FURTHER EXPLORATIONS OF AQUEOUS HUMOUR DRAINAGE IN ENUCLEATED HUMAN AND BOVINE EYES

By

Patrick A. Scott

B.S., Biology/Pre-Medicine
Canisius College, 2002

A THESIS PRESENTED TO THE GRADUATE FACULTY IN PARTIAL FULFILLMENT OF THE REQUIREMENTS FOR THE DEGREE OF

MASTER OF SCIENCE

AT THE
NEW ENGLAND COLLEGE OF OPTOMETRY

MAY 10, 2006

©2006 Patrick A. Scott
All Rights Reserved

The author hereby grants the New England College of Optometry permission to reproduce and to distribute publicly paper and electronic copies of this thesis document in whole or in part

FURTHER EXPLORATIONS OF AQUEOUS HUMOUR DRAINAGE IN ENUCLEATED HUMAN AND BOVINE EYES

By

Patrick A. Scott

A THESIS PRESENTED TO THE GRADUATE FACULTY IN PARTIAL FULFILLMENT OF THE REQUIREMENTS FOR THE DEGREE OF

MASTER OF SCIENCE

AT THE
NEW ENGLAND COLLEGE OF OPTOMETRY

MAY 10, 2006

©2006 Patrick A. Scott
All Rights Reserved

This manuscript has been read and accepted by the Thesis Examination Committee in satisfaction of the thesis requirement for the degree of Master of Science

Signature of Author _____
Patrick A. Scott
May 10, 2006

Certified by _____
Haiyan Gong
Thesis Supervisor

Thesis Committee

_____
Thomas Freddo

_____
Darryl Overby

_____
Mark Zorn

Accepted by _____
David Troilo
Chairmen, Department Committee on Graduate Studies

FURTHER EXPLORATIONS OF AQUEOUS HUMOUR DRAINAGE IN ENUCLEATED HUMAN AND BOVINE EYES

By

Patrick A. Scott

Submitted to the Department of Vision Science
On May 10, 2006 in partial fulfillment of the
Requirements for the Degree of Master or Science in
Vision Science

ABSTRACT

Primary open-angle glaucoma (POAG) is the most common form of glaucoma in individuals over forty-years of age in North America. In POAG, outflow resistance is pathologically elevated due to a malfunctioning or impairment of the filtration mechanisms with the eye; consequently, prolonged elevation of IOP may ultimately lead to irreversible blindness. The human eye appears to be particularly vulnerable to POAG when compared to eyes of non-human species. The reason for this increased susceptibility remains unknown. An interesting corollary of this distinction is that all studies of non-human mammalian eyes performed to date demonstrate a volume-related increase in outflow facility when undergoing prolonged intraocular perfusion. This phenomenon, known as "washout", does not occur in the human eye. Currently, is unclear what physiological mechanisms are involved in governing the washout effect. Washout is a reversible process and a correlation is observed between the degree of physical separation between the juxtacanalicular connective tissue (JCT) and basal lamina of the inner wall of the aqueous plexus (bovine equivalent of Schlemm's canal) and changes in outflow facility in enucleated bovine eyes. In these studies, we focused on

structural differences between species that do and do not exhibit the washout effect, developed a better method for tracing and investigating the macroscopic patterns of aqueous humor drainage in bovine eyes. Our studies demonstrated that the measured increase in outflow facility due to washout correlates with JCT/inner wall separation from the bovine aqueous plexus. In human eyes, which do not exhibit washout, neither of these changes occurred after prolonged intraocular perfusion. Compared to bovine eyes, there are more elastic fiber connections in the JCT of the human eye that may limit JCT/inner wall separation, thereby potentially explaining the lack of washout in human eyes. A preliminary study was performed to investigate whether changes in outflow facility correlate with changes in outflow patterns before and after washout in bovine eyes. Outflow patterns were examined using confocal microscopy and two colors of fluorescent microspheres to probe for changes in outflow patterns before and after washout. Our results showed the pre-washout macroscopic pattern of outflow appeared punctate whereas the post-washout pattern appears more uniform. Changes in outflow facility did not correlate with the area available for outflow through the inner wall of the bovine aqueous plexus. A better understanding of the mechanisms that augment the total area for outflow could be exploited to increase outflow facility in eyes with elevated IOP.

Thesis Supervisor: Haiyan Gong, M.D., Ph.D.

Thesis Committee: Thomas F. Freddo, O.D., Ph.D.
Darryl R. Overby, Ph.D.
Mark Zorn, Ph.D.

ACKNOWLEDGEMENTS

I would like to thank Professor Haiyan Gong (Boston University School of Medicine, Department of Ophthalmology; New England College of Optometry, Department of Biomedical Science) for all the expert training and guidance she provided me with throughout this project. Professor Gong has been an exemplary role model.

I thank Professor Thomas F. Freddo (Vice-Chairman for Research, Boston University School of Medicine, Department of Ophthalmology; New England College of Optometry, Department of Biomedical Science) for providing me with guidance, motivation, constructive-criticism, and stimulating conversation. His expert advice and knowledge of science and ophthalmology were invaluable for the completion of this project,

I am grateful to Professor Darryl R. Overby (Tulane University, Department of Bioengineering) for his time and effort in the development of this project. His former studies in aqueous humor hydrodynamics provided the bedrock for the formation and design of this project.

I thank Professor Mark Zorn (New England College of Optometry, Department of Biomedical Science) for his thoughtful comments and his thorough review of this thesis.

I would like to acknowledge support from The Glaucoma Research Foundation, National Eye Institute, grant #EY09699, The Massachusetts Lions Eye Research Fund to Boston University School of Medicine, and the National Institute of Health T-35 Summer Training Grant. The technical assistance of Rozanne Richman, M.S., is most gratefully appreciated.

TABLE OF CONTENTS

Abstract……3

Acknowledgements……..…5

Chapter 1: Introduction to Aqueous Humor Outflow…….11
1.1 The Aqueous Humor Outflow Pathway……..14
1.1.1 Aqueous Humor…….14
1.1.2 Conventional Outflow Route and Related Structures…….15
1.1.2a Uveal and Corneoscleral Meshwork……...15
1.1.2b Juxtacanalicular Connective Tissue (Cribriform Meshwork)…….16
1.1.2c Schlemm's Canal & Inner Wall Endothelial Cells……..…17
1.1.2d Collector Channels and Aqueous Veins…….18
1.1.2e Aqueous Pump Mechanism…….19
1.1.3 Unconventional Outflow Route……..19
1.2 Aqueous Humor Outflow Resistance……..21
1.2.1 Aqueous Humor Outflow Resistance Within the Uveal and Corneolscleral Meshwork……21
1.2.2 Aqueous Humor Outflow Resistance Within the Aqueous Veins and Schlemm's Canal……22
1.2.3 Aqueous Humor Outflow Resistance Within the Inner Wall Endothelium of Schlemm's Canal……23
1.2.4 Aqueous Humor Outflow Resistance Within the Juxtacanalicular Connective Tissue……26
1.2.5 Site of Aqueous Humor Outflow Resistance in Primary Open-Angle Glaucoma…….27
1.3 Specific Aims of Project……..29
1.3.1 Specific Aim #1……..30
1.3.2 Specific Aim #2……..31
1.3.3 Specific Aim #3……..33

Chapter 2A: A Brief History of the Washout Effect……34

Chapter 2B: Comparative Studies Between Species that Do and Do Not Exhibit a Washout Effect……..37
2B.1 Abstract…….37
2B.2 Introduction……...39
2B.3 Materials and Methods……..41
2B.3.1 Experimental Ocular Perfusion…….43
2B.3.2 Outflow Perfusion Procedure……44
2B.3.2a Experimental Perfusion of Bovine Eyes……..45
2B.3.2b Experimental Perfusion of Human Eyes……..45
2B.3.3 Tissue Processing for Microscopy……46

2B.3.3a Morphologic Evaluation of Inner Wall/JCT Separation……..46
2B.3.4 Statistical Methods……..50
2B.4 Results…….50
2B.4.1 Outflow Facility in Human and Bovine Eyes…….51
2B.4.2 Morphological Evaluation……...53
2B.5 Discussion……...62

Chapter 3A: A Review of Aqueous Humor Filtration Studies……...67
3A.1 Aqueous Humor Outflow Filtration Studies……..67
3A.1.1 Relevant Conclusions From Previous Aqueous Humor Outflow Filtration Studies……...72
3A.1.2 Comparative Differences in Outflow Morphology Between Human and Bovine Eyes……..75

Chapter 3B: Relationship Between Outflow Facility and Patterns of Aqueous Humor Drainage in the Bovine Eye –A Preliminary Study……...75
3B.1 Abstract…….75
3B.2 Introduction……..77
3B.3 Materials and Methods…….80
3B.3.1 Ocular Perfusion Apparatus……..80
3B.3.2 Outflow Perfusion Procedures……..…80
3B.3.2a Short-Duration Perfusion…….81
3B.3.2b Long-Duration Perfusion……..……82
3B.3.3 FluoSpheres……..83
3B.3.4 Removal of Free-Floating FluoSpheres from the Anterior Chamber during Anterior Chamber Exchange…….83
3B.3.5 Confocal Microscopy……86
3B.4 Results……...88
3B.4.1 Outflow Facility……..……88
3B.4.2 Confocal Imaging of Pre- and Post-Washout Micropshere Outflow Patterns……..…89
3B.4.2a Comparing Outflow Facility with Pre- and Post-Washout Microsphere Distribution…….93
3B.5 Discussion…….97

Chapter 4: Conclusions and Recommendations for Future Work……...102
4.1 Comparative Studies Between Species that Do and Do Not Exhibit a Washout Effect……103
4.2 Relationship Between Outflow Facility and Patterns of Aqueous Humor Drainage in the Bovine Eye– A Preliminary Study……...105
4.3 Future Work……..……106

Appendix…….108

Bibliography……...112

CHAPTER 2 – FIGURES

FIGURE NUMBER	FIGURE TITLE	PAGE
2.1	Ocular Perfusion Apparatus	43
2.2	Morphologic Assessment of Separation Between The Inner Wall/JCT in the Bovine Eye	48
2.3	Electron Microscopy Image of Cell-Matrix vs. Matrix-Matrix Separation in Bovine Eyes	49
2.4	Outflow Facility for Short- and Long-Duration Perfusions at 15 mmHg in Human and Bovine Eyes	52
2.5A	Light Micrograph of Bovine Aqueous Plexus After Short-Duration Perfusion	55
2.5B	Light Micrograph of Bovine Aqueous Plexus After Long-Duration Perfusion	55
2.6A	Correlation of Absolute Value of Pre-Fixation Outflow Facility and JCT/Inner Wall Separation Scores	56
2.6B	Correlation of Outflow Facility and JCT/Inner Wall Separation Scores	56
2.7A	Transmission Electron Micrograph of the Bovine Aqueous Plexus After Long-Duration Perfusion	57
2.7B	Transmission Electron Micrograph of the Bovine Aqueous Plexus After Short-Duration Perfusion	57
2.8A	Light Micrograph of Human JCT/Inner Wall After Short-Duration Perfusion	60
2.8B	Light Micrograph of Human JCT/Inner Wall After Long-Duration Perfusion	60
2.9A	Transmission Electron Micrograph of Human JCT/Inner Wall After Short-Duration Perfusion	61
2.9B	Transmission Electron Micrograph of Human JCT/Inner Wall After Long-Duration Perfusion	61

CHAPTER 3 – FIGURES

FIGURE NUMBER	FIGURE TITLE	PAGE
3B.1	Perfusion System with Computer	80
3B.2	Anterior Chamber Removal of FluoSpheres	84
3B.3	Visible FluoSpheres/30 microliter Sample/1 ml Exchanged vs Exchange Volume	85
3B.4	Confocal Image of the Bovine Aqueous Plexus Effective Filtration Area	87
3B.5	Punctate Micropshere Distribution in Control Eyes	90
3B.6	Radial Sections of Aqueous Humor Drainage Patterns in the Bovine Aqueous Plexus using Confocal Microscopy	92
3B.7	Experimental % FluoSphere Distribution vs % Change in Outflow Facility in Pre- and Post-Washout Bovine Eyes	96
3B.8	Segmental Outflow in Bovine Eyes at 15 mmHg	99

CHAPTER 4 – FIGURES

FIGURE NUMBER	FIGURE TITLE	PAGE
4.1	Frontal Sectioning along the Bovine Aqueous Plexus	107

CHAPTER 2 – TABLES

TABLE NUMBER	TABLE TITLE	PAGE
2.1	Outflow Facility for Short- and Long-Duration Perfusions At 15 mmHg in Human and Bovine Eyes	51
2.2	Inner Wall Separation Scores for Short- and Long-Duration Perfusions in Bovine Eyes	56
2.3	Inner Wall Separation Scores for Short- and Long-Duration Perfusions in Human Eyes	58

CHAPTER 3 – TABLES

TABLE NUMBER	TABLE TITLE	PAGE
3B.1	Data for Visible Microspheres per 30 μL/1mL Exchange Sample	85
3B.2	Outflow Facility for Short-Duration Perfusions at 15 mmHg in Bovine Eyes	88
3B.3	Outflow Facility for Short-Duration Perfusions at 15 mmHg in Bovine Eyes	89
3B.4	Short-Duration (Control) Perfusion % Microsphere Distribution (Pre-Washout) vs % Change in Outflow Facility	94
3B.5	% Microsphere Distribution vs % Change in Outflow Facility	95

CHAPTER 1: INTRODUCTION TO AQUEOUS HUMOR OUTFLOW

Aqueous humor, a clear nutritive fluid derived from the blood, pressurizes the eye by various means that have puzzled researchers for over a century. Prior to 1873, aqueous humor was thought to be a stagnant fluid within the eye (Seidel, 1921). It was Leber, who in 1873 (Leber, 1873), proposed that aqueous humor was the result of an ongoing dynamic process involving the eye and the circulatory system. Later, it became apparent that aqueous humor played a more central role in maintaining the necessary backpressure, a.k.a. intraocular pressure (IOP), that that is responsible for optimizing the structural and optical properties within the eye as well as providing nutritive substances and a means for metabolic waste removal for the avascular tissues within the eye. As such, disrupting the delicate balance between aqueous humor inflow and outflow may lead to elevation of IOP, a known risk factor for primary open-angle glaucoma (POAG).

In glaucoma, aqueous humor outflow may be impaired for various reasons. The manifestation of glaucoma is often idiopathic, i.e. POAG, and if untreated may result in irreversible blindness. Systemic conditions such as venous congestion may elevate episcleral venous pressure impairing aqueous humor drainage causing increased IOP. The body's immune system may cause an abrupt rise in IOP secondary to inflammation of the trabecular meshwork (trabeculitis) when an inciting agent such as the herpes zoster virus is active within the eye. Despite all of the accrued knowledge on the pathogenesis, treatment, and management of glaucoma, our understanding of the basic mechanisms involved in regulating aqueous humor outflow resistance remains unclear in both the normal and glaucomatous human eye.

POAG is the most common form of glaucoma in individuals over forty-years of age

in North America (Kanski, 2000). Eyes with POAG exhibit a chronic progressive loss of retinal ganglion cells, a specific optic neuropathy, and characteristic visual field loss. In POAG, outflow resistance is increased due to malfunction or impairment of the filtration mechanism within the trabecular meshwork. Current hypotheses for the pathophysiological development of POAG include: (1) increased mechanical stress at the level of the lamina cribrosa (Quigley et al., 1983) secondary to elevated IOP disrupts vital axonal transport processes that result in retinal ganglion cell death, (2) impairment of the angioarchitecture supplying the anterior optic nerve, i.e. "watershed" zones – areas of compromised choroidal circulation that may deprive the anterior optic nerve of nutrients and a means of metabolic waste disposal (Hayreh, 1994); defects or malfunctions of the autoregulatory mechanisms involved in controlling blood flow from the retinal vasculature to the optic nerve (Pillunat, Stadtmeister, Wilmanns et al., 1985; Robert, Steiner, and Hendrickson, 1989), as well as nocturnal systemic hypotension (Hayreh, Zimmerman, Podhajsky, et al., 1994), and (3) elevated levels of extracellular glutamate within the vitreous secondary to retinal ischemia and apoptosis (Dreyer, Zurakowski, Schumer, et al., 1996).

Interestingly, the human eye appears to be particularly vulnerable to POAG when compared to eyes of non-human species (Gelatt, 1977). The reason for this increased susceptibility remains unknown. The use of animal models in glaucoma has contributed significantly to our current understanding of aqueous humor outflow in both normal and glaucomatous human eyes; however, these results are also disappointing in that they have yet to provide a definitive locus for the primary resistive moiety within the human eye. Morphometric studies of the primary outflow pathway at the electron microscope level

have failed to determine the primary resistive moiety in the normal human eye as well as the added resistance in eyes with POAG. Unfortunately, this lack of fundamental knowledge has prevented the development of an effective anti-glaucoma therapy that could be used to selectively target and weaken the primary resistive moiety to allow for decreased outflow resistance in the conventional pathway.

The goal of this thesis is to investigate the mechanism(s) responsible for the generation of aqueous humor outflow resistance in the human and bovine eye in hopes that such knowledge may be applied in future studies to better understand the hydrodynamic mechanisms involved in regulating aqueous humor outflow resistance in glaucomatous human eyes.

1.1 THE AQUEOUS HUMOR OUTFLOW PATHWAY

Aqueous humor outflow resistance within the eye is needed to create positive IOP to keep the eye from collapsing. IOP provides stabilizing pressure that keeps the refracting components of the eye in their proper alignment and orientation to maximize clarity of the optical image on the retina as well as upholding the structural integrity of the eye (Millar and Kaufman, 1995).

1.1.1: *Aqueous Humor*

Aqueous humor is a clear nutritive fluid derived from an ultra-filtrate of blood plasma in the microvasculature of the ciliary body stroma. It is secreted by the non-pigmented ciliary epithelium into the posterior chamber at a rate of 2.5 μL/min. This metabolically rich fluid contains 1/100 of the protein content of blood plasma and serves as a source of nutrition for the avascular lens, cornea, and trabecular meshwork. The low protein concentration decreases the potential for light scatter (Tyndall Effect) and glare that would otherwise be detrimental to the quality of the optical image projected onto the retina. Aqueous humor enters the posterior chamber of the eye after being secreted from the non-pigmented epithelium located on the apical ends of the ciliary processes of the pars plicata. Aqueous humor then flows anteriorly between the intraocular lens and iris pigmented-epithelium where it arrives and quickly traverses the pupillary aperture to enter the anterior chamber. In the anterior chamber, in the horizontal facing eye, it circulates in a convective flow current, rising posteriorly due to the warm iris vasculature and falling anteriorly behind the cooler corneal endothelium. Aqueous humor exits the anterior chamber via two major drainage pathways; the conventional route, a.k.a.

trabecular meshwork route, and the unconventional pathway, a.k.a. uveoscleral route (Bill, 1965, 1966; Bill and Phillips, 1971). The conventional outflow pathway is responsible for the majority (70-90%) of aqueous humor outflow whereas the uveoscleral outflow route drains 34±12% (Townsend and Brubaker, 1980; Toris, 1999) of total aqueous outflow.

1.1.2: Conventional Outflow Route (Trabecular) and Related Structures

The conventional outflow pathway begins with aqueous humor flowing into the iridocorneal angle where it arrives at the inner boundary of the trabecular meshwork. The trabecular meshwork extends from the scleral spur posteriorly to Schwalbe's line (termination of Descemet's membrane in the cornea) anteriorly. The trabecular meshwork is a wedge shaped tissue composed of 12-20 trabecular layers posteriorly and 3-5 layers anteriorly at its apex near the cornea (Tripathi, 1974; Gong, Tripathi R and Tripathi B, 1996). The trabecular meshwork is divided into the uveal, corneoscleral, and cribriform meshwork.

1.1.2a: Uveal and Corneoscleral Meshwork

Aqueous humor traverses the uveal meshwork, the inner most portion of the trabecular meshwork that faces the anterior chamber, followed by the deeper corneoscleral meshwork. The trabecular meshwork is arranged in a funnel-like manner with larger openings (25 to 75 microns side-to-side) observed between the intersecting beams of the innermost portion of the uveal meshwork. Lining the trabecular beams are versatile endothelial cells able to perform a wide variety of functions including

phagocytosis, cellular migration, production of extracellular matrix elements, and lysosomal and matrix-degradation (Yue, 2000). These beams or cords are arranged in a radial net-like pattern (Tripathi, 1974) while the outer portions of the uveal and corneoscleral meshwork are arranged circumferentially forming flat perforated sheets. The arrangement of the uveal and corneoscleral meshwork forms a system of aqueous flow channels comprised of a series of progressively smaller tortuous pathways (2-15 microns in diameter) (Tripathi, 1974). The progressively decreasing pore size from inner to outer meshwork, combined with the phagocytic activity of the trabecular meshwork cells, causes the trabecular meshwork to behave as a "self-cleaning" filter that eliminates debris and particulates that would otherwise obstruct aqueous humor outflow.

1.1.2b: Juxtacanalicular Connective Tissue (Cribriform Meshwork)

Abutting the outermost sheet of the corneoscleral meshwork is an amorphous tissue the juxtacanalicular connective tissue (JCT). The JCT lacks a basal lamina and is composed of fibroblast-like cells (Rohen, Futa, and Lutjen-Drecoll, 1981), extracellular matrix material, and also contains endothelial cells that lack regular organization. The extracellular matrix material appears to contain ground substance, fine fibrils, and an elastic-like fiber system that surrounds many openings located in the JCT (Rohen and Unger, 1959). The elastic-like fiber system, far more robust in human eyes as compared to other species, connects the inner wall endothelium with the trabecular lamellae, while a separate set of fibers branch off into bundles and form elastic-sheaths that connect inner wall endothelial cells to their subendothelial basement membrane (Rohen et al., 1981).

After aqueous humor has passed through the JCT it must now traverse the inner wall of Schlemm's canal in order to exit the eye into the greater venous circulation.

1.1.2c: Schlemm's Canal and Inner Wall Endothelial Cells

The inner wall of Schlemm's canal is lined with a single layer of non-fenestrated endothelial cells that rest on a discontinuous basement membrane. A unique feature of the inner wall of Schlemm's canal is the presence of endothelial cells that experience a basal-to-apical directed pressure gradient. The precise mechanism by which aqueous humor passes into the lumen of Schlemm's canal is not fully understood; however, most authorities believe small pores found in unique bulges of the endothelium, known as giant vacuoles, and other areas of the inner wall represent pathways for aqueous egress into Schlemm's canal (Inomata, Bill, and Smelser, 1972). Cytoplasmic processes extend downward from the endothelial cells to an incomplete subendothelial layer composed of parachute-like cells; JCT cells form the tether of the parachute while inner wall endothelial cells form the parachute itself. This parachute-like configuration may anchor the inner wall and its endothelium allowing it to withstand pressure-induced distention secondary to hydrodynamic stress across the inner wall/JCT region. Johnstone (1979) reported a progressive change in configuration in response to gradual change in IOP (25-35 mmHg in monkey eyes) suggesting the endothelial cell processes serve as architectural subunits that resist elevated IOP.

Two distinct types of pores have been studied: "border pores" or intercellular pores – found between adjacent endothelial cells, and "I pores" or intracellular pores – found on the basal and abluminal sides of the endothelial cells (Ethier, Coloma, Sit, and

Johnson, 1998). While their potential involvement in outflow resistance is currently unknown, studies suggest the number of pores is decreased in glaucomatous human eyes (Johnson, Chan, Read, Christensen, Sit, and Ethier, 2002; Allingham, deKater, and Ethier, 1992). It has also been shown that pore density and artifacts increase secondarily with the volume of fixative perfused through and eye (Sit, Coloma, Ethier, and Johnson, 1997). However, a recent study (Yektashenas, Read, Ethier, and Johnson, 2006) used cationized ferritin as a marker of true pores in the inner wall endothelium and showed a significant portion of these pores were labeled suggesting a significant fraction of outflow enters these pores into Schlemm's canal. Interestingly, glaucomatous eyes still show far less pores than normal eyes when artifacts and the volume of fixative that is perfused is taken into account.

1.1.2d: Collector Channels and Aqueous Veins

Aqueous humor travels circumferentially (Moses, 1979) in the lumen of Schlemm's canal and exits via approximately 30-35 collector channels (Theobald, 1934; Ashton, 1951) from the outer wall of Schlemm's canal. The collector channels then lead to venous plexi (deep scleral plexus, intrascleral plexus, and episcleral plexus, respectively) and then finally drain into the episcleral veins to join the greater venous circulation. Shunt vessels leading directly to the episcleral plexus sometimes bypass the venous plexi and these vessels are known as the aqueous veins of Ascher (Ascher, 1942).

1.1.2e: Aqueous Pump Mechanism

The physiological manner by which aqueous humor leaves the eye is also currently under hot debate. It is generally accepted that in the conventional outflow pathway aqueous humor is carried by bulk flow (Bill and Maepea, 1994); however, a recent paper by Johnstone (2004) argues otherwise suggesting that oscillating IOP pumps aqueous humor from the anterior chamber. Whether or not any credence or general support for this alternative mechanism has been accepted is unclear at this time. A more in depth treatise on ocular outflow by means of a pumping mechanism can be found in Johnstone (2004).

1.1.3: Unconventional Outflow Route

The second major pathway, the uveoscleral route, begins with aqueous humor passing through the anterior face of the ciliary body. Aqueous humor flows between the ciliary muscle fasicles into a potential space between the ciliary body and the lamina fusca of the sclera known as the supraciliary space. Posterior to and continuous with the supraciliary space is the suprachoroidea through which aqueous humor then passes as it traverses the sclera directly or may re-enter the venous circulation back across the endothelium of the vortex ampullae. The uveoscleral route is responsible for approximately 34±12% (Townsend and Brubaker, 1980; Toris, 1999) of aqueous humor outflow in the human eye and is almost evenly distributed with the trabecular route in monkey eyes (Bill, 1965; Nilsson, 1989; Sperber and Bill, 1984; Gabelt et al., 2003). The uveoscleral pathway has been targeted with prostaglandin analogs (i.e. $PGF_{2\alpha}$ Latanprost) to enhance aqueous humor outflow along this route. However, studies have

also shown an increase in pigment between the ciliary fasicles of the anterior longitudinal muscle in rhesus monkeys suggesting this pathway may also develop resistance to outflow (Lutjen-Drecoll, Tamm, and Kaufman, 1988a, 1988b; Gabelt et al., 2003). It has also been reported by Toris (1999) that uveoscleral outflow decreases with age.

1.2 AQUEOUS HUMOR OUTFLOW RESISTANCE

Over the past 130 years, understanding the filtration characteristics of the conventional aqueous humor outflow pathway has been a goal sought by many researchers interested in discerning the regulatory mechanism(s) involved in governing aqueous humor outflow resistance in the human eye.

In 1873, Leber was the first to propose that aqueous humor was part of an ongoing process originating in the circulatory system (Leber, 1873). Leber's contention was further supported by numerous studies (Schwalbe, 1870; Knies, 1875; Smith, 1888; Thomassen, 1947; Seidel, 1923; Ascher, 1942; Goldmann, 1946). Leber's disputation of previously established dogma regarding the primary role of aqueous humor in the eye necessitated re-evaluation, which has lead to our current understanding of the formation, secretion, and egression of aqueous humor as well as its metabolic role within the eye. Although much progress has been made in understanding the aqueous humor drainage system in human eyes one central question still unanswered today is: where in the outflow pathway is the primary resistance to aqueous humor generated and by what mechanism? In the following section, we review previous and current views on aqueous humor outflow resistance and the various tissues that were and are now thought to be involved in maintaining outflow resistance.

1.2.1: Aqueous Outflow Resistance Within the Uveal and Corneoscleral Meshwork

The outflow resistance encountered in the uveal and corneoscleral meshwork has been shown theoretically (McEwen, 1958) and experimentally (Grant, 1963) to be negligible given the vast number and large size of the openings in this tissue. Furthermore, it has been demonstrated (Johnstone and Grant, 1973) that a widening of

these openings occurs with increasing IOP, which, intuitively, should decrease outflow resistance; however, since an increase in outflow resistance (Johnson and Kamm, 1983) is observed with increasing IOP, the corneoscleral meshwork is ruled out.

1.2.2: Aqueous Outflow Resistance Within Aqueous Veins and Schlemm's Canal

Other structures of the outflow pathway including aqueous veins have been studied to determine their relative contribution to overall outflow resistance. Various studies (Rosenquist, Epstein, and Melamed, 1989; Maepea and Bill, 1989, 1992) showed that these channels generate negligible resistance (10% or less) and that resistance within the intrascleral vessels varies with changes in IOP.

Schlemm's canal has also been studied extensively to determine if its size and dimensions contribute to the bulk of aqueous humor outflow resistance (Johnson and Kamm, 1983; Moses, 1979, 1981). Schlemm's canal collapses during states of increased IOP (Van Buskirk, 1976) and this observation has led some investigators to hypothesize that collapse of the canal lumen may lead to added outflow resistance in POAG (Nesterov, 1970). In contrast, Johnson and Kamm (1983) demonstrated that eyes perfused at pressures of 50 mmHg show a completely collapsed Schlemm's canal (Johnstone and Grant, 1973), but the outflow facility measured at this pressure (Brubaker, 1975) was significantly higher than that observed in glaucomatous eyes. Therefore, Johnson and Kamm (1983) concluded that collapse of Schlemm's canal could not provide the added resistance observed in POAG and that other physiological mechanisms must be involved. However, Allingham et al. (1996) disputed Johnson and Kamm (1983) arguing that the dimensions of Schlemm's canal and inner wall endothelial lining may be important structural features that regulate outflow resistance in POAG and warrant

further consideration. Allingham et al. (1996) noted a 37% decrease in the inner wall length of Schlemm's canal secondary to inner wall/outer wall apposition leading to a decrease of 36% in the effective filtration area (EFA = fraction of total area of the JCT/inner wall involved in aqueous humor filtration at any given instant; Bárány, 1967) in POAG eyes (Allingham, deKater, Ethier, 1996). The nature of the involvement of Schlemm's canal and its contribution to total outflow resistance in both the normal and glaucomatous eye require further study.

1.2.3: Aqueous Outflow Resistance Within the Inner Wall Endothelium of Schlemm's Canal

The inner wall endothelium of Schlemm's canal has also been studied extensively to determine its role in contributing to outflow resistance within the eye. The inner wall endothelium of Schlemm's canal, a non-fenestrated tissue with tight junctions, has the highest hydraulic conductivity of any endothelial tissue in the human body (Johnson and Erickson, 2000). The inner wall endothelium possesses large pores through which fluid is believed to flow into Schlemm's canal. The majority of these pores allow for intracellular transport of fluid, while a small, but significant, fraction is intercellular (Ethier et al., 1998). Previous filtration studies (Seidel, 1923; Johnson, Johnson, and Kamm, 1990; Huggert, 1955; Huggert, Holmberg, Esklund, 1955) as well a recent study (Yektashenas et al., 2006) confirmed that fluid is transported through these pores into Schlemm's canal. Studies (Bill and Svedbergh, 1972; Grierson, Lee, Moseley, and Abraham, 1979; Erikkson and Svedbergh, 1980; Moseley, Grierson, and Lee, 1983) have shown that these pores account for only 10% of aqueous outflow resistance; however, this is still debated due to artifacts that occur with fixation. Although the resistance of

the pores may be negligible by themselves, it has been hypothesized (Johnson, Shapiro, Ethier, Kamm, 1992) that the proximity of these pores to the JCT may cause the formation of aqueous streamlines or a so-called “funneling effect” that greatly increases outflow resistance. Johnson et al. (1992) hypothesized their funneling model based on the work of Grierson et al. (1979) who showed a decrease in outflow resistance due to a three-fold increase in inner wall porosity after pilocarpine administration. . Johnson et al., 1992 proposed that a hydrodynamic mechanism known as “pore funneling” may augment outflow resistance by confining fluid through those regions of the JCT nearest pores in the inner wall and thereby decrease the available area for aqueous humor drainage. Moreover, pore funneling may cause a hydrodynamic interaction where the resistance of the JCT and inner wall are coupled resulting in additional outflow resistance. In other words, when the resistance of both the JCT and inner wall are considered together as a functional unit, the combined resistance of the JCT and inner wall is greater than sum of these structures measured individually. Convergence of aqueous streamlines occurs at the pores because the greatest drop in pressure across the inner wall occurs near pores. Thus, the effective filtration area for entering Schlemm’s canal is decreased, which inversely increases outflow resistance due to pore funneling along the inner wall. However, the funneling effect will only occur if certain physiological conditions are met: (1) pores in the inner wall endothelium are static open structures – if vacuole formation is dynamic, that is, where some are in a state of filling while others are in a state of draining, outflow through the JCT region will be more uniform and eliminate pore funneling, (2) uniform permeability of the JCT – open spaces in the JCT would diminish the funneling effect, and (3) uniform size and spacing between

inner wall pores – non-uniform pore distributions will cause significant flow variability thus diminishing the funneling effect (Johnson et al. 1992). Interestingly, two studies (Ethier et al., 1998; Sit et al., 1997) disputing the funneling hypothesis found no correlation between outflow facility and inner wall pore density. However, other studies (Allingham, 1992; Johnson et al., 2002) have shown a decrease in the number of pores in glaucomatous eyes (160 pores/mm^2) as compared to the normal eye (835 pores/mm^2) suggesting outflow resistance may be exacerbated due to pore funneling in glaucomatous eyes. Support for the funneling hypothesis also comes from a study (Sabanay, Gabelt, Tian, Kaufman, and Geiger, 2004) using H-7, an agent known to reversibly increase outflow facility in monkeys in vivo monkey eyes (Tian, Kaufman, Volberg, Gabelt, and Geiger, 1998; Tian, Gabelt, Peterson, Kiland, and Kaufman, 1999). In that study, infusion of the H-7 compound led to a more uniform distribution of tracer particles from a punctate distribution along the inner wall as predicted by elimination of the funneling effect.

Despite numerous studies of the inner wall of Schlemm's canal much remains unknown about the role endothelial cells play in regulating IOP. A recent study (Ethier, Read, and Chan, 2004) that investigated the cytoarchitecture and the potential role that F-actin may play in modulating both inner and outer wall endothelial cell alignment. Ethier et al. (2004) attempted to characterize the biomechanical environment of Schlemm's canal in vivo to determine if shear stress exerted by the flow aqueous humor affected endothelial cell cytoarchitecture. Ethier et al. (2004) found a statistically significant coalignment of the inner and outer wall endothelial cells that tended to increase as collector channel ostia are approached. F-actin distribution and changes in

cytoarchitecture between inner and outer wall cells appeared to be related to differences in their respective biomechanical environments. Also of particular interest, Bill et al. (1972) noted aqueous humor within Schlemm's canal influenced the orientation of endothelial cells and their borders. More studies are needed to determine how stress factors such as the pressure associated force across the inner wall affect F-actin distribution as well as the response of both inner and outer wall endothelial cells to changes in their micro-environments. One might contemplate whether F-actin is involved in the molecular tethering of the inner wall to the underlying JCT matrix and how its distribution may change after the washout effect (See Chapter 2A & 2B).

1.2.4: Aqueous Humor Resistance Within the Juxtacanalicular Connective Tissue

Currently, it is widely accepted that most of the outflow resistance in the conventional pathway is generated from extracellular matrix material in the JCT. The process of elimination was largely a part of this distinction given the negligible resistance of other outflow structures and tissue. The small openings and tortuous pathways in the JCT make it a likely candidate for harboring the primary resistive moiety. If the open spaces within the JCT contain extracellular matrix gel, hydrodynamic calculations closely approximate the order of magnitude that could provide significant resistance to aqueous humor outflow (Johnson, 1987). The glycosaminoglycans (GAGs) comprising the extracellular matrix are negatively charged and have been shown to generate flow resistance in other tissues (Maepea and Bill, 1992). Maepea and Bill (1992) provided evidence using micropipette techniques that showed most of the outflow resistance is located approximately 7-14 microns upstream from the inner wall at a pressure of 9

mmHg. Interestingly, at more physiologic pressures, outflow resistance localized closer to the inner wall. However, it is not known whether the human JCT region contains a gel-like matrix that completely fills the space between JCT cells since most conventional electron microscopy tissue preparation techniques cause secondary degradation of GAGs. A recent study (Gong, Ruberti, Overby, Johnson, and Freddo, 2002), using a technique called quick-freeze/deep-etch (QFDE), revealed an elaborate view of the extracellular matrix in the JCT that showed micro-sized optically empty spaces. Gong et al. (2002) pointed out that although optically empty space is still observed with QFDE, it is unclear as to whether this technique is able to preserve GAGs in their uncollapsed state.

A recent debate at the 2002 International Society of Eye Research (ISER) meeting resulted in an agreement by experts that neither inner wall endothelial cells nor extra-cellular matrix material within the JCT could be clearly ruled out in the generation of aqueous humor outflow resistance. One expert, Dr. David Epstein, pointed out that even if the funneling hypothesis is accepted, the pores generating the funneling effect pass through the cells of the inner wall. Therefore, the inner wall cells may be important 'modulators' of outflow resistance generated by the extracellular matrix upstream of these cells (http://www.glaucom.com/Meetings/4-3/iser.htm).

1.2.5: Site of Aqueous Humor Resistance in Primary Open-Angle Glaucoma

Although the primary site for generation of aqueous humor outflow resistance is believed to be in the JCT in normal human eyes (Johnson, 1987; Maepea, 1992), less is known about the locus of the added resistance in eyes with POAG. One study showed, after complete surgical trabeculotomy in an enucleated glaucomatous eye, outflow

facility approached similar facility rates observed in enucleated healthy human eyes (Grant, 1963). This suggests that the elevated outflow resistance in POAG eyes most likely resides between the anterior chamber and Schlemm's canal. Additionally, increased thickening of the cortical zone of the trabecular endothelial cells and an overall decrease in the number of these cells may exacerbate outflow resistance in eyes with POAG (Duane, 1971).

As previously mentioned (See Section 1.2.2), Schlemm's canal was once thought (Nesterov, 1970) and is still debated by some (Allingham et al., 1996) to be involved in generating outflow resistance in eyes with POAG.

Given the findings of previous research, it appears that the generation of outflow resistance in POAG resides in the JCT or endothelial cells of the inner wall of Schlemm's canal or both. However, it is not the goal of this thesis to determine the primary site of outflow resistance in POAG, rather, we attempt to further understand the generation of outflow resistance in the bovine and normal human eye, in hopes that such knowledge will aid future studies in determining the cause of the added outflow resistance in the glaucomatous human eye.

1.3 SPECIFIC AIMS OF PROJECT

Although washout is not observed in human eyes (Erickson-Lamy, Schroeder, Bassett-Chu, and Epstein, 1990) it occurs in all non-human species studied to date (Barany, 1962,1964; Epstein, et al., 1982; Erickson and Kaufman, 1981; Erickson-Lamy, et al., 1988; Gaasterland, et al., 1978; Fourman and Fourman, 1989; Gaasterland, et al., 1979; Hashimoto and Epstein, 1980; Kaufman, et al., 1988; Overby, et al., 2002; Rao, et al., 2001; Ruben, Moses, and Grodski, 1985; Van Buskirk and Brett, 1978; Yan, et al., 1991). The human eye may have a unique morphology that prevents the washout effect from occurring; however, the underlying mechanism(s) involved in washout are poorly understood.

Overby et al. (2002) showed the structural correlate to the increase in outflow facility during washout is detachment of the JCT from the inner wall of the aqueous plexus (AP) - bovine equivalent of Schlemm's canal (Tripathi, 1971). Washout in bovine eyes (Overby et al., 2002) and monkey eyes (Sabanay et al., 2004) was shown to be a reversible process suggesting constituents involved in tethering the inner wall to the underlying JCT may play an integral role in regulating outflow resistance. It is unknown if washout is caused by JCT/inner wall separation or if some other mechanism is involved in decreasing outflow resistance in non-human eyes. Also unknown, is if trabecular drainage pathways are altered secondarily by the washout effect. This project proceeds with the following specific aims:

Specific Aim #1: *Determine structural differences that distinguish eyes that do and do not exhibit the washout effect.*

Specific Aim #2: *Review previous filtration studies and conclusions therein to develop a better method for tracing patterns of aqueous humor outflow in enucleated bovine eyes.*

Specific Aim #3: *Investigate the relationship between outflow facility and patterns of aqueous humor drainage in enucleated bovine eyes.*

1.3.1: Specific Aim #1

Overby et al. (2002) recently documented that, in bovine eyes, the structural correlate to the facility increase during washout is separation of the inner wall of the aqueous plexus from the underlying JCT. Molecular constituents involved in tethering the inner wall to the underlying JCT may give way to a pressure-associated force across the inner wall of the bovine aqueous plexus causing separation of the inner wall from the underlying JCT. Separation of the inner wall from the JCT may decrease outflow resistance by increasing the effective area for aqueous humor to filter into the aqueous plexus.

Overby et al. (2002) suggested that washout occurs in the bovine eye as a mechanism to regulate IOP. Studies (Johnstone and Grant, 1973; Grierson and Lee, 1974) have previously documented that elevated IOP places mechanical stress upon the connecting fibrils between the inner wall and JCT causing protrusion of the inner wall from the underlying JCT region. Thus, the molecular constituents and connecting fibrils

that tether the inner wall and underlying JCT may be involved in regulating outflow resistance.

Interestingly, in human eyes, washout does not occur (Erickson-Lamy et al., 1990). The human eye, when compared with eyes of all other species, has a more developed elastic-like cribriform plexus extending from the tendons of the ciliary muscle to the endothelial cells of the inner wall of Schlemm's canal (Rohen et al., 1981). This elastic-like network may provide structural support that resists JCT/inner wall separation as well as contribute to the regulation of steady outflow resistance in human eyes (Erickson-Lamy et al., 1990). ***We hypothesize that if the structural correlate for washout in bovine eyes is separation between the inner wall and JCT then similar morphological changes should not be found in human eyes subjected to prolonged intraocular perfusion.***

In Chapter 2B, we investigate our hypothesis by performing a morphological evaluation in both bovine (with washout) and human eyes (without washout) after both short and long-duration intraocular perfusion.

1.3.2: Specific Aim #2

Previous tracer studies have provided insight into the filtration characteristics and mechanisms of the human conventinonal aqueous outflow pathway. Filtration studies were pursued because it was indicated that the characteristic flow dimensions responsible for generating outflow resistance would not be determinable from morphological studies alone (McEwen, 1958; Bill and Svedbergh, 1972; Johnson et al., 1983; Ethier, Kamm, Palaszewski Johnson, and Richardson, 1986; Johnson et al., 1990). This indeterminacy persists due to the limitations of standard techniques that are not sensitive enough nor

well suited for examining small changes in cellular ultrastruture (i.e., extracellular matrix of the JCT). For example, preparing tissue samples for electron microscopy causes degradation of GAGs that may or may not occupy the open spaces observed in the JCT. Therefore, extrapolating outflow resistance based on the structural dimensions and parameters within this region would be highly speculative without substantial proof that GAGs occupy the open spaces. If these open spaces within the JCT are not filled with GAGs or an extracellular matrix-like material, then the predicted JCT outflow resistance is two orders of magnitude lower, as predicted by mathematical models, than the resistance needed to satisfy physiological conditions within the eye. Therefore, without visualizing GAGs in their preserved state in the JCT, a complete analysis of the hydrodynamics involved in generating outflow resistance can not be determined from morphological studies of the JCT. In addition, Johnson et al. (1990) extended the previous assertion and concluded that filtration studies would provide little information regarding the dimensions of flow limiting passages in the aqueous outflow system. We, however, disagree with the previous assertion that little information can be gained from filtration studies to understand the hydrodynamics of the aqueous outflow pathway. Our technique that we have developed examines fluid dynamics at a more macroscopic level (10-100 microns), whereas most of the previous filtration studies investigated outflow hydrodynamics at a microscopic level (0.1-10 microns) with emphasis on the heterogeneity of pores and pore funneling in the JCT/inner wall region. In other words, our study considers the macroscopic pathway of aqueous humor outflow and how these macroscopic passageways may regulate outflow facility in bovine eyes.

In Chapter 3A, we review pertinent methods, materials, results and conclusions

from previous tracer studies that helped us to design the protocol of our preliminary study in Chapter 3B.

1.3.3: Specific Aim #3

In Chapter 3B, we investigate the relationship between the change in outflow facility observed with washout and changes in patterns of aqueous humor drainage in bovine eyes. We attempt to determine if changes in aqueous outflow drainage patterns correlate with changes in outflow facility. ***We hypothesize that post-washout drainage patterns will demonstrate a more uniform pattern along the inner wall of the aqueous plexus due to a decrease in tethering between the inner wall and JCT that increases the effective area for aqueous humor filtration along the inner wall, while pre-washout outflow patterns will show a more punctate tracer pattern due to the lack of inner wall/JCT separation.*** Investigating patterns of aqueous humor outflow before and after washout in bovine eyes may provide possible clues into the mechanisms regulating outflow resistance and IOP in the bovine eye.

CHAPTER 2A: A BRIEF HISTORY OF THE WASHOUT EFFECT

All non-human mammalian eyes studied to date (Barany, 1962,1964; Epstein et al., 1982; Erickson and Kaufman, 1981; Erickson-Lamy et al., 1988; Gaasterland et al, 1978; Fourman and Fourman, 1989; Gaasterland et al., 1979; Hashimoto and Epstein, 1980; Kaufman et al., 1988; Overby et al., 2002; Rao et al., 2001; Ruben et al., 1985; Van Buskirk and Brett, 1978; Yan et al., 1991), demonstrate an increase in aqueous humor outflow facility when undergoing prolonged intraocular perfusion. This phenomenon, known as "washout", does not occur in the human eye (Erickson-Lamy et al., 1990), which instead exhibits a steady state of outflow resistance. It is not known why washout does not occur in the human eye. It is especially interesting that even non-human primate eyes exhibit washout (Epstein et al., 1982; Erickson and Kaufman, 1981; Gaasterland et al. 1978, Gaasterland et al., 1979; Kaufman et al., 1988; Peterson and Jocson, 1974). Washout has been observed in both living and postmortem eyes, as well as young eyes (Erickson and Kaufman, 1981).

Washout in non-human eyes is a well-known if not well-explained phenomenon originally thought to be time-dependent (Erickson et al., 1981; Kaufman et al., 1988), but a more recent study has documented that the effect is actually perfusion volume-dependent (Johnson, et al., 1991).

Several hypotheses have been put forward to explain the mechanisms governing washout. Originally, washout was believed to be a "washing out" or erosion of GAGs, particularly hyaluronic acid, from the extracellular matrix in the trabecular outflow pathway (Bárány and Scotchbrook, 1954; Bárány, 1955). However, studies have reported, using biochemical analyses of rabbit trabecular meshwork, no significant

change occurs in GAG composition upon exposure to GAG-degrading enzymes that would otherwise alter outflow dynamics (Knepper, Farbman, and Tesler, 1984). Most importantly, neither a decrease in IOP nor an increase in outflow facility was found with either single or multiple intracameral injection of GAG- degrading enzymes, hyaluronidase or chondroitinase, in living cynomolgus monkey eyes (Hubbard, et al., 1997).

Another hypothesis was that "washout" occurs due to a dilution of plasma-derived protein originating from an anterior segment protein depot located at the root of the iris where it is supplied by the ciliary body (Bartels, Lawrence, and Kolodny, 1992; Freddo, et al., 1990; Johnson, et al., 1993). It was proposed that a decrease in protein diffusion from this depot causes the dilution of plasma-derived proteins leading to less protein accumulation and entanglement within the extracellular matrix, resulting in decreased outflow resistance (Bartels et al., 1992; Epstein, Hashimoto, and Grant, 1978; Laurent and Pietruszkiewicz, 1961). Later, studies of aqueous humor composition in the bovine eye revealed that decreases in outflow facility are not due to general levels of dominant serum proteins, i.e. albumin and γ-globulin, but may be attributed to interactions between particular serum proteins contributing to the resistance (Sit, et al., 1997).

A more recent hypothesis accounting for the possible mechanism of washout is elimination of the so-called funneling effect as previously discussed in Section *1.2.3*.

Overby et al. (2002) recently document that, in bovine eyes, the structural correlate to the facility increase during washout is a detachment of the JCT from the inner wall of the aqueous plexus - bovine equivalent of Schlemm's canal (Tripathi, 1971). This result suggests that hydrodynamic coupling between the inner wall of the aqueous plexus

and JCT plays an important role in the maintenance of outflow resistance. Elimination of the funneling effect was suspected to have decreased outflow resistance; however, colloidal gold perfused in this experiment was difficult to locate along the inner wall and prevented an adequate investigation of the pore-funneling hypothesis. Overby et al. (2002) was unable to determine the cause of the sparse colloidal gold labeling underneath the inner wall, but it is possible that altered binding characteristics, altered outflow patterns, or other phenomenon were involved.

It has been previously documented (Johnstone and Grant, 1973; Grierson and Lee, 1974) that elevated IOP induces a pressure difference across the inner wall of Schlemm's canal by placing mechanical stress upon the connecting fibrils between the inner wall and JCT causing protrusion of the inner wall from the underlying JCT region. The ability of the inner wall to separate from the JCT in non-human eyes thus suggests that this distention may occur as an autoregulatory response to elevated IOP.

In Chapter 2B, we attempt to describe the role washout may play in governing aqueous humor outflow resistance and what morphological correlates may distinguish eyes that do and do not exhibit a washout effect.

CHAPTER 2B: COMPARATIVE STUDIES BETWEEN SPECIES THAT DO AND DO NOT EXHIBIT A WASHOUT EFFECT

2B.1 ABSTRACT

Ocular perfusion studies from all non-human species performed to date consistently demonstrate a perfusion-volume-dependent increase in aqueous outflow facility, known as the "washout" effect. However, this "washout" effect does not occur in human eyes. We have recently documented that, in bovine eyes, the washout associated increase in facility correlates with the extent of physical separation between the juxtacanalicular connective tissue and the inner wall endothelium lining the aqueous plexus (the bovine equivalent of Schlemm's canal). We hypothesize that if washout truly correlates with inner wall/JCT separation then this separation should not occur in human eyes that do not exhibit the washout effect, even after prolonged perfusion. Eight enucleated human and eight bovine eyes were used in this study. Aqueous outflow facility was measured at 15 mmHg for long-duration (3 h) or short-duration (30 min to 1 h) perfusion (n = 4 for each group). All eyes were perfusion-fixed at 15 mmHg, and examined morphologically with both light and electron microscopy. In bovine eyes, outflow facility increased 81% (p = 0.049) from 1.06 ± 0.06 μl/min per mmHg (mean ± SEM) at baseline to 1.92 ± 0.30 μl/min per mmHg after 3 h due to washout. The pre-fixation outflow facility in long-duration eyes (1.92 ± 0.30 μl/min per mmHg) was 2-fold greater than pre-fixation facility in short-duration eyes (0.92 ± 0.11 μl/min per mmHg; p = 0.0387). In human eyes, washout was not observed; baseline outflow facility was similar between both groups (0.18 ± 0.02 vs 0.25 ± 0.08 μl/min per mmHg; p = 0.518); however, pre-fixation outflow facility in long-duration eyes showed a 40% *decrease* compared to baseline outflow

facility in those same eyes ($p = 0.017$, paired Student's *t*-test). In bovine eyes, significant expansion and rarefaction of the JCT and inner wall/JCT separation was much more prevalent in long-duration eyes, and data from all bovine eyes revealed a correlation between the extent of inner wall/JCT separation and the absolute value of outflow facility measured immediately prior to fixation ($p = 0.0024$) as well as the washout-induced increase in outflow facility ($p = 0.0006$). In human eyes, no significant morphologic differences were observed between long- and short-duration perfusion, with no observed change in inner wall/JCT separation or expansion between the two groups. Morphologica analysis revealed that the previously described "cribriform plexus" of elastic like fibers was more extensive in the JCT of human eyes, appearing to form numerous connections to the inner wall endothelium. The cribriform plexus appears to function as a mechanical tether that maintains inner wall/JCT connectivity in human eyes by opposing hydrodynamic forces generated during perfusion, potentially explaining the lack of washout in humans.

2B.2 INTRODUCTION

Primary open-angle glaucoma (POAG) is a potentially blinding disease, occurring in 1/100 individuals over 40 years of age (Kwon and Caprioli, 2005) and affecting 60-70 million people worldwide (Quigley, 1996). The human eye appears to be particularly vulnerable to POAG when compared to eyes of non-human species (Gelatt, 1977). The reason for this increased susceptibility remains unknown. An interesting corollary of this distinction is that all non-human mammalian eyes studied to date (Barany, 1962,1964; Epstein et al., 1982; Erickson and Kaufmann, 1981; Erickson-Lamy et al., 1988; Fourman and Fourman, 1989; Gaasterland et al., 1978; Gaasterland et al., 1979; Hashimoto and Epstein, 1980; Kaufman et al., 1988; Overby et al., 2002; Rao et al., 2001; Ruben et al., 1985; Van Buskirk and Brett, 1978; Yan et al., 1991), demonstrate a "washout effect."

The "washout effect" is a phenomenon in which perfusion of an eye at physiological pressure results in a volume-dependent increase in the measured facility of aqueous humor outflow. Washout was originally believed to result from a "washing out" of extracellular glycosaminoglyans (Barany and Scotchbrook, 1954; Barany, 1955) or proteoglycans (Ethier et al., 1986; Jackson and James, 1982; Levick, 1987) from the outflow pathway, but biochemical studies have failed to detect an appreciable change in either sulfated proteoglycans (Johnson et al., 1993) or hyaluronic acid (Knepper et al., 1984) from the outflow pathway following prolonged perfusion. While the rate of facility increase during washout can be slowed by perfusion with either serum (Kee et al., 1996) or serum proteins (Epstein et al., 1978) or by perfusion with either pooled homologous aqueous humor (Barany and Woodin, 1955) or mock aqueous humor with similar

biochemical constituents (Gaasterland et al., 1979), the washout effect cannot entirely be eliminated (Barany and Scotchbrook, 1954; Van Buskirk and Brett, 1978).

Possibly the most intriguing aspect of the washout effect, however, is that it does not occur in the human eye (Erickson-Lamy et al., 1990). This suggests that there is some unique aspect of outflow anatomy or physiology that distinguishes human eyes from most other species, including from non-human primate eyes that exhibit washout during perfusion both in vivo (Barany, 1962, 1964; Erickson and Kaufman, 1981; Gaasterland et al., 1978, 1979; Kaufman et al., 1988) and in vitro (Epstein, 1982; Hashimoto and Epstein, 1980; Peterson et al., 1974), despite their anatomical similarity to humans. A thorough understanding of the mechanism of washout, and the reason for its absence in humans would likely provide important insight into the fundamental mechanisms that generate outflow resistance. Such understanding might also permit us to artificially induce a washout-like response in human eyes as a means of reducing intraocular pressure in glaucoma.

Two recent studies (Overby et al., 2002; Sabanay et al., 2004) have documented that washout is a reversible process in both bovine and monkey eyes. A structural correlate to the facility increase during washout in bovine appeared to be the degree of separation of the JCT from the inner wall of the aqueous plexus –the bovine equivalent to Schlemm's canal (Tripathi, 1971). This separation was proposed to increase outflow facility by disrupting a hydrodynamic interaction between the inner wall and JCT known as "funneling" (Johnson et al., 1992). The funneling theory states that the patterns of outflow through the JCT are confined to those regions nearest the pores in the inner wall, and this flow confinement reduces the filtration area through the JCT, thereby increasing

its effective hydrodynamic resistance. Based upon our prior work in bovine eyes, we hypothesized that washout resulted from a disruption in the connectivity between inner wall and JCT that decreased outflow resistance by eliminating the funneling effect. The washout hypotheses and funneling theory emphasize the role of cellular and extracellular matrix adhesions that maintain the connectivity between the inner wall and JCT in the face of an opposing pressure gradient and thereby influence outflow resistance by controlling the local hydrodynamic patterns of outflow.

In this study, we hypothesize that if the structural correlate for washout is separation between the inner wall and JCT in bovine eyes, then similar morphological changes should not be found in human eyes subjected to prolonged perfusion. To determine whether the absence of washout in human eyes relates to morphological differences unique to the human outflow pathway, morphological changes following prolonged perfusion were compared between bovine eyes that exhibit washout and human eyes that do not exhibit washout. A corollary of our hypothesis is that the absence of washout in the human eye may result from an enhanced connectivity between the inner wall and JCT, which would have important consequences for the regulation of outflow resistance in this species.

2B.3 MATERIALS AND METHODS

Four pairs of enucleated bovine eyes were obtained from a local abattoir (Arena and Sons, Hopkinton, MA) and delivered on ice within 6 hours post-mortem. Eyes with discernible damage or accumulated blood in the angle of the anterior chamber were not used. Eight human eye bank eyes from donors with no known history of eye disease

(ranging from 33 to 89 years of age) were obtained from National Disease Research Interchange (Philadelphia, PA) within 24 hours of death. Each eye was confirmed to be grossly normal by examination under a dissecting microscope. Donor eyes were used in accordance with the tenets of the Declaration of Helsinki.

2B.3.1: Outflow Perfusion Apparatus

A constant-pressure ocular perfusion system/apparatus (University of Wisconsin Medical Electronics Lab, Madison, Wisconsin) was used in all perfusions. (See Figure 2.1)

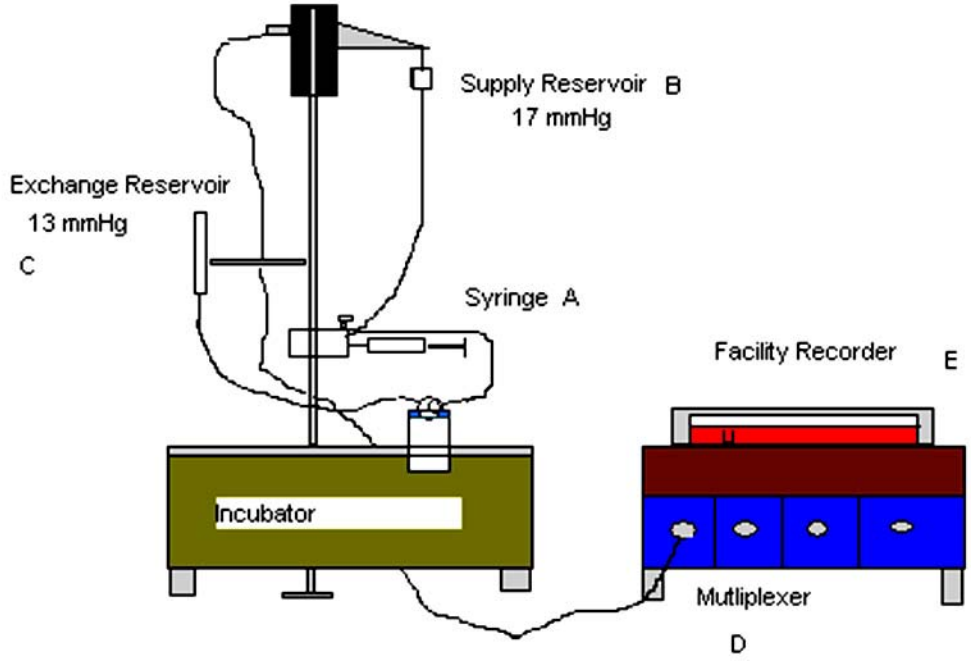


Figure 2.1 Outflow Perfusion Apparatus: This specific representation exhibits positioning of the supply reservoir and waste reservoir to maintain constant pressure of 15 mmHg during anterior chamber exchange. Fluid perfused is injected from the syringe pump (A), it then passes through the 3-way stopcock valve to accumulate in the supply reservoir (B), the 3-way stopcock is then turned to allow for fluid to descend down the tubing into the eye. The exchange reservoir collects the anterior chamber content during anterior chamber exchange. Changes in the supply reservoir volume are converted into electrical signals at the multiplexer (D) and then recorded on a computerized strip chart (E) to determine outflow facility values. Drawing by Patrick Scott and built by University of Wisconsin Medical Electronics Lab, Madison, Wisconsin.

2B.3.2: Outflow Perfusion Procedure

Dulbecco's phosphate-buffered saline (PBS; Life Technologies, Grand Island, NY) containing 5.5 mM D-glucose (collectively referred to as DPBS) was used as mock aqueous humor in all perfusions. Each eye to be perfused was placed in a beaker with the cornea facing upward and submerged with saline just above the limbus. A fluid supply reservoir was positioned above the limbus at a height equal to 15 mmHg, which was chosen based on previous studies (Barany and Woodin, 1955; Erickson-Lamy et al., 1988; 1990) to have shown significant washout in bovine eyes perfused at a constant-pressure of 15 mmHg. A perfusion needle (23-guage for bovine, 25-gauge for human) was then inserted intracamerally through the cornea. The tip of the needle was placed into the posterior chamber of the eye to prevent anterior chamber deepening that would otherwise lead to an artificial increase in outflow facility (Francois, Rabaey, and Neetens, 1955; Ellingsen and Grant, 1971). Anterior chamber fluid exchange was achieved using a second needle attached to tubing leading to an exchange receptacle. During the perfusion the exchange receptacle line was clamped.

During anterior chamber fluid exchange the supply reservoir was positioned at a height 2 cm H_2O (17 mmHg) above 15 mmHg and the exchange receptacle at a height 2 cm H_2O (13 mmHg) below. This protocol ensured that the average pressure within the eye was never >2 cm H_2O away from 15 mmHg. Approximately 2 ml of fluid had to be exchanged to flush the anterior chamber and fluid lines. After the exchange, receptacle tubing was clamped and perfusion-fixed (30 minutes for bovine eyes and 1 hour for human eyes). During the perfusion, a piece of cotton soaked in DPBS was placed on any exposed cornea to keep it moist.

2B.3.2a: Human Short-Duration Anterior Chamber Perfusion Procedure

1 hour was allowed for stabilization of outflow facility to achieve a baseline measurement. The outflow facility was measured for an hour after baseline in 4 human eyes. Eyes were then perfusion-fixed with universal fixative (2% paraformaldehyde and 2.5% glutaraldehye in PBS; pH 7.3) under the same pressure for 1 hour.

2B.3.2b:Human Long-Duration Anterior Chamber Perfusion Procedure

Same protocol as *human short-duration*; however, outflow facility was recorded for 4 hours and then perfusion-fixed for 1 hour using the same fixative.

2B.3.2c: Bovine Short-Duration Anterior Chamber Perfusion Procedure

Four eyes were allowed to stabilize for 20-30 minutes after which outflow facility was measured for 30 minutes. Eyes then underwent perfusion-fixation for 30 minutes.

2B.3.2d: Bovine Long-Duration Anterior Chamber Perfusion Procedure

Same protocol as *bovine short-duration*; however, 4 eyes were perfused for 3 hours and then perfusion-fixed for 30 minutes as well.

The human and bovine long-duration eyes were perfused for different durations (4 and 3 hours, respectively) to allow ample time for washout to occur. We were uncertain if washout would occur in the human eye after three hours of perfusion, therefore we continued perfusing human eyes for one additional hour.

All studies adhered to the ARVO Statement for the Use of Animals in Ophthalmic and Vision Research.

2B.3.3: Morphological Evaluation

Sections from 4 quadrants of each eye were prepared for examination by light and transmission electron microscopy.

2B.3.3a: Light Microscopy

Anterior segments of the eyes were divided into 4 quadrants (designated Superior, Inferior, Nasal, and Temporal) and cut into meridional sections (1-2 mm) that were post-fixed in 2% osmium tetroxide and 1.5% potassium ferrocyanide in dH_2O for 2 hours. The samples were then dehydrated in a graded series of ethanols and embedded in Epon-Araldite. Semithin radial sections (3 µm) were then cut and stained with 0.1% Toluidine Blue to identify the outflow region and to localize the inner wall. Micrographs were taken at a magnification of 747x and analyzed for the degree of separation of the JCT from the inner wall.

2B.3.3b: Assessing Inner wall/JCT Separation

A trained masked observer (HG) was presented with micrographs of the inner wall and JCT from both human and bovine eyes and was instructed to identify regions along the inner wall that exhibited separation from the underlying matrix (Figure 2.2). Micrographs were measured by hand, using a display monitor. The total length and the length exhibiting inner wall and JCT separation were measured to the nearest millimeter in >8 micrographs/eye. When examining inner wall/JCT separation, the degree of separation observed was assessed based on a scale of 0 (no separation), + (approximately less than 1/3 of total length of the inner wall), ++ (approximately more than 1/3 but less than 2/3 of the total length of inner wall), and +++ (approximately more than 2/3 of the total length of the inner wall). This grading system is analogous to the one previously

previously used by Overby et al. (2002) for electron micrscopy, but evaluating as we do here allows for a much larger field of view to appreciate morphologic changes over tissue-level dimensions that may be more relevant for influencing outflow resitance. We did not quantify other dimensions of JCT/inner wall separation because any increase in separation length hypothetically coincides with increased outflow facility and therefore other dimensions assume a secondary importance. Figure 2.2 shows an example micrograph for each score. Two types of separation have previously been described to occur between the inner wall and JCT (Overby et al., 2002): (i) separation between the extracellular matrix of the JCT and the basal lamina of the inner wall (matrix-matrix separation) and (ii) separation between the basal lamina of the inner wall and the endothelial cells lining the aqueous plexus (cell-matrix separation) (Fig 2.3). At the level of magnification used for light microscopy (40x), the basal lamina underlying the inner wall could not clearly be identified. Therefore, to more closely examine the inner wall/JCT separation and to distinguish between cell-matrix and matrix-matrix separation, electron micrographs of the inner wall and JCT (3300x) were examined from all 4 quadrants and were compared to determine whether morphological differences were evident between bovine and human eyes and between eyes following short and long-duration perfusions.

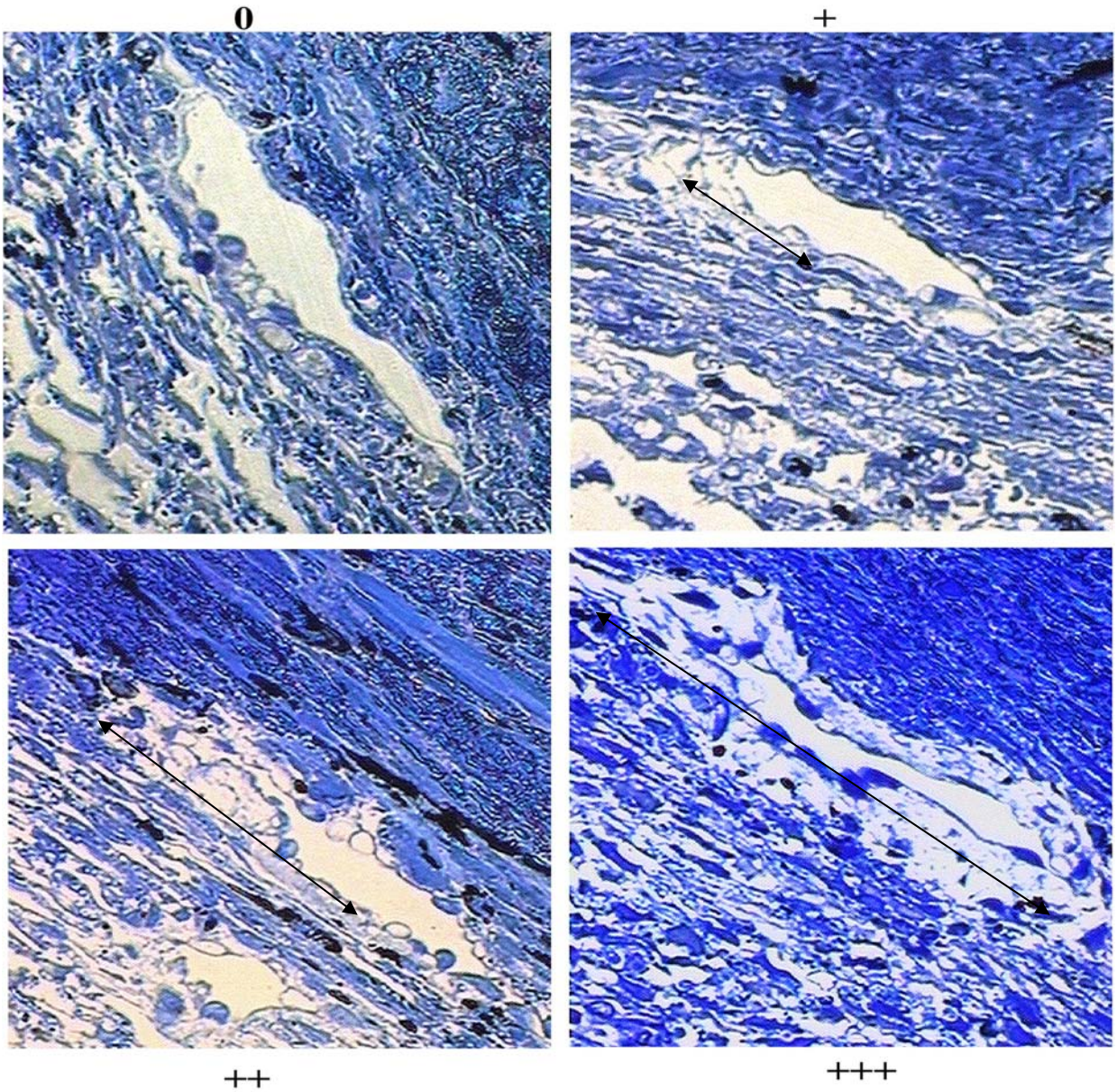


Figure 2.2 *Morphological assessment of separation between the inner wall/JCT in the bovine eye.* The degree of inner wall/JCT separation observed in each section was assessed based on a scale of 0 (no separation), + (~less than 1/3 of total length of the inner wall), ++ (~more than 1/3 but less than 2/3 of the total length of inner wall), and +++ (~more than 2/3 of the total length of the inner wall). The length of the double-headed arrows corresponded to the estimated length of inner wall/JCT separation in each case. (Magnification 747X)

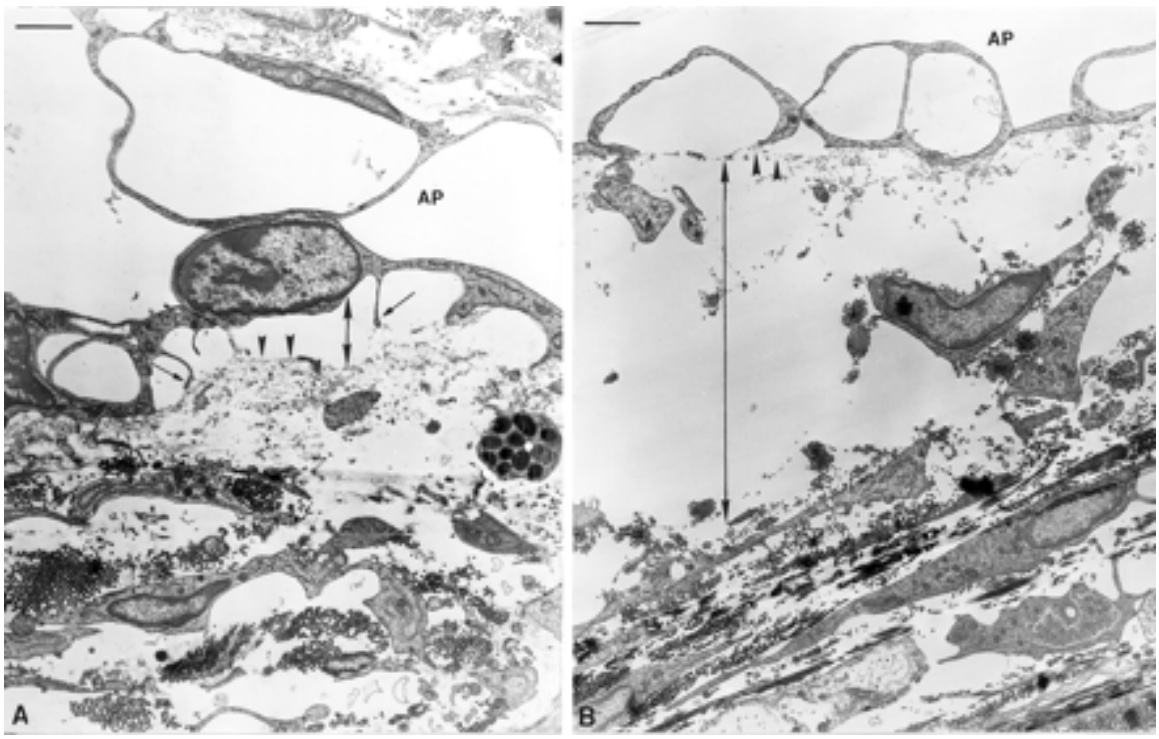


Figure 2.3 *Electron Microscopy Images of Cell-Matrix vs Matrix-Matrix Separation in the Bovine Eye* (**A**) Cell–matrix separation (*double-headed arrow*) occurred between the endothelial cell and basal lamina (*arrowheads*) along the inner wall of the aqueous plexus (AP). In this image, two inner wall cells were displaced into the lumen, but retained contact with the basal lamina through multiple cellular processes (*arrows*). The extracellular matrix within the JCT remained well organized beneath the site of cell–matrix separation. A giant vacuole was seen extending from the outer wall. (**B**) Matrix–matrix separation (*double-headed arrow*) occurred between the basal lamina (*arrowheads*) of the inner wall and the underlying JCT matrix. The basal lamina remained attached to the inner wall cell, and together they were displaced from the JCT. Bars, 2 µm. (Photo and description from Overby et al. 2002 in *Investigative Ophthalmology and Visual Science*. 2002;43:3455-3464.)

2B.3.3c: Transmission Electron Microscopy

Ultra-thin sections (90 nm) from each of the four quadrants of each eye, were cut with an ultramicrotome, counterstained with uranyl acetate and lead citrate, and examined with an electron microscope (Model 300: Philips, Eindhoven, The Netherlands). Micrographs from the four quadrants of both human and bovine eyes, taken along the inner wall of Schlemm's canal (or AP) at an original magnification of 3300X, were compared to determine if differences were evident between bovine and human, and between eyes from short and long perfusions. Representative micrographs were also examined to determine how change seen at the light microscopic levels responded to the electron microscopy grading system of Overby et al (2002).

2B.3.4: Statistical Methods

Two-tailed Student's t-test and linear regression analysis were applied (Systat for the Macintosh, ver. 5.2.1; Chicago, IL) with a required significance level of 0.05. For the regressions, the residuals (the difference between the fitted value of the dependent parameter and its measured value) were examined and in all cases appeared random when plotted against the independent variables.

2B.4 RESULTS

2B.4.1: Outflow Facility

A summary of outflow facility data from all human and bovine eyes is presented in Table 2.1. The average baseline facility for the short and long-duration perfused bovine eyes began at 0.97 ± 0.06 (mean±SEM) μL/min/mmHg, which was significantly higher than the average human baseline facility 0.21 ± 0.04 (mean±SEM) μL/min/mmHg.

Outflow Facility (μL/min/mmHg)							
Bovine				***Human***			
C_0:Baseline		**C_1:Pre-Fixation**		**C_0:Baseline**		**C_1:Pre-Fixation**	
Short	*Long*	*Short*	*Long*	*Short*	*Long*	*Short*	*Long*
1.09	1.18	0.79	1.77	0.23	0.47	0.24	0.41
0.82	1.16	1.22	2.72	0.21	0.27	0.16	0.19
0.72	0.94	0.76	1.92	0.13	0.09	0.12	0.05
0.95	0.96	0.90	1.28	0.16	0.15	0.15	0.04
Mean							
0.89	1.06	0.92	1.92	0.18	0.25	0.17	0.17
SD.							
0.16	0.13	0.21	0.60	0.05	0.17	0.05	0.17
SE							
0.08	0.06	0.11	0.30	0.02	0.08	0.03	0.09
p-value 0.158		0.037		0.518		0.959	

Table 2.1 *Outflow Facility for Short and Long-Duration Perfusions at 15mmHg in Human and Bovine Eyes* Bovine eyes undergoing long-duration perfusion show an increase of 81% (p=0.049), whereas, bovine short-duration, human short and long-duration perfusions show no significant change in outflow facility.

In bovine eyes, long-duration perfusion led to washout with an increase in outflow facility of 80.52% ($p<0.043$) above baseline facility after three hours. In contrast, human eyes did not exhibit an increase in outflow facility after long-duration (four hours) perfusion ($p>0.085$). Both the human and bovine short-duration perfusions failed to exhibit an increase in aqueous outflow from their respective baselines. The percent change in outflow facility during DPBS perfusion in the human and bovine eyes is shown in Figure 2.4.

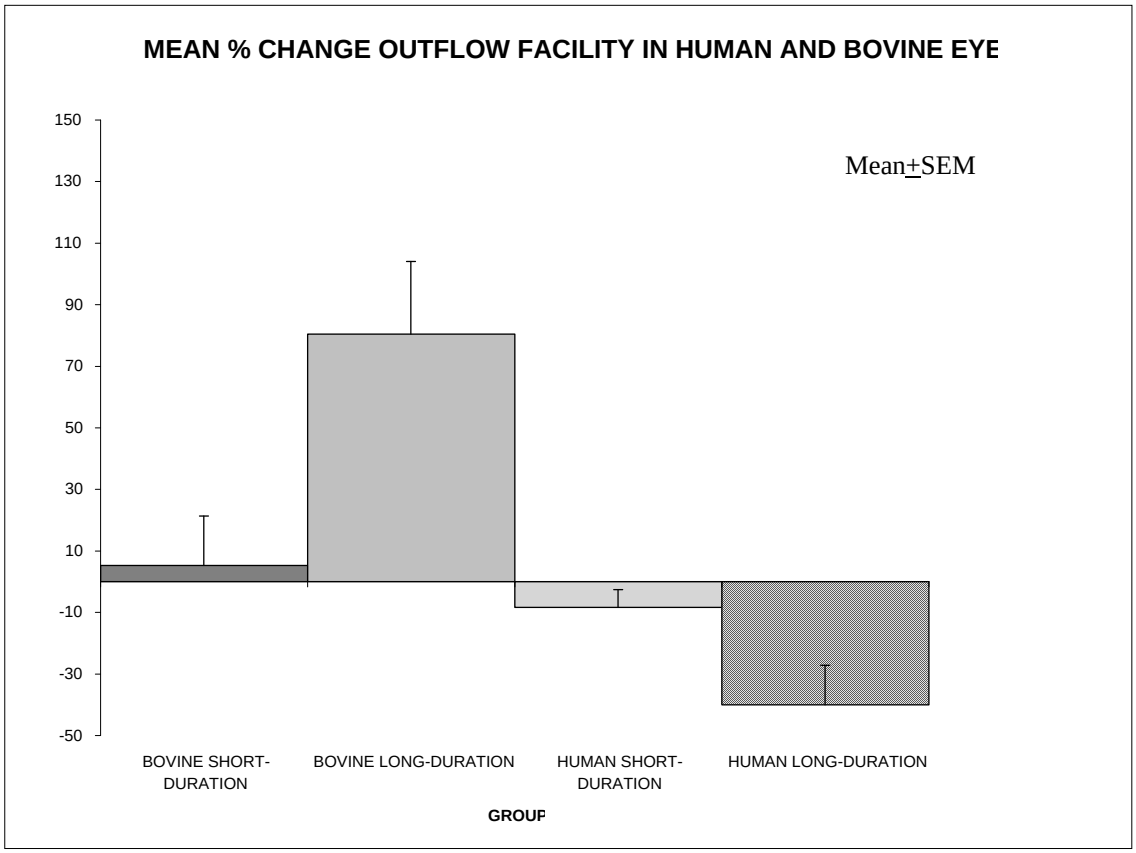


Figure 2.4 *Outflow Facility for Short and Long-Duration Perfusions at 15mmHg in Human and Bovine Eyes* Bovine eyes undergoing long-duration perfusion show an increase of 81% (p=0.049), whereas, no similar increase occurred in human short and long-duration perfusions (p=0.085).

2B.4.2: Morphological Evaluation

2B.4.2a: Light Microscopy

In bovine eyes, significant morphological differences were seen in the inner wall and JCT region between the short-duration (Figure 2.5.A.) and long-duration perfusion (Figure 2.5.B.). Significant separation of the inner wall from underlying JCT after long-duration perfusion was observed in bovine eyes. Bovine long-duration perfusions had an average inner wall/JCT separation score of 1.31$\pm$0.19 (mean$\pm$SEM) after three hours of perfusion from baseline. Very little separation of the inner wall from the underlying JCT was observed in the eyes with short-duration perfusion. Bovine short-duration perfusions had an average inner wall/JCT separation score of 0.65$\pm$0.08 (mean$\pm$SEM) after 30 minutes of perfusion from baseline. Morphologic examination based on our grading analysis (Figure 2.2) revealed significant separation of the inner wall from the underlying JCT after long-duration perfusion (Table 2.2) that correlated ($p<0.0006$) with the washout induced increase in outflow facility (Figure 2.6). Very little distention or separation of the inner wall from the underlying JCT was observed in the eyes with short-term perfusion.

An interesting aside, although not a focus of this study, we observed giant vacuoles along the inner wall of the aqueous plexus in both short and long-duration perfusion eyes; however, in long-duration eyes giant vacuoles were sparse in areas of the inner wall that had separated from the underlying JCT, whereas in short-duration eyes it appears that there was less inner wall/JCT separation but more giant vacuoles along the inner wall. A quantitative analysis of vacuole distribution was not performed in this study; however, this observation warrants further study and is currently underway in our laboratory.

In human eyes, morphologic examination failed to reveal any identifiable separation of the JCT from the inner wall of Schlemm's canal after both short (Figure 2.7.A.) and long-duration perfusion (Figure 2.7.B.). The structural integrity of the cribriform meshwork immediately beneath the inner wall was maintained and uncompromised. Schlemm's canal demonstrated an open lumen along the entire length of the inner wall. In human eyes, giant vacuoles were observed spatially homogenous along the inner wall of Schlemm's canal with a similar distribution between short and long-duration perfusions.

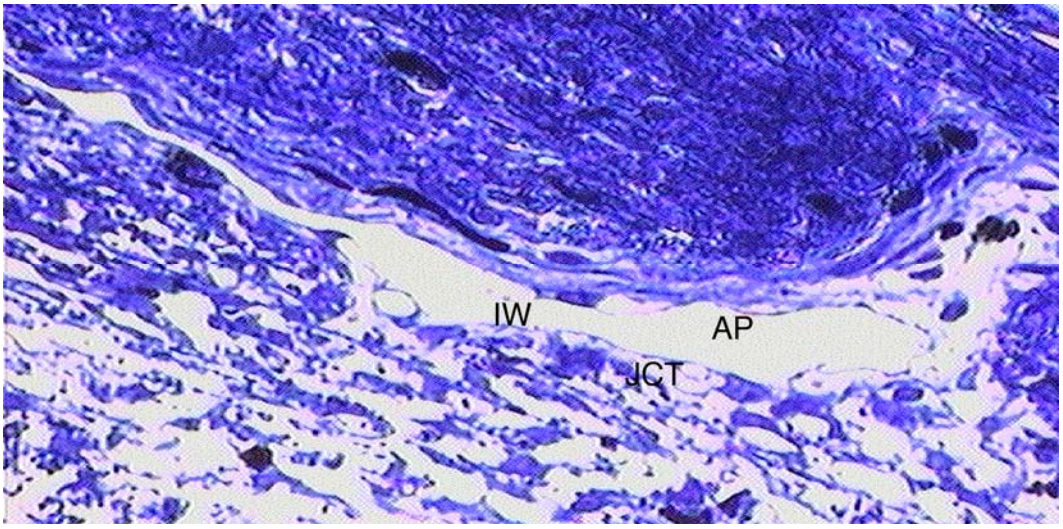


Figure 2.5.A *Light Micrograph of Bovine Aqueous Plexus after Short-Duration Perfusion.* No distention or separation between the JCT and inner wall (IW) of the bovine aqueous plexus (AP) is observed. The JCT/inner wall region appears organized and intact. (Magnification 747X)

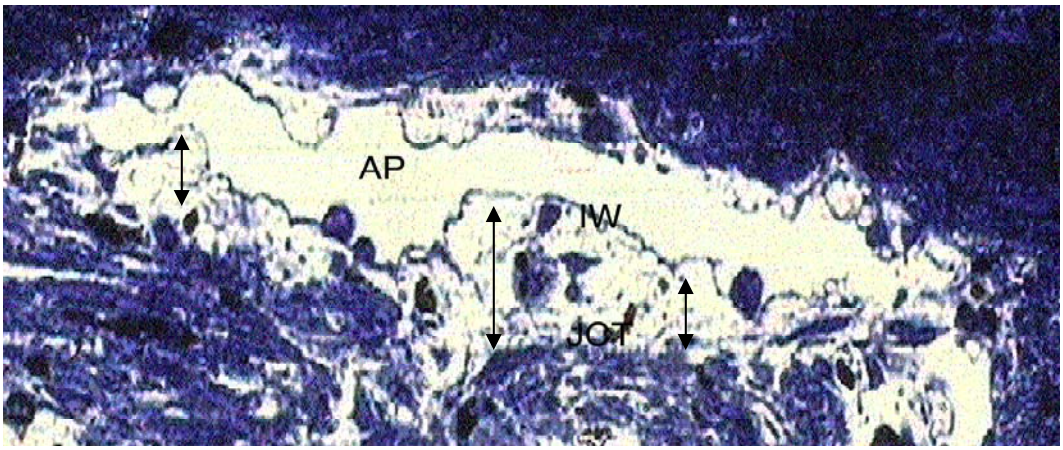


Figure 2.5.B *Light Micrograph of Bovine Aqueous Plexus after Long-Duration Perfusion.* A clear separation (double headed arrows) can be seen between the JCT and the inner wall of the aqueous plexus (AP). The inner wall distends into the lumen of the AP while the underlying tissue appears disorganized. Giant vacuoles are sparse in areas of inner wall/JCT separation. (Magnification 747X)

Inner Wall Separation Scores

	Bovine Short-Duration			**Bovine Long-Duration**	
Eye	*#Micrographs*	*Average Score*	*Eye*	*#Micrographs*	*Average Score*
3OD	10	0.80	2OD	8	1.25
6OS	13	0.77	3OS	9	1.56
7OD	7	0.57	4OS	8	1.63
8OS	8	0.47	7OS	10	0.80
Mean		0.65			1.31
SD.		0.16			0.38
SE		0.08			0.19

Table 2.2 *Inner Wall Separation Scores for Short and Long-Duration Bovine Eyes* Bovine eyes undergoing long-duration perfusion show an increase of two-fold compared to short-duration eyes.

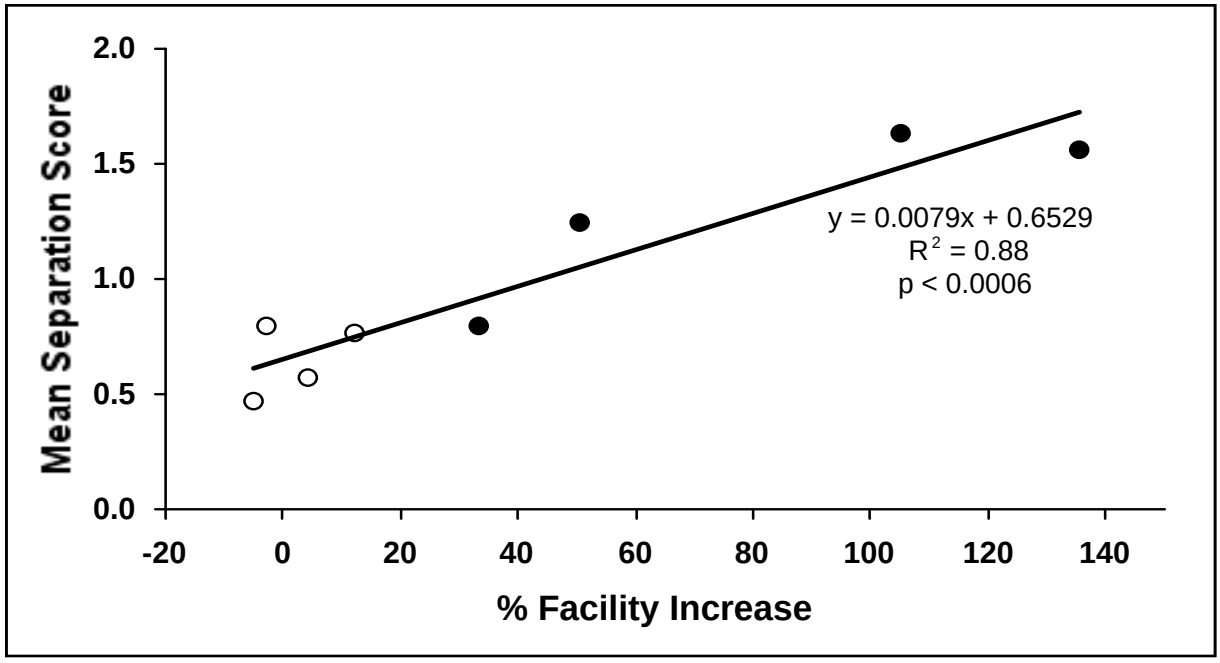


Figure 2.6 *Correlation of Outflow Facility and JCT/Inner Wall Separation Scores* Morphologic examination revealed significant distension of the underlying JCT after short (open circles) and long (filled circles) perfusion in bovine eyes that correlated with the washout induced increase in outflow facility ($p<0.0006$).

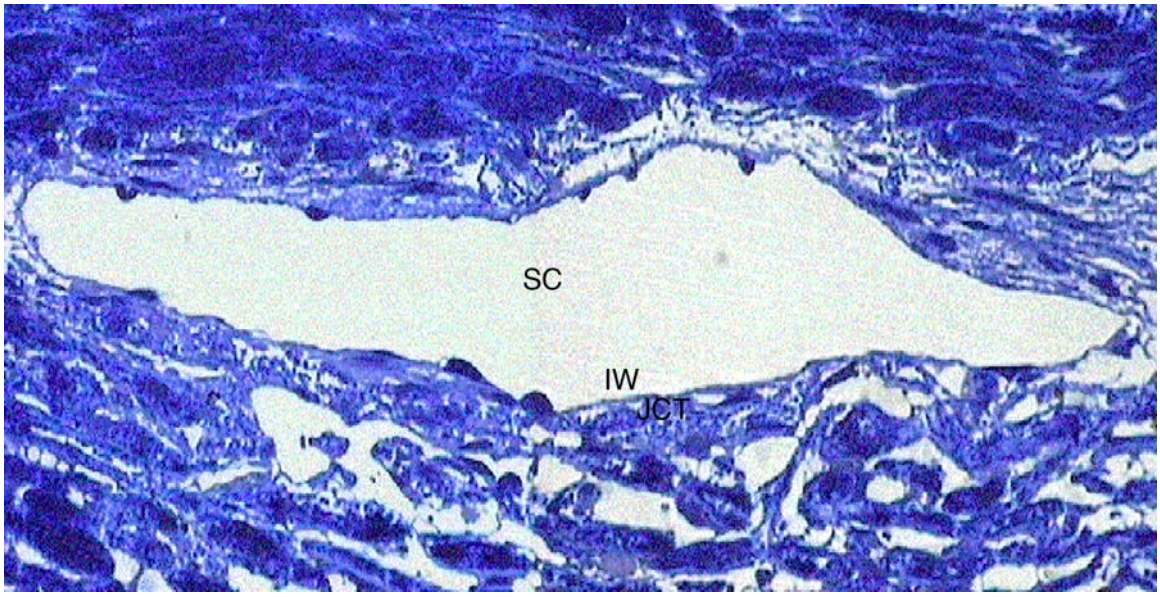


Figure 2.7.A *Light Micrograph of Human JCT/Inner Wall Region after Short-Duration Perfusion.* No distention or separation between the JCT and inner wall (IW) of Schlemm's canal (SC) is observed. The JCT/inner wall region appears organized and intact. (Magnification 747X)

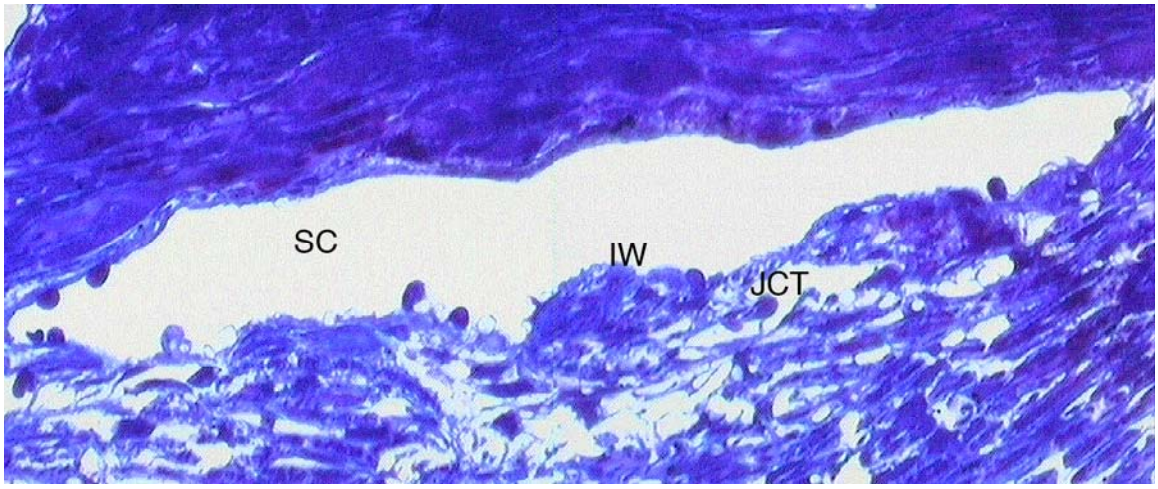


Figure 2.7.B. *Light Microscope Picture of Human JCT/Inner Wall Region after Long-Term Perfusion.* No distention or separation between the JCT and inner wall of Schlemm's canal is observed. The JCT/inner wall region appears organized and intact. (Image Magnification 747X)

Human Short-Duration			**Human Long-Duration**		
Eye	*#Micrographs*	*Average Score*	*Eye*	*#Micrographs*	*Average Score*
61894OS	41	0	31202OS	50	0
80994OS	32	0	30802OS	31	0
52402OD	44	0	22502OS	25	0
60302OS	49	0	32502OS	34	0
Mean		0			0
SD.		0			0
SE		0			0

Table 2.3 *Inner Wall Separation Scores for Short and Long-Duration Human Eyes* Human eyes undergoing long-duration perfusion show no separation.

2B.4.2b: Transmission Electron Microscopy

In bovine eyes, following short-duration perfusion, very little separation of the JCT from the inner wall was observed (Figure 2.8.A). Giant vacuoles were seen along the inner wall of the aqueous plexus. The basement membrane of the inner wall retained its characteristic discontinuity along the inner wall of the aqueous plexi. However, compared to the short-duration perfused bovine eyes, a greater amount of JCT area was separated from the inner wall in the long-duration perfused bovine eyes (Figure 2.8.B). The observed separation of the inner wall from the underlying JCT was attributed to matrix-matrix separation – characterized by a loss of adhesion and discernible separation between the basal lamina and the extra-cellular matrix of the JCT and is usually associated with a loose or "relaxed" JCT matrix (See Figure 2.3.B). The basement membrane remained tethered to the inner wall even after distention of the inner wall to the outer wall. The structural integrity of the endothelial cells appeared to be intact, as

did that of the giant vacuoles. Small amounts of elastic fiber were observed in the JCT region, very few were observed immediately underneath the basement membrane of the inner wall (Figure 2.8.A &B).

In human eyes, no significant separation of the JCT from the inner wall of Schlemm's canal was found after both short and long-duration perfused eyes (Figure 2.9.A, B respectively). Compared to bovine eyes (Figure 2.8.A, B), there was a more complex array of elastic fibers in the JCT region, especially in the area immediately underneath the basement membrane of the inner wall. Elastic fibers were commonly observed attached to the endothelial cells of Schlemm's canal at the edges of giant vacuoles (Figure 2.9.A & B).

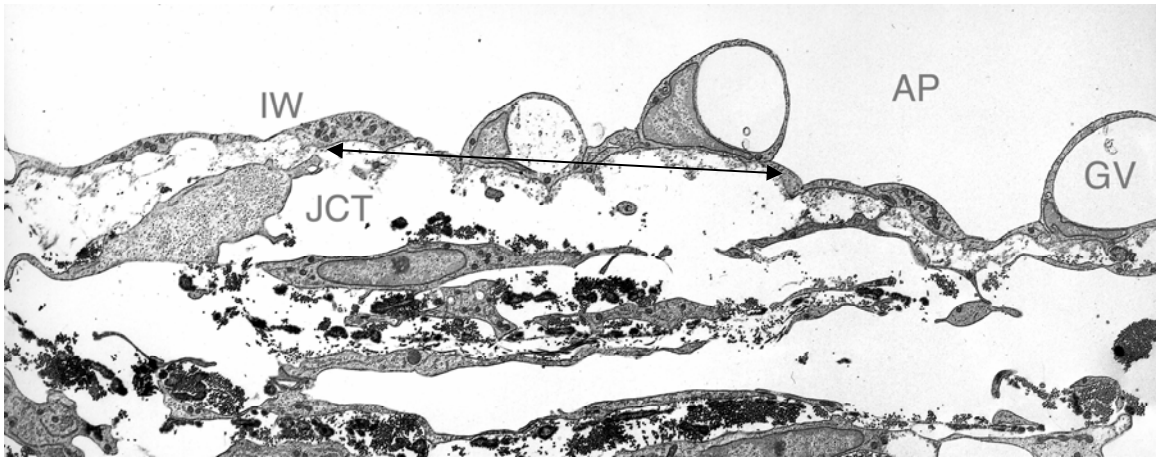


Figure 2.8.A *Transmission Electron Micrograph of Bovine Aqueous Plexus after Short-Duration Perfusion*. The distention or separation of the JCT and discontinuations in the IW lining endothelial cells of the aqueous plexus (AP) are not observed (no breaks in the inner wall are shown by double headed arrows). Giant vacuoles (GV) are seen along the inner wall. (Magnification X4690)

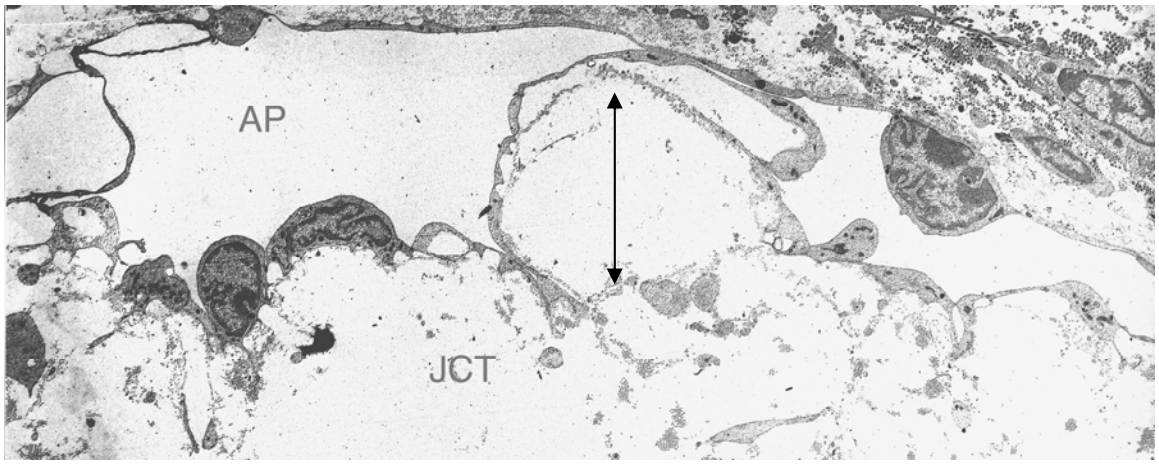


Figure 2.8.B *Transmission Electron Micrograph of Bovine Aqueous Plexus after Long-Duration Perfusion.* Significant separation (double headed arrow) between the inner wall (IW) of the bovine aqueous plexus (AP) and underlying JCT region is observed. Less giant vacuoles was seen in the region where inner wall/JCT separation occurs. (Magnification X4690)

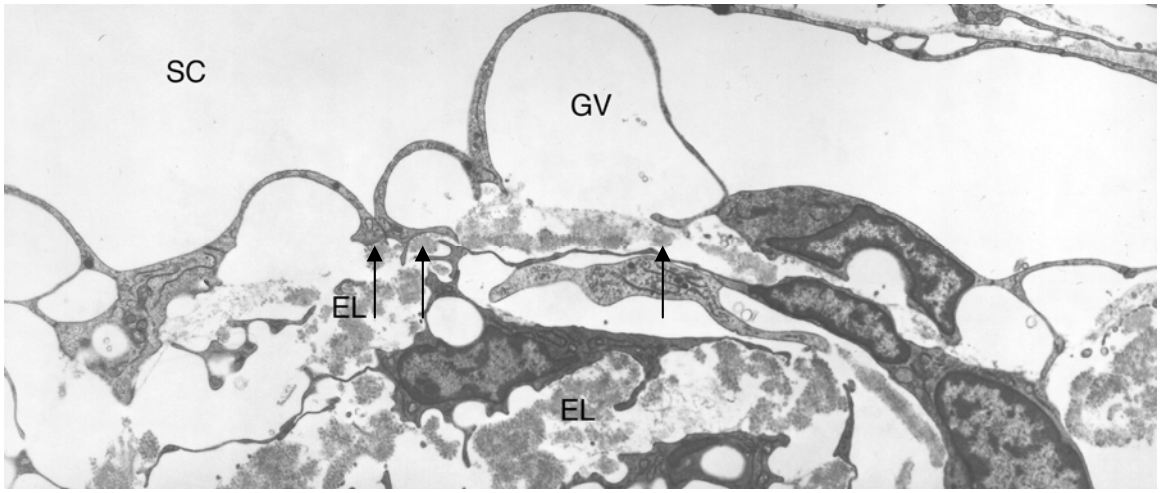


Figure 2.9.A *Transmission Electron Micrograph of Human Schlemm's Canal after Short-Duration Perfusion.*

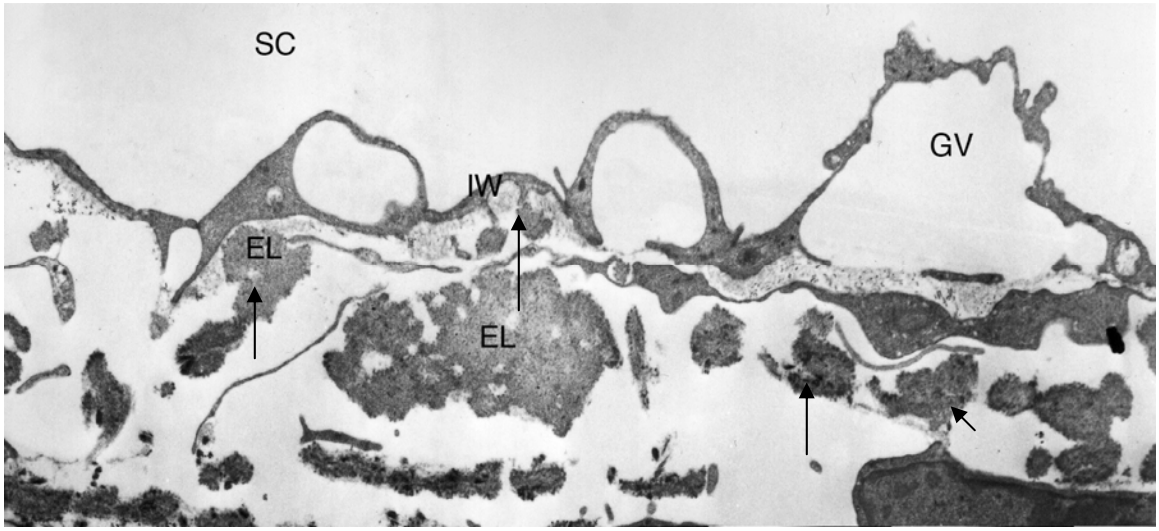


Figure 2.9.B *Transmission Electron Micrograph of Human Schelmm's Canal after Long -Duration Perfusion.*

No separation is observed between the inner wall (IW) of Schlemm's canal (SC) and the underlying JCT in both short and long-duration perfusion. Giant vacuoles are seen along the IW of SC with a similar distribution in both short and long-duration. Compared to bovine eyes (Figure 2.7A & B) there is more complex array of elastic fibers (EL) (indicated by arrows) in the JCT region, especially in the area immediately underneath the inner wall (IW). (Magnification X8910)

2B.5 DISCUSSION

In this study, we have documented that the separation of the inner wall from the JCT, a finding previously documented to correlate with the washout effect in bovine eyes, does not occur in human eyes. Our findings suggest that it is the unique morphological features in the human JCT that account for the lack of washout in human eyes.

The finding that separation between the JCT region and the inner wall of the aqueous plexus is a primary morphological correlate for the washout effect in bovine eyes was first documented by Overby et al. (2002), who did an extensive evaluation of these changes at the electron microscopic level. In those studies, long-duration perfusions were done and the eyes with washout were compared to the morphological appearance of the meshwork in eyes after the perfusion pressure was allowed to drop to zero for one hour. In these latter cases, outflow facility returned nearly to the level of resistance present at the baseline of the perfusion.

In the present study we compared the morphology of short-duration baseline perfusion with long-duration perfusion but we completed our morphological assessments at the light microscopic level in order to obtain data over a wider sampling of the meshwork. What we found was that the morphological correlates between our long duration perfusions and Overby's were very similar, both showed separation between the JCT region and the inner wall.

Of additional interest our morphological findings in pre-washout baseline eyes were remarkably similar to the morphological appearance of the eyes in Overby's studies that were allowed to return to baseline, suggesting that washout is reversible and that the pre-

washout facility and its morphology are similar to that found in an eye subjected to washout and allowed to recover.

Our facility data in human eyes is consistent with a previous study performed by Erickson-Lamy et al. (1990), whose perfusion study first documented the lack of a washout phenomenon in enucleated human eyes. Morphological examination of the perfused eyes was not performed in their study. The prior work of Overby et al. (2002) suggested that separation of the inner wall from the JCT represents the structural correlate of the washout effect. For this to a valid conclusion, mandates the converse be true as well, that is, human eyes that do not exhibit washout should also fail to exhibit separation of the inner wall from the JCT. By documenting a lack of separation between the inner wall and the JCT in perfused human eyes, the current study not only provides the morphological data not present in the original work of Erickson-Lamy et al. (1990), it also validates the conclusion of Overby et al. (2002) regarding the morphological correlate for washout.

The results of both Overby et al. (2002) and our present study strongly suggest that the connecting fibrils and molecular constituents responsible for tethering the inner wall basal lamina to the JCT are important regulators of aqueous outflow resistance in bovine eyes. In addition, in human eyes we observed a dense irregularly arranged amorphous elastic network extending from the tendon of the ciliary musculature to the inner wall endothelium (the ‘cribriform plexus’) as previously reported (Rohen et al., 1981). In this study, electron micrographs were used to perform a qualitative comparison of human and bovine JCT morphology that showed less elastic fibers in the JCT region of bovine eyes than that of human eyes, especially in the region immediately underneath the

inner wall of Schlemm's canal. Our data suggest that this tenacious tethering of the inner wall with the underlying JCT may limit protrusion of the JCT region, thereby accounting for the lack of washout in the human eye. Moreover, previous studies in human eyes (Johnstone, 1974, 1979; Grierson, Lee, Abraham, and Howes, 1978) have reported extensive connections exist between the inner wall cells and the underlying JCT whereby inner wall cells send processes down into the JCT to form a parachute like structure. These connections may anchor the inner wall and its endothelium to withstand pressure-induced distention secondary to hydrodynamic stress across the JCT/inner wall tissue region possibly contributing to the inner wall tethering and absence of washout in the human eye. Johnstone (1979) reported a progressive change in configuration in response to gradual change in IOP (25-35 mmHg in monkey eyes) suggesting the endothelial cell processes serve as architectural subunits to resist elevated IOP. Inner wall endothelial cell processes may be important constituents in tethering of the inner wall to the JCT in human eyes; however, it is not known if similar morphological ultrastructure is found in bovine eyes.

We hypothesize that washout occurs in the bovine as a result of a mechanical breakdown in the connectivity between inner wall and JCT adhesions (10-100 microns) whereby the funneling effect is eliminated at a macro-scale level. Elimination of the funneling effect, due to washout, may allow for a more uniform distribution of flow in areas where inner wall separation has occurred. Whether or not washout in this study resulted from elimination of the funneling effect on a micro-scale mandates further investigation.

Given the rather different anatomy of the bovine and human anterior chamber angle, it might be reasonable to expect that their outflow physiology might easily differ as we have seen. Surprisingly, however, the monkey eye, which bears far greater anatomical similarity to the human rather than the bovine eye, also exhibits washout (Epstein et al., 1982; Erickson and Kaufman, 1981; Gaasterland et al. 1978, Gaasterland et al., 1979; Kaufman et al., 1988; Peterson and Jocson, 1974). In future studies, we hope to exploit this dichotomy, examining monkey eyes to further refine the elements of the ultrastructure that are most critical to defining whether or not washout will occur.

In summary, we investigated the mechanism(s) for the increase in outflow facility during washout in the bovine eye and examined the mechanism accounting for the lack of washout in human eyes. Our study suggests that constituents involved in the tethering of the inner wall and JCT are important regulators in outflow resistance and therefore represent possible targeting for new pharmacological strategies that disrupt the connectivity between the inner wall and the JCT.

Finally, based upon our observations

i. ***Washout in the bovine eye correlates with separation of JCT from the inner wall of Schlemm's canal, which does not occur in human eyes and may possibly account for the lack of washout.***

ii. ***Human eyes uniquely possess an enhanced mechanical connectivity between the inner wall of Schlemm's canal and underlying JCT region that resists the separation between the JCT and inner wall that attends washout in bovine eyes.***

iii. ***Morphological comparison of electron micrographs shows human eyes appear to have more elastic fiber in the JCT region, especially in the region immediately underneath the inner wall of Schlemm's canal, that may aid in inner wall/JCT tethering; whereas, the bovine eye exhibits less elastic fiber in***

the JCT region, which may allow for easier separation of the inner wall/JCT tissue region.

CHAPTER 3A: A REVIEW OF AQUEOUS HUMOR FILTRATION STUDIES

3A.1 AQUEOUS HUMOR OUTFLOW FILTRATION STUDIES

To further understand the generation of aqueous humor outflow resistance many investigators have studied the filtration characteristics of the aqueous outflow system. Before proceeding with the development of our tracer study protocol (see chapter 3B), it is necessary to review some of the relevant methods and results of earlier tracer studies to understand how we developed our technique for tracing patterns of aqueous humor drainage in bovine eyes.

Although Leber was the first to propose aqueous humor was not a stagnant fluid he contended that colloidal gold suspensions could not pass through the outflow system, whereas, Schwalbe, thought otherwise (Huggert, 1955). Schwalbe's disputation was correct. His contention led to the investigation of tracer particles after intraocular perfusion to study the hydrodynamics of aqueous humor outflow. The earlier particle studies focused on determining the caliber of the openings in the trabecular pathway that may have a significant role in generating outflow resistance (Barany, 1959; Huggert, 1955, 1957; Huggert et al., 1955), while later studies were directed towards understanding fluid dynamics within the outflow pathway.

3A.1.1: Relevant Conclusions from Previous Aqueous Outflow Filtration Studies

Numerous studies were performed by Huggert using various particulate solutions to study outflow hydrodynamics (Huggert, 1955, 1957; Huggert et al., 1955). Huggert's goal was to determine pore size distribution in the aqueous outflow system. Huggert

hypothesized that heteroporosity was responsible for capturing filtered particles via steric hindrance, that is, particles too large to pass through the pores would become trapped. Huggert deduced his finding by comparing the distribution of particles (~0.1 μm, ~2.5 μm) in perfusate collected from the aqueous veins with the distribution of particles entering the anterior chamber. The results of this study suggest that below a certain critical size all particles should pass through the outflow pathway.

Later, Barany, having a different interpretation of Huggert's study, reanalyzed Huggert's data and results. Barany believed there would be significant capture for all sizes of particles via direct interception onto sticky walls of the trabecular meshwork and inner JCT region (Barany, 1959). Barany contended trabecular endothelial cells were "sticky" since they phagocytose material. Essentially, sticky wall capture implies larger particles should be captured by direct contact while smaller particles would be captured by indirect contact due to their large Brownian motion. In Brownian motion, electrostatic interactions and London dispersive forces are involved in particle capture (Spielman, 1977). After Barany reanalyzed Huggert's data, the mechanism(s) involved in particle capture remained unclear. Johnson et al. (1990) attempted to settle the disputation between Huggert and Barany by performing a similar experiment using enucleated human and bovine eyes. Johnson et al. (1990) was able to show significant capture of all particles sizes (0.176 μm and 0.46 μm). In the JCT, the capture rates of the 0.176 μm particles, which are smaller than most of the openings in the JCT, differed significantly between the calf (92%) and the human (45%). Thus, it was concluded that steric hindrance was not involved in capturing particles in the openings of the human aqueous outflow system. However, steric hindrance cannot be ruled out with certainty because of

the possibility of open spaces in the JCT containing extracellular matrix material (Ethier et al., 1986). In the bovine eye, however, particle capture in the bovine eye is due to both steric hindrance and sticky wall capture (Johnson et al., 1990). Johnson et al. (1990) also points out that the site of aqueous humor filtration is distinct from the site of outflow resistance, which suggests particle distribution within the JCT does not reflect or delimit the primary site of aqueous humor outflow resistance.

Tracer particles have also been used to investigate the possibility of segmental flow (Hann, Bahler, Johnson, 2005; de Kater, Melamed, Epstein, 1989; Melamed, Freddo, Epstein, 1986; Ethier and Chan, 2001; Epstein and Rohen, 1991), preferential outflow routes, and patterns of aqueous humor drainage in glaucomatous and non-glaucomatous human eyes (de Kater et al., 1989). The observation that pigment in the anterior chamber, as viewed during gonioscopy, appears segmentally distributed has prompted studies of segmental drainage pathways. Moreover, a histological study of the trabecular meshwork region found pigmented regions of the anterior chamber angle to correspond with the loci of the collector channel ostia (Tanchel NA, et al. *IOVS* 1984; 25:ARVO Abstract 7). This suggests that outflow may be preferential and tends to prefer those regions with a greater drop in pressure across the inner wall of Schlemm's canal (i.e. where collector channel ostia are located).

Particle studies of human eyes have led to various interpretations of the hydrodynamic mechanisms involved in governing aqueous humor drainage. One study (deKater et al., 1989) suggested uniform labeling in all regions of the trabecular meshwork, while another study (Ethier et al., 2001) demonstrated segmental labeling in all quadrants in human eyes. A more recent study (Hann et al., 2005), using cationic

ferritin, also demonstrated segmental labeling and the existence of preferential fluid pathways in the trabecular meshwork. Hann et al. (2005) concluded that cationic ferritin labeled and non-labeled regions of the trabecular outflow pathway do not differ ultrastructurally, and no differences were observed in cellular or extracellular matrix morphology that would account for segmental flow distribution. Hann et al. (2005) suggests preferential flow pathways may be created by several factors such as: dimensions and relationships of aqueous channels, variations in concentrations and permeability of extracellular matrix, aqueous channel interconnections, ease of passage across the endothelial barrier, and downstream resistance due to the presence of collector channel ostia. Hann et al. (2005) also reports the existence of "backwaters" or "dead ends" that are present in the trabecular meshwork not easily reached by aqueous humor. Moreover, they observed an absence of basement membrane in areas of the JCT where the extracellular matrix was distended causing the inner wall/JCT tissue region to protrude into the lumen of Schlemm's canal. The protrusions into the lumen of Schlemm's canal showed abundant labeling of cationic ferritin. Hann et al. (2005) also commented that enucleated eyes contain more preferential flow pathways due to the loss of ciliary muscle tone. Since live eyes are undergoing a continuous expansion and contraction of the ciliary muscle, which tugs on the corresponding ciliary muscle tendons that extend to the inner wall, it is thought that spaces in the trabecular meshwork and JCT are altered increasing activity of alternate flow channels, i.e. the outflow facility enhancing effect observed with topical administration of pilocarpine (Grierson, Lee, and Abraham, 1978; Rohen, Lutjen, and Barany, 1967; Lutjen-Drecoll and Kaufman, 1993). Hann et al. (2005) speculate a very interesting point in the conclusion of their study: the

loss of accommodation and concurrent loss of contraction of the ciliary muscle may lead to a decrease in interconnections of aqueous flow channels and an increase in preferential flow pathways with a consequent loss of overall aqueous humor drainage.

The relationship, if any, between changes in outflow facility and changes in patterns of aqueous humor drainage is unknown. In our study in Chapter 2, we demonstrated that the bovine eye undergoes an increase in outflow facility with prolonged perfusion, while bovine eyes perfused for a short duration do not. Our previous study (Chapter 2), as well as Overby et al. (2002), also demonstrated that the degree of inner wall separation from the underlying JCT correlates with outflow facility after prolonged intraocular perfusion. We speculated that the degree of tethering of the inner wall with the underlying JCT tissue region was involved in regulating outflow resistance, and when detached, decreases outflow resistance by increasing the effective filtration area for aqueous humor drainage into the aqueous plexus. Therefore, to better understand the mechanism regulating outflow resistance within the bovine eye we extended our study from Chapter 2 and investigated the possible relationship that changes in outflow facility may have with changes in patterns of aqueous humor drainage.

In our study in Chapter 3B, we examined the relationship between outflow facility and patterns of aqueous humor drainage with scanning laser confocal microscopy and fluorescent microspheres. Fluorescent microspheres were used to probe for changes in aqueous humor outflow patterns before and after washout in bovine eyes. Confocal laser microscopy is an excellent technique that does not require tissue processing for examining optic sections of the inner wall/JCT region in bovine eyes. Fluorescent microspheres, unlike latex microspheres, can be viewed in optic sections with the

confocal laser microscope. Another advantage of using the confocal laser microscope in conjunction with fluorescent microspheres is two colors of fluorescent microspheres can be used to map and compare changes in the distribution and patterns of aqueous humor outflow before and after washout.

We therefore proceed with a preliminary study in Chapter 3B with the goal of ***determining if there is a relationship between changes in outflow facility and changes in patterns of aqueous humor drainage to better understand the mechanism of outflow resistance in the bovine eye.*** However, before proceeding to our study of aqueous humor drainage patterns it is important to review differences and similarities of the aqueous humor outflow pathway between the human and bovine eye.

3A.1.2: Comparative Differences in Outflow Morphology Between Human (Primate) and Bovine Eyes

Each mammalian order has its own unique evolutionary adaptation for aqueous humor egression. Some interspecies differences are marked while others are subtle when compared to the human eye, i.e. presence of pectinate ligament, aqueous plexi, and Sondermann's channels are found in ungulate eyes, but not in the human eye. These differences in aqueous outflow morphology and physiology have been studied in non-human eyes to develop an animal model of POAG. Although glaucoma studies with animal models have been rewarding, our knowledge of the fundamental principles governing IOP is minimal at best.

Average IOP in vivo bovine eyes is 16.5±5.5 mmHg (Booffel, 1964); whereas, in the human eye it is 15.5±2.6 mmHg (Schottenstein, 1996). The bovine anterior chamber

angle is distinct from that found in the human eye and consists of at least three different regions (Flugel, Tamm, and Lutjen-Drecoll, 1990): *i*. a pectinate ligament/uveal meshwork with large spaces of Fontana, *ii*. a trabecular meshwork more reticular than lamellar, and *iii*. a loosely arranged connective tissue between the trabecular meshwork and ciliary muscle consisting of small loosely arranged longitudinal bundles. Only the anterior portion of the bovine uveal meshwork is presumed to carry aqueous fluid (Johnson et al., 1990). Aqueous humor then passes through the reticular meshwork – the calf equivalent of the human trabecular meshwork (Rohen, 1986). The reticular meshwork of the bovine eye contains cells between which are spaces filled with collagen and elastic fibers and also areas of optically empty space (Flugel, 1990), which apparently interconnect forming an elaborate system of tortuous pathways (Erickson-Lamy et al., 1988). It is not known whether the human JCT region contains a gel-like matrix completely filling the space between JCT cells since conventional tissue embedding methods for electron microscopy secondarily degrade GAGs. However, a technique called quick-freeze/deep-etch (QFDE) used in a study (Gong et al., 2002) revealed an elaborate view of the extracellular matrix in the JCT that still showed micro-sized optically empty spaces. Gong et al. (2002) pointed out that although optically empty space is observed with QFDE, it is unclear as to whether this technique is sensitive enough to visualize GAGs in their uncollapsed state.

The bovine and other lower mammalian eye contains a series of aqueous channels termed “aqueous plexus” (AP) (Tripathi, 1971, 1972a) that drain aqueous humor from the anterior chamber. The lumens of the aqueous plexus travel circumferentially around the eye and are discontinuous in certain loci while continuous in other regions. The

measured distance from the uveal meshwork to the aqueous plexus is less in the bovine than in the human ~ 50 microns (Johnson et al., 1990). In the bovine eye, distinguishing the JCT from the reticular meshwork is tedious since the size of the openings (5-10 μM) tends to remain stable between the JCT and inner aspects of the reticular meshwork (Johnson et al., 1990). Aqueous humor then passes through the remaining reticular/JCT region arriving at the basal side of the inner wall endothelial cells. The endothelial cells of the inner wall of the aqueous plexus are joined by zonulae occludentes forming a continuous single-layered membrane quite similar to the inner wall endothelial lining of the human eye (Tripathi and Tripathi, 1972a). Prominent nuclei and giant vacuoles are also present in both species (Tripathi, 1971). Given the large size of the bovine, it is not surprising that all linear dimensions of the bovine outflow system are approximately 1.6 times as large as the human's with the exception of the radial dimension of the trabecular meshwork (Johnson et al., 1990). The anatomy and morphology of the aqueous outflow pathway in human eyes has been previously described in Chapter 1.

We now proceed accordingly with our filtration study after having reviewed pertinent findings from previous tracer studies as well as the differences and similarities between human and bovine aqueous humor outflow morphology.

CHAPTER 3B: RELATIONSHIP BETWEEN OUTFLOW FACILITY AND PATTERNS OF AQUEOUS HUMOR DRAINAGE IN THE BOVINE EYE – A PRELIMINARY PERFUSION STUDY

3B.1 ABSTRACT

The goal of this study was to determine whether changes in outflow facility correlate with changes in aqueous outflow patterns in the trabecular meshwork/juxtacanalicular connective tissue (TM/JCT) before and after washout in enucleated bovine eyes. 10 bovine eyes were perfused at 15 mmHg with Dulbecco's PBS, containing 5.5 mM glucose (DPBS), while outflow facility was continuously measured. Two colors of fluorescent microspheres (0.5 μm; 0.002% v/v) were used to probe for changes in outflow patterns before and after washout in bovine eyes. *Short-duration perfusion*: (*n*=5), 0.5 mL DPBS containing pre-washout red tracer (RT), followed by anterior chamber exchange with Karnovsky's fixative and perfusion-fixation at 15 mmHg. *Long-duration Perfusion*: (*n*=5), 0.5 mL DPBS containing pre-washout tracer, then 5 mL of DPBS without tracer to induce washout, followed by 0.5 mL of DPBS containing post-washout green tracer (GT) and perfusion-fixation. Sections were cut in the radial direction to the limbus in all quadrants, nuclei were stained with To-Pro 3, and sections examined using confocal laser microscopy to visualize the tracer distribution within the TM/JCT. The total length (TL) and the tracer-decorated length (L) of the inner wall were measured in >3 images/eye, and the average percent effective filtration length (PEFL=L/TL) in each eye was calculated. The distribution of the pre-washout RT was similar in both short and long-duration perfusion, exhibiting a punctate pattern within the TM/JCT that tended to cluster near collector channel ostia. After long-duration perfusion

and washout in 5 eyes, outflow increased by 177.8±35.6% (p=0.008). The post-washout GT pattern was more uniform along the inner wall of the bovine aqueous plexus (AP) as compared to the pre-washout RT tracer pattern. The PEFL in short-duration eyes (41.96±6.7%) was similar to both the pre-washout (44.10±10.1%) and post-washout in long-duration perfusions (47.3±9.40%, p=0.82). In conclusion, compared to short-duration and pre-washout outflow patterns appear punctate, whereas post-washout drainage patterns appear more uniform along the AP. Changes in outflow facility do not appear to correlate with the area available for flow through the TM/JCT in radial sections. A better understanding of the mechanisms that augment the total area for flow could be exploited to increase facility in eyes with elevated intraocular pressure. The macroscopic pattern of aqueous humor outflow is highly segmental at 15 mmHg.

3B.2 INTRODUCTION

Primary open-angle glaucoma (POAG), a potentially blinding disease, is associated with an impairment or malfunctioning of the filtration mechanisms within the trabecular meshwork that causes elevated outflow resistance. Currently, the mechanisms governing aqueous humor outflow resistance remain unexplained in both the normal and glaucomatous human eye.

It is generally accepted that the bulk of outflow resistance is generated in the juxtacanalicular connective tissue (JCT) while some argue the inner wall endothelium of Schlemm's canal may plays a more central role (Epstein and Rohen, 1991; Johnson et al., 1992; Ethier et al., 1998). Previous studies (Ellingsen and Grant, 1972; Bill and Svedbergh, 1972) have shown that the inner wall of Schlemm's canal only accounts for 10% of the aqueous outflow resistance. These studies provide the support for the hypothesis that the primary resistive moiety is proximal to the inner wall of Schlemm's canal, thus, localizing it to within the JCT; however, the characteristics of resistance to aqueous humor outflow are sensitive to different perfusion pressures (Rosenquist et al., 1989).

The JCT contains small preferential pathways lying directly underneath Schlemm's canal and are believed to represent the actual filtering area of the inner wall of the canal (Rohen, 1986). It has been proposed that pores in the inner wall endothelium, while offering negligible resistance alone, may increase outflow resistance by modulating the flow of aqueous humor with the JCT towards these discrete pores in turn causing a hydrodynamic interaction known as the "funneling effect" (Johnson et al.,

1992) (See Section 1.2.3). The increase in outflow facility observed in non-human eyes exhibiting washout may be related to elimination of the funneling effect (See Chapter 1.2.3). Although studies (Sit et al., 1997; Ethier et al., 1998) have failed to demonstrate the funneling effect on a microscale level (0.1- 10 microns), investigating these hydrodynamic flow patterns on a macroscale level (10-100 microns), that is, taking into account JCT and inner wall connectivity as well as the structural correlate of washout - separation of the inner wall from the JCT (Overby et al., 2002; See Chapter 2), may provide insight into the hydraulic mechanisms governing aqueous humor outflow resistance in bovine eyes.

In light of Overby et al. (2002), Sabanay et al. (2004), and our study in Chapter 2B, we consider the molecular constituents involved in tethering large regions along the inner wall and JCT that may increase outflow resistance macroscopically (10-100 microns) by regulating patterns of aqueous humor outflow. Separating these large regions of tenacious tethering may lead to a more uniform distribution of aqueous humor outflow along the inner wall as predicted by the funneling hypothesis.

In this study, we have attempted to determine if there is a relationship between changes in aqueous outflow facility and changes in patterns of aqueous humor drainage in enucleated bovine eyes. To investigate this relationship we take advantage of the washout effect whereby outflow resistance is decreased after prolonged intraocular perfusion in non-human eyes.

We hypothesize that washout occurs in the bovine eye as a result of disrupting the connectivity between inner wall and JCT adhesions (10-100 microns) whereby the funneling effect is eliminated. Elimination of the funneling effect, due to washout, may

allow for a more uniform distribution of aqueous flow in areas where inner wall separation has occurred, which may account for the decreased outflow resistance observed with washout. Therefore, we consider the presence of preferential drainage patterns before and after washout. ***We hypothesize that post-washout drainage patterns will demonstrate a more uniform pattern along the inner wall of the AP due to a decrease in tethering between the inner wall and JCT increasing the effective area for aqueous humor filtration along the inner wall, while pre-washout outflow patterns will show a more punctate tracer pattern due to the lack of inner wall/JCT separation.***

To test our hypothesis, fluorescent microspheres and confocal microscopy were used to visualize changes in hydrodynamic patterns of outflow before and after washout. Investigating the relationship between changes in outflow facility and changes in patterns of aqueous humor drainage may supplement our current understanding of the washout mechanism and how this phenomenon might be utilized to develop an effective anti-glaucoma treatment in human eyes.

3B.3: MATERIALS AND METHODS

Ten enucleated bovine eyes were obtained from a local abattoir (Arena and Sons, Hopkinton, MA) and delivered on ice within 6 hours post-mortem. Eyes with discernible damage or accumulated blood in the angle of anterior chamber were not used.

3B.3.1: Outflow Perfusion Apparatus

The perfusion apparatus used was described previously (See Chapter 2.1.1); however, the strip chart recorder was abandoned because it was too labor intensive and replaced with software (Labview) that converted voltage into outflow facility (Fig. 3B.1)

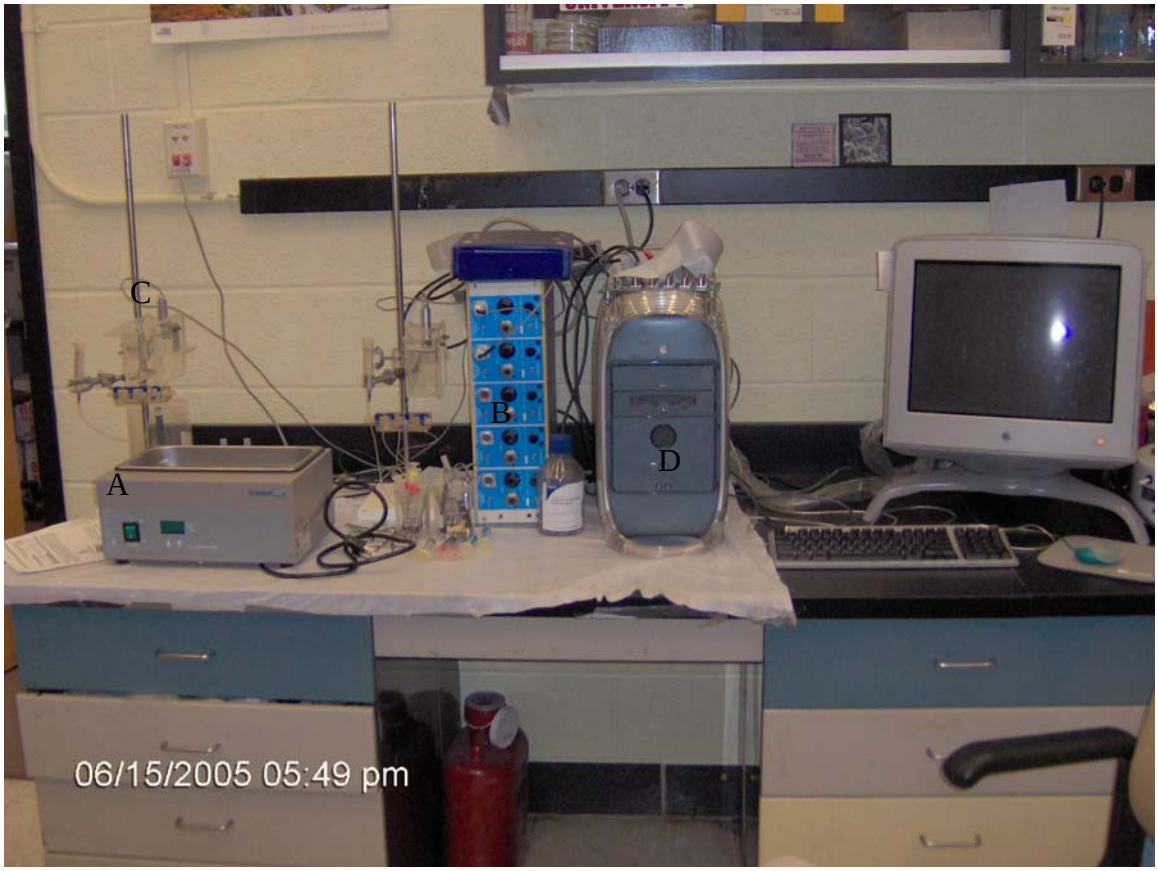


Figure 3B.1 *Perfusion System and Computer* (A) water bath used to heat bovine specimens, (B) multiplexer, (C) rods to adjust supply and waste reservoirs, and (D) computer with Labview Software.

3B.3.2: Outflow Perfusion Procedure

Dulbecco's phosphate-buffered saline (PBS; Life Technologies, Grand Island, NY) containing 5.5 mM D-glucose (collectively referred to as DPBS) was used as mock aqueous humor in all perfusions. Each eye to be perfused was placed in a beaker with the cornea facing upward and submerged with saline just above the limbus. A fluid supply reservoir was positioned above the limbus at a height equal to 15 mmHg, which was chosen based on previous studies (Barany and Woodin, 1955; Erickson-Lamy et al., 1990; Erickson-Lamy et al., 1988) to have shown significant washout in bovine eyes perfused at a constant-pressure of 15 mmHg. A perfusion needle (23-guage) was then inserted intracamerally through the cornea. The tip of the needle was placed into the posterior chamber of the eye to prevent anterior chamber deepening that would otherwise lead to an artificial increase in outflow facility (Francois et al., 1955; Ellingsen and Grant, 1971). Anterior chamber fluid exchange was achieved using a second needle attached to tubing leading to an exchange receptacle. During the perfusion the exchange receptacle line was clamped.

During anterior chamber fluid exchange the supply reservoir was positioned at a height 2 cm H_2O (17 mmHg) above 15 mmHg and the exchange receptacle at a height 2 cm H_2O (13 mmHg) below. This protocol ensured that the average pressure within the eye was never >2 cm H_2O away from 15 mmHg. During the perfusion, a piece of cotton soaked in DPBS was placed on any exposed cornea to keep it moist.

3B.3.2a: Short-Duration Perfusion (n=5) (One Color Tracer)

30 minutes was allowed for stabilization of outflow facility to achieve a baseline measurement. The anterior chamber was exchanged with 7.0 ml 5.5 mM D-glucose

DBPS + red fluorescent microspheres (500 nm, 0.002% v/v) after which outflow facility was measured until 0.5 ml of DPBS+RT (~30 minutes) drained from the supply reservoir to adequately trace the outflow pathway within the eye. After, the anterior chamber was exchanged with 7.0 ml of 2% paraformaldehyde and 2.5% glutaraldehye in PBS (pH 7.3) and perfusion-fixed with 0.5 ml (~30 minutes) at 15 mmHg.

3B.3.2b: Long-Duration Perfusion (n=5) (Two Color Tracer)

30 minutes was allowed for stabilization of outflow facility to achieve a baseline measurement. The anterior chamber was exchanged with 7.0 ml 5.5 mM D-glucose DBPS + red fluorescent microspheres (500 nm, 0.002% v/v) after which outflow facility was measured until 0.5 ml of DPBS+RT (~30 minutes) drained from the supply reservoir to adequately trace the outflow pathway within the eye. After, the anterior chamber was exchanged with 7.0 mL DPBS to remove any suspended pre-washout tracer particles, outflow facility was measured until 5.0 ml of DBPS perfused through the eye in order to induce washout (~3-4 hours). 30 minutes was allowed for stabilization of outflow facility to achieve a baseline measurement. The anterior chamber was exchanged with 7.0 ml 5.5 mM D-glucose DBPS + yellow-green fluorescent microspheres (500 nm, 0.002% v/v) after which outflow facility was measured until 0.5 ml of DPBS+GT (~30 minutes) drained from the supply reservoir to adequately trace the outflow pathway within the eye. The anterior chamber was then exchanged and perfusion-fixed with 0.5 ml of 2% paraformaldehyde and 2.5% glutaraldehyde in PBS (pH 7.3) under the same pressure.

3B.3.3: FluoSpheres

Fluorescent microspheres were used in this study to probe for changes in patterns of aqueous humor drainage in bovine eyes. One color of microspheres (RT) were used in the short-duration to trace the outflow pathway. Two colors of microspheres (RT & GT) were used in the long-duration to trace the pre and post-washout (RT & GT) pathways. The short-duration outflow pattern was then compared with the pre-washout pattern in long-duration eyes, while the post-washout pathway was compared to the pre-washout pathway in long-duration eyes. The concentration (0.002%) and size (0.50 μm) of fluorescent microspheres (Molecular Probes FluoSpheres, Carlsbad, CA) used in this study were based upon Johnson et al. (1990) who selected a concentration of 4×10^{-6} and 0.176 & 0.46 μm size because it was shown to be dilute enough to avoid the possibility that captured microspheres would impede outflow thereby inhibiting change of outflow characteristics. The pre and post-washout FluoSpheres were carboxylate-modified microspheres with distinct emission/excitation wavelengths (Red 580/605 nm λ, Yellow-Green 505/515 nm λ, respectively) suspended in DBPS (0.002% v/v).

3B.3.4: *Removal of Free-Floating FluoSpheres from the Anterior Chamber During Anterior Chamber Exchange*

In bovine eyes undergoing washout it was necessary to ensure that no free-floating FluoSpheres remained suspended in the anterior chamber. Free-floating pre-washout tracers in eyes undergoing a three-hour induction of washout were removed from the anterior chamber by exchanging 7 mL of DPBS. Each successive 1 mL was exchanged from the waste reservoir, a 30 microliter sample was taken from each milliliter exchanged, and examined under the confocal microscope at 20X magnification (See

Figure 3B.2). Each successive 30 microliter sample per successive 1 ml exchanged decreased in the number of visible microspheres until the 7th mL, in which no microspheres were observed within the field of view (See Figure 3B.3 & Table 3B.1). This ensured that no pre-washout or washout free-floating microspheres remained suspended or were stirred up in the aqueous humor during the anterior chamber exchange that would otherwise deposit later in the experiment compromising the integrity of the pre and post-washout aqueous humor drainage patterns.

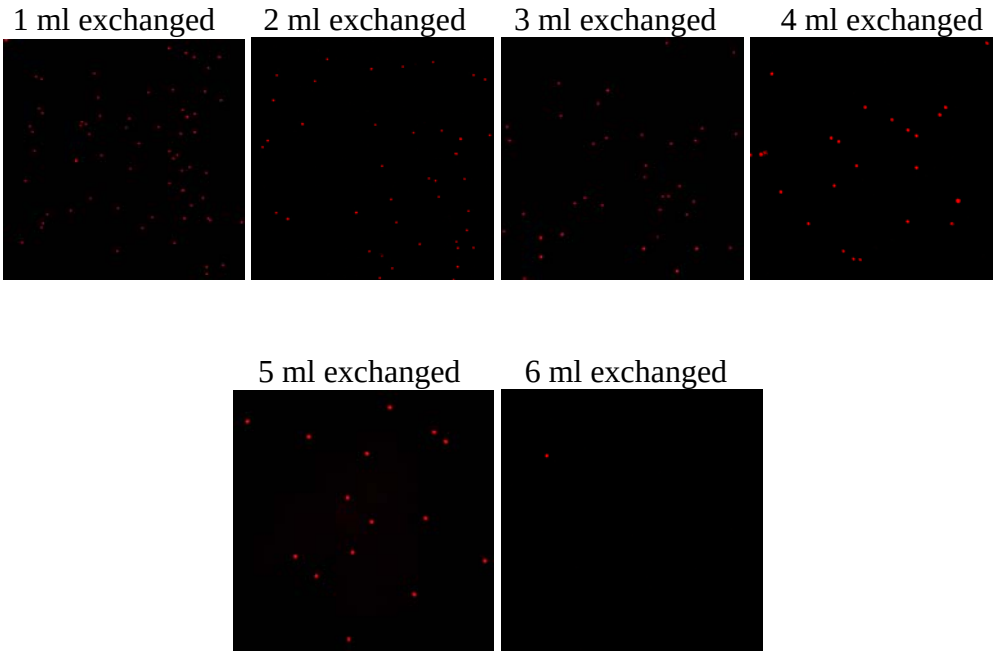


Figure 3B.2 *Anterior Chamber Removal of Fluorescent Microspheres.* The number of visible fluorescent microspheres decreases with each successive 1.0 ml exchanged sample from the waste collection reservoir during anterior chamber exchange. Each image above represents a randomly selected field of view (Image magnification 20X) of a 30 microliter sample of each successive 1.0 ml exchanged. The imaging demonstrates that almost all microspheres are removed from the anterior chamber after exchanging 6.0 ml.

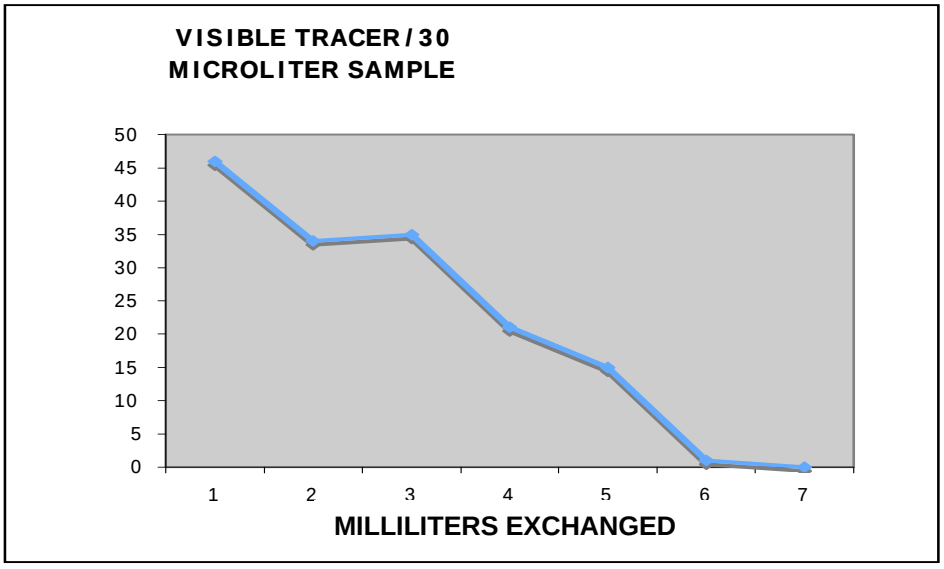


Figure 3B.3 *Visible Microspheres per 1.0 ml Sample vs Exchange Volume***.** This graph shows visible microsphere distribution decreasing as a function of volume exchanged per 30 microliter sample taken from each milliliter exchanged. Microspheres visible within a constant field of view (Image Magnification 20X) of a randomly selected area from each successive 1.0 ml sample exchanged up to 6.0 ml total exchange.

Data of Visible Microspheres/30 ul Sample/1ml Exchanged Viewed during Confocal Microscopy

Volume of DPBS Exchanged	Number of Microspheres Visible Per 30 ul
1.0 ml	46
2.0 ml	34
3.0 ml	35
4.0 ml	21
5.0 ml	15
6.0 ml	1

Table 3B.1 *Data of Visible Microspheres per 1.0 ml Exchanged Sample* The data from the table above shows the number of visible microspheres visible in a constant field of view of a randomly selected area on a slide of a 30 microliter sample taken from each successive milliliter exchange. Microsphere distribution decreases with greater exchange volume.

All studies adhered to the ARVO Statement for the Use of Animals in Ophthalmic and Vision Research

3B.3.5: Confocal Microscopy

Anterior segments of the eyes were then divided into 4 quadrants (designated Superior, Inferior, Nasal, and Temporal) and cut into meridional sections (1-2 mm). Each sample was then stained with Topro-3 (Molecular Probes, Inc., Eugene, OR, USA) for 30 minutes to allow visualization of cell nuclei followed by three successive five-minute washes in PBS. All sections were then examined using (Carl Zeiss 510 Axiovert 100M Laser Scanning Microscope/Software version 3.2 PS2, Heidelberg, Germany). A multi-track channel system was then used to visualize the fluorescent microspheres under 20X magnification. The distributions of the two fluorescent tracers were measured along the inner wall for comparison of drainage patterns and effective filtration length (distribution) of flow. Image analysis software (Carl Zeiss MicroImage Software, NY) was used to measure the total length of inner wall (*TL*) and the apparent length (*L*) of inner wall exhibiting tracer labeling in each image (n=3 to 21 images per eye). The effective filtration length (i.e., the 1-dimensional equivalent to effective filtration length observed on a micrograph) was calculated as *L/TL* for each image and averaged over all images per eye. The effective filtration length represents the percent distribution along the inner wall, but not the pattern of aqueous humor drainage. Furthermore, the effective filtration length is a quantitative measure used to compare the percent distribution of microspheres along the inner wall before and after washout, whereas the tracer patterns are qualitative assessments as observed in respective micrographs. Figure 3B.4 demonstrates how the distribution or effective filtration length was measured along the inner wall of the bovine aqueous plexus.

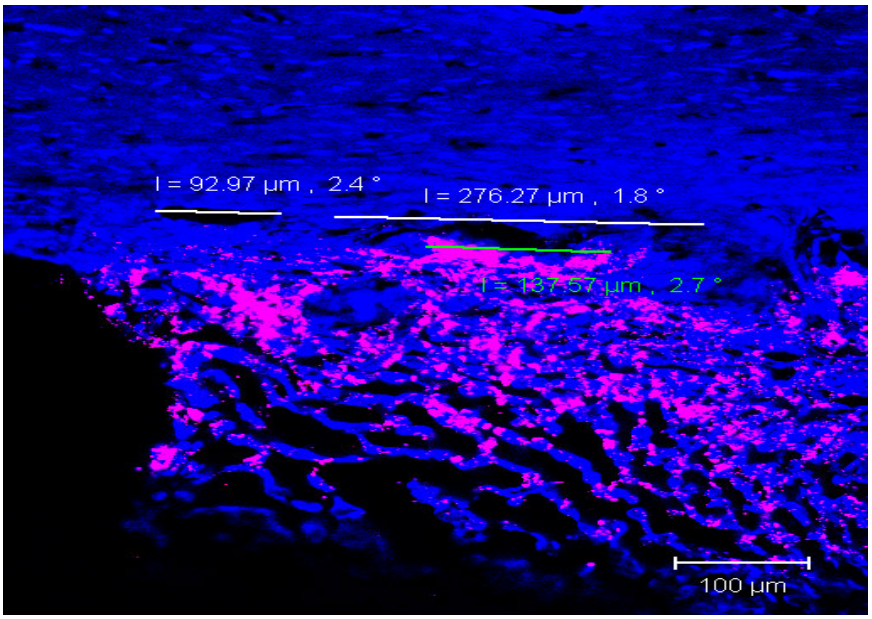


Figure 3B.4 *Confocal Image of the Bovine Aqueous Plexus Effective Filtration Area (EFA) in redial section* The EFA was calculated by measuring the total length of inner wall (TL) (white line) and the apparent length (L) (green line) of inner wall exhibiting tracer labeling in each image (n=3 to 21 images per eye). The effective filtration length (i.e., the 1-dimensional equivalent to effective filtration area observed on a micrograph) was calculated as L/TL for each image and averaged over all images per eye.

3B.4 RESULTS

3B.4.1: Outflow Facility

A summary of outflow facility data from short-duration perfusion bovine eyes is presented in Table 3B.2. Short-duration perfusion eyes show an average increase of 28.9 ± 6.0% μL/min/mmHg from baseline facility (C0) to pre-fixation (C1).

Outflow Facility (μL/min/mmHg)

Bovine

EYE	C0:BASELINE	C1 (PRE-FIX)	%C0-C1/C0	FIX C	%FIX-C1/FIX
CONT1	0.96	1.24	29.2%	0.77	-37.9%
CONT3	1.61	1.99	23.6%	1.54	-22.6%
CONT4	0.96	1.33	38.5%	1.53	15.0%
CONT5	1.65	2.37	43.6%	0.91	-61.6%
CONT6	2.83	3.1	9.5%	1.31	-57.7%
MEAN	1.60	2.01	28.9%	1.21	-33.0%
SD	0.76	0.77	13.4%	0.36	31.1%
N	5	5	5	5	5
SEM	0.34	0.34	6.0%	0.16	13.9%

Table 3B.2 *Outflow Facility for Short-Duration Perfusions at 15mmHg in Bovine Eyes* Bovine eyes undergoing short-duration perfusion show an average outflow facility of 2.01±0.34 μL/min/mmHg with percent increase of 28.9±6.0 μL/min/mmHg (%C1-C0/C0) from baseline (C0) to pre-fixation (C1). C0 = measurement made after 30 minute stabilization period, C1 = measurement after 0.5 ml of DPBS+tracer particle, and FIX C = measurement after 0.5 ml of fixative perfusion.

A summary of outflow facility data from long-duration perfusion bovine eyes is presented in Table 3B.3. The pre-washout average outflow facility was 1.99±0.32% μL/min/mmHg after 0.5 ml DPBS+red FluoSpheres, and a change in outflow facility of 69.15 ±17.16% μL/min/mmHg from pre-washout (after red tracer perfusion) to post-washout (green tracer perfusion) facility values. The total average change in outflow

facility from C0 to post-washout was 177.8±35.6% μL/min/mmHg (p=0.008). However, the average change in outflow facility from C0 (baseline) to C1 (after red tracer perfusion) is 62.67±5.87%, (mean±SEM) while the short-duration average change in outflow facility from C0 (baseline) to C1 is 28.9±6.0 % (mean±SEM). The % change in outflow facility between pre and post-washout values is 69.15±17.16% (mean±SEM) and is insignificant (p=0.79).

High-Volume Outflow Facility (μL/min/mmHg)

				Bovine				
EYE	C0 :Baseline	C1:pre-washout	%C0-C1/C0	C2:post-washout	%C2-C1/C1	%C2-C0/C0	FIX	FIX-C3/FIX
EXP1	1.89	2.77	46.56	4.02	45.13	112.7%	2.22	-44.8%
EXP2	1.54	2.45	59.09	4.03	64.45	161.7%	2.31	-42.7%
EXP4	1.21	2.21	82.64	4.44	100.9	266.9%	2.7	-39.2%
EXP5	0.61	1.01	65.57	2.16	113.86	254.1%	1.12	-48.1%
EXP6	0.94	1.499	59.47	1.82	21.41	93.6%	0.8	-56.0%
MEAN	1.24	1.99	62.67	3.29	69.15	177.8%	1.83	-46.2%
SD	0.50	0.72	13.13	1.21	38.36	79.6%	0.82	6.4%
N	5	5	5	5	5	5	5	5
SEM	0.22	0.32	5.87	0.54	17.16	35.6%	0.37	2.9%
unpaired p				0.02				
paired p				0.007	0.79			
tstat p						0.008		

Table 3B.3 *Outflow Facility for Long-Duration Perfusions at 15mmHg in Bovine Eyes* Bovine eyes undergoing high-volume perfusion show an average percent increase of 177.8±35.6 μL/min/mmHg (p=0.008) from baseline to post-washout (%C2-C0/C0). No significant change occurred between C2 and C1 (p=0.79). C0 = measurement after 30 minute stabilization period, C1 = measurement after pre-washout microsphere perfusion, C2 = measurement after post-washout microsphere perfusion, Fix = measurement after 0.5 ml of fixative perfusion.

3B.4.2:Confocal Imaging of Pre and Post-Washout Microsphere Outflow Patterns in Radial Sections

In control eyes, the pre-washout pattern of microsphere pattern showed punctate labeling along the inner wall of the bovine aqueous plexus (Figure 3B.4). This punctate pattern may possibly be related to preferential flow towards discrete pores along the inner

wall endothelium secondary to pore funneling. Figure 3B.5 demonstrates the punctate decorating along the inner wall in an eye after 0.5 ml DPBS + red tracers.

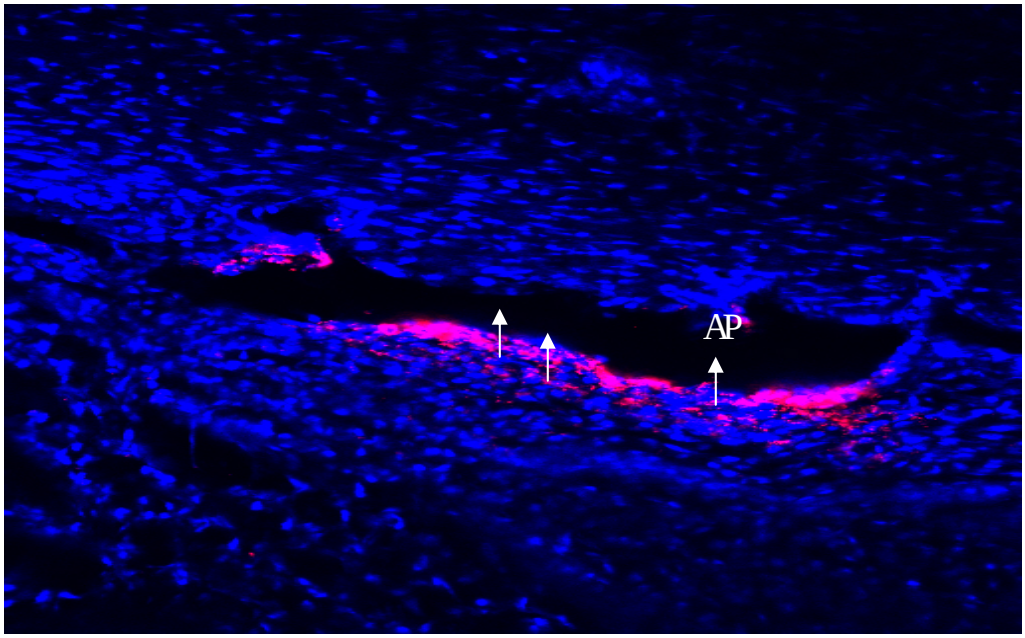


Figure 3B.5 *Punctate Pattern of Microspheres in Control Eyes* Punctate decorating (arrows) along the inner wall in an eye after 0.5 ml DPBS + red tracers. AP = aqueous plexus.

Figure 3B.6A shows the pre and post-washout microsphere labeling along the inner wall of the aqueous plexus. Figure 3B.6B shows the pre-washout microsphere labeling (red tracer) as punctate along the inner wall of the bovine aqueous plexus as compared to the post-washout microsphere decorating (green tracer) that has a more uniform pattern along the inner wall Figure 3B.6C. The pre-washout tracer is confined within the post-washout tracer demonstrating areas of co-localization (yellow) in this image. Examination of the pre and post-washout aqueous humor drainage patterns in all confocal images (n=72) consistently showed the pre-washout pathways having less uniform or more punctate patterns of aqueous humor drainage (possibly representing

preferential outflow routes) while the post-washout showed more uniform or less punctate decorating along the inner wall and in areas where the pre-washout tracer absent.

We are confident that the pre-washout microsphere patterns represent the outflow pathway before washout and were not altered by prolonged perfusion. After comparing the short-duration outflow patterns and the pre-washout outflow patterns in long-duration perfusions we found no changes in the pre-washout outflow patterns that would suggest prolonged perfusion would compromise or alter the pre-washout patterns. The short-duration and pre-washout outflow patterns in the long-duration perfusion both show a punctate pattern. If the representation of the pre-washout patterns were altered in the long-duration perfusions (possibly due to dislodging and recapture of microspheres after prolonged perfusion), then it would most likely show a decrease in labeling along the inner wall and have a much lower percent effective filtration length along the inner wall as well. However, in this study, no changes were observed between the short-duration and pre-washout outflow patterns in the long-duration perfusions, and the effective filtration length was also similar between the short-duration and pre-washout microsphere distribution, which further supports the integrity of the pre-washout microsphere pattern and distribution. However, to be certain of our assertion, further studies in which the perfusate is collected and analyzed at different times during the washout induction for evidence of pre-washout microsphere dislodgment are warranted.

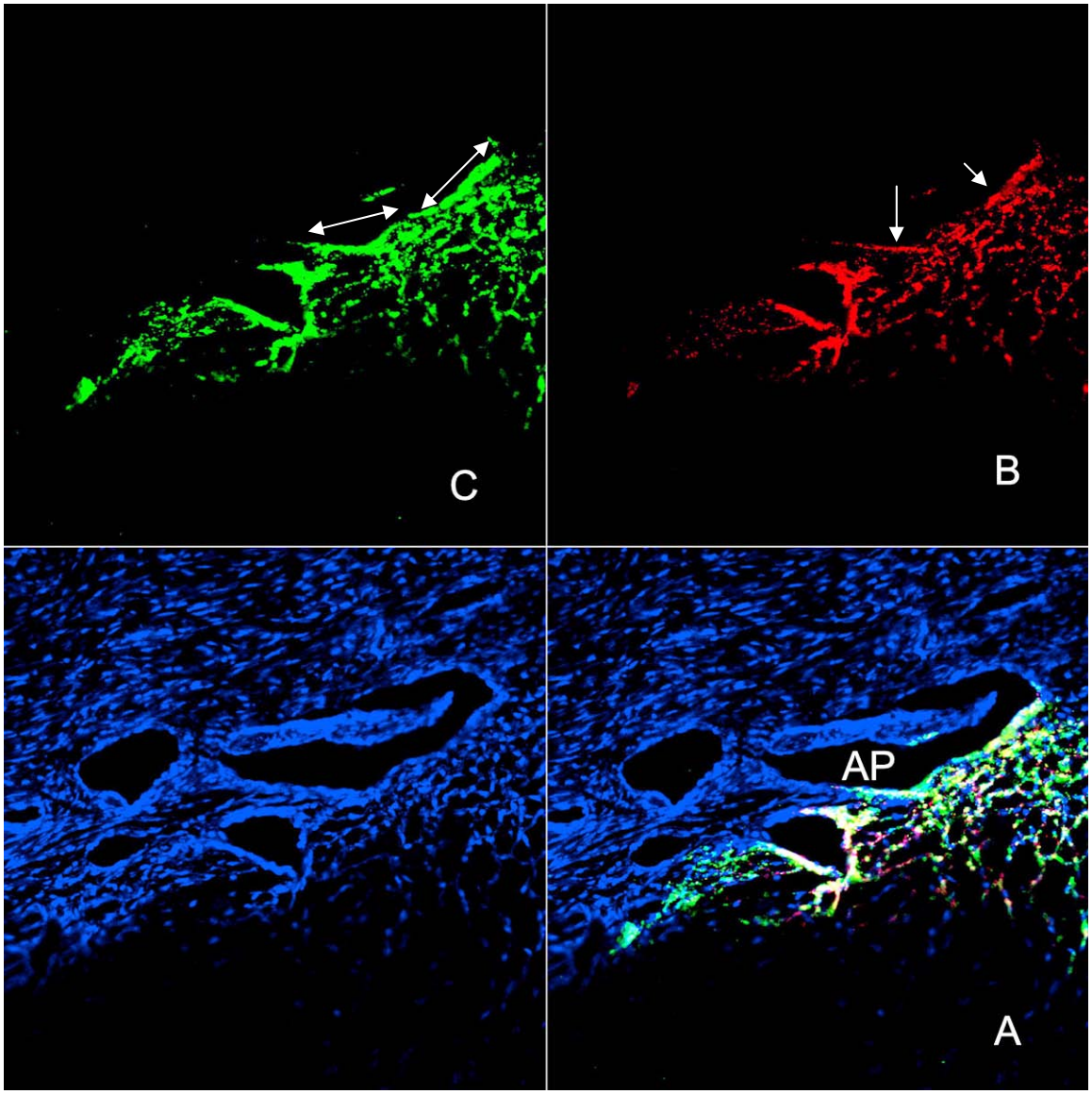


Figure 3B.6 *Radial Sections of Aqueous Humor Drainage Patterns in the Bovine Aqueous Plexus using Confocal Microscopy* (A) superimposed image of the bovine aqueous plexus (AP) with pre and post-washout microsphere labeling (yellow = colocalization); (B) pre-washout tracer labeling showing punctate aqueous outflow patterns (single headed arrows) along the inner wall; (C) green beads have a greater uniform distribution (double headed arrows) and density along the inner wall.

3B.4.2a: Comparing Pre and Post-Washout % Microsphere Distributions vs % Change in Outflow Facility

Table 3B.5 summarizes the average facility during pre-washout tracer perfusions in the control (pre-washout only) group. The average baseline outflow facility was 1.18±0.22 (mean±SEM) ul/min/mmHg with an average change in outflow facility of 30.44±4.36% (mean±SEM) (See Appendix Table 1A and Table 1B: *Pre and Post-Washout Microsphere Distribution Percentages Along the Inner Wall of the Bovine Aqueous Plexus*).

In control eyes, in which only the pre-washout patterns of aqueous humor drainage were assessed after 0.5 ml DPBS+red tracer were perfused, the % pre-washout microsphere distribution was 41.96±6.7% (mean±SEM), CONT5 and CONT6 were removed from calculating this value due to the low number of confocal images (n=2 and n=4, respectively) in these eyes.

In experimental eyes, the average % pre-washout microsphere distribution was 44.1±10.1% (mean±SEM), while the post-washout % microsphere distribution was 47.3±9.4% (mean±SEM) (See Table 3B.5). There was no significant change in the % microsphere distribution before and after washout in experimental eyes; however, this does not imply that the patterns of aqueous humor drainage before and after washout are not similar, but simply indicates that the distribution of the microspheres along the inner wall of the bovine aqueous plexus are similar.

EYE	BASELINE C	PRE-WASHOUT C	% PRE-WASHOUT BEAD DIS	%CHANGE C BETWEEN BASELINE AND PRE-WASHOUT
CONT1	0.96	1.24	49.1	29.2
CONT3	1.61	1.99	28.68	23.6
CONT4	0.96	1.33	48.1	38.5
MEAN	1.18	1.52	41.96	30.44
SD	0.38	0.41	11.51	7.55
N	3	3	3	3
SEM	0.22	0.24	6.65	4.359

Table 3B.4 *Short-Duration (Control) Perfusion % Microsphere Distribution (Pre-Washout) vs % Change in Outflow Facility* The average % pre-washout bead distribution in low-volume (control) eyes is 41.96±6.65% (mean±SEM). The average % change in outflow facility between baseline and after 0.5 ml DPBS + red tracer was 30.44±4.36% (mean±SEM) *µl/min/mmHg*.

Table 3B.5 summarizes the % microsphere distribution in experimental eyes before (pre-washout) and after washout (post-washout) versus the % change in outflow facility before and after washout. In experimental eyes, the average increase in outflow facility from baseline to after perfusion of 0.5 ml DPBS+red microspheres is 63.59±7.49% (mean±SEM) ml/min/mmHg with an average pre-washout % distribution of microspheres of 44.1±10.1% (mean±SEM), while the post-washout change in outflow facility (measured from pre-washout facility value until after 5.0 ml of DPBS followed by 0.5 ml DPBS+green tracer was perfused) was 70.33±22.09% (mean±SEM) ml/min/mmHg with an average % post-washout microsphere distribution of 47.3±9.4% (mean±SEM) (p=0.82). No correlation (p=0.76) was observed between microsphere distribution and the % change in outflow facility (See Figure 3B.7).

PRE-WASHOUT DATA

	Baseline C	Pre-Wash C	%Bead Dis	%Facility Increase
EXP1	1.890	2.770	58.44	46.56
EXP4	1.210	2.210	58.63	82.64
EXP5	0.610	1.010	15.84	65.57
EXP6	0.940	1.500	43.49	59.57
Mean	1.163	1.873	44.100	63.588
SD	0.544	0.775	20.131	14.979
SEM	0.272	0.388	10.065	7.490

POST-WASHOUT DATA

	Pre-Wash C	Post-Wash C	%Bead Dis	%Facility Increase
EXP1	2.77	4.020	57.78	45.13
EXP4	2.21	4.440	67.55	100.90
EXP5	1.01	2.160	25.97	113.86
EXP6	1.5	1.820	38.05	21.41
Mean	1.873	3.110	47.338	70.33
SD	0.775	1.312	18.801	44.19
SEM	0.388	0.656	9.400	22.09
p-value	0.190	0.167	0.822	0.79

Table 3B.5 *% Microsphere Distribution vs % Change in Outflow Facility* The average % pre-washout bead distribution is 44.1±10.1% (mean≠SEM), average % pre-washout change in outflow

facility 63.59±7.49% (mean±SEM) *µl/min/mmHg*, while post-washout change in outflow facility was 70.33±22.09% (mean±SEM) µl/min/mmHg with an average % post-washout microsphere distribution of 47.3±9.4% (mean±SEM) (p=0.82).

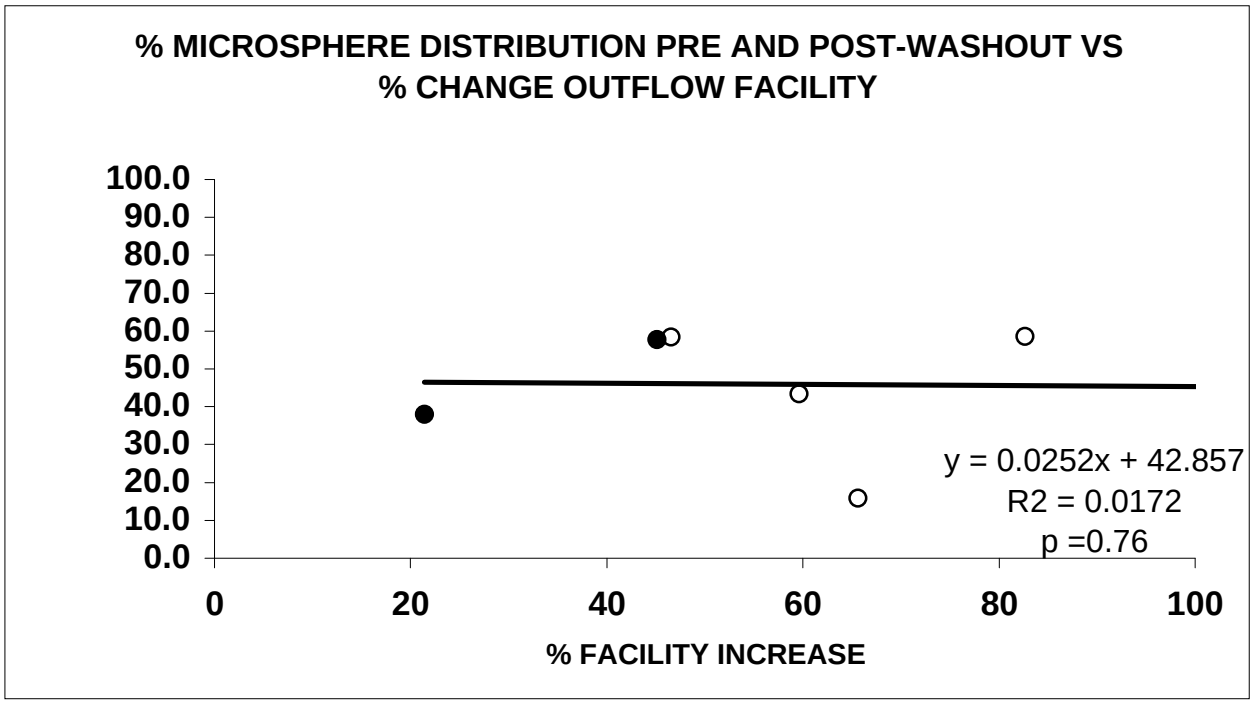


Figure 3B.7. *Experimental (Pre and Post-Washout) % Microsphere Distribution vs % Change in Outflow Facility*. The average % pre-washout bead distribution (open circles) is 44.1±10.1% (mean±SEM), average % pre-washout change in outflow facility 63.59±7.49% (mean±SEM) *µl/min/mmHg*, while the post-washout change in outflow facility was 69.15±17.16% (mean±SEM) µl/min/mmHg with an average % post-washout microsphere distribution (closed circles) of 47.3±9.4% (mean±SEM). There is no correlation (p=0.76) between % microsphere distribution or % change in outflow facility.

3B.5 DISCUSSION

In this study, we investigated the relationship between changes in outflow facility and changes in patterns of aqueous humor drainage before and after washout. We took advantage of the increase in outflow facility with washout and compared the pre and post-washout pathways by analyzing fluorescent microsphere patterns with a confocal scanning laser microscope. Furthermore, we were able to differentiate pre and post-washout outflow pathways by using two colors of microspheres to trace each route (red tracer = pre-washout, green tracer = post-washout) to compare drainage patterns and tracer labeling along the inner wall of the bovine aqueous plexus in the same eye.

In light of our results in Chapter 2B and the work of Overby et al. (2002), which suggest that washout is caused by separation of the inner wall from the JCT, we suspected this separation may alter fluid dynamics that regulate the passage of aqueous humor through the inner wall/JCT region. We have documented that bovine eyes exhibiting washout have a more uniform outflow pattern along the inner wall of the bovine aqueous plexus, whereas, the pre-washout pattern is more puntcate. The results of this study support our hypothesis that post-washout drainage patterns will demonstrate a more uniform pattern along the inner wall of the aqueous plexus due to a decrease in tethering between the inner wall and JCT increasing the effective area for aqueous humor filtration along the inner wall, while pre-washout outflow patterns will show a more punctate tracer pattern due to the lack of inner wall/JCT separation. Our results suggest that the punctate labeling observed in short-duration perfusions and the pre-washout phase of the long-duration perfusions may be caused by large areas (10-100 microns) of

tethering between the inner wall and JCT that cause aqueous humor outflow to converge toward discrete pores in the inner wall. The uniform pattern observed in the post-washout phase of the long-duration perfusions is thought to be due to a loss of connectivity between the inner wall and JCT that increases the effective filtration area (inversely decreasing outflow resistance) along the inner wall for aqueous humor to enter the aqueous plexus. However, in our study, the effective filtration area in the short-duration, and both the pre and post-washout phases of the long–duration perfusions did not differ significantly (p=0.82). A logical assumption is that the pre-washout microspheres may have been dislodged from the inner wall/JCT region and passed out of the eye given the prolonged period (~3 h) for inducing the washout effect. However, the pre-washout outflow distribution and the short-duration (red tracer only) distribution were similar and suggest that the pre-washout decorating was not disrupted during the three-hour washout induction. Even more interesting was that the post-washout effective filtration area also did not differ significantly (p=0.76) from both the short-duration and pre-washout effective filtration area. A more likely explanation for the similarity between the short-duration and long-duration perfused eyes is segmental outflow. In both short and long-duration perfusions we observed areas of the aqueous plexus that had sparse microsphere labeling while other areas, particularly near the collector channel ostia, were heavily decorated (See Figure 3B.8).

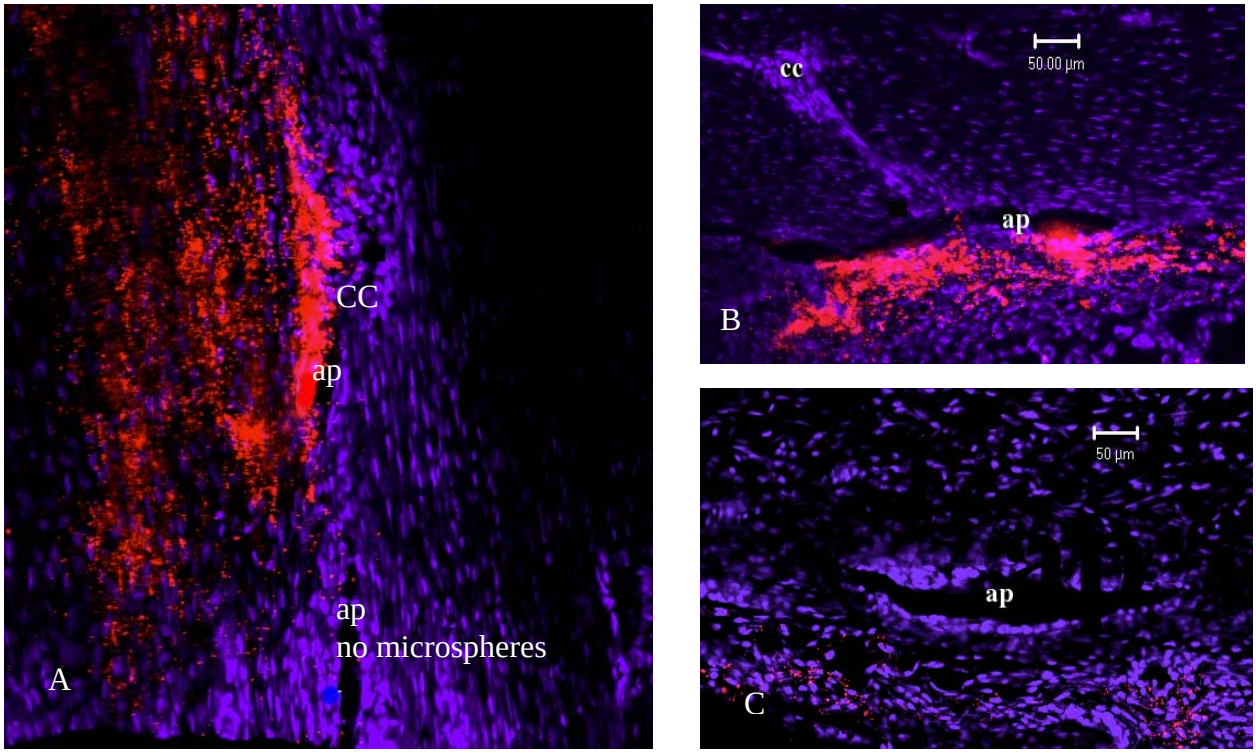


Figure 3B.8 *Segmental Outflow in Bovine Eyes at 15 mmHg* (A) tangential section showing intense labeling of the inner wall of the aqueous plexus (ap) with microspheres near the collector channel ostium (CC) while no microsphere labeling is observed along the inner wall distal to the CC, (B) radial section showing diffuse microsphere labeling along the inner wall near the CC, and (C) no microsphere decorating along the inner wall.

In support of our finding, previous filtration studies (Hann et al., 2005; de Kater et al., 1989; Melamed et al., 1986; Ethier and Chan 2001; Epstein and Rohen, 1991) have

provided evidence that aqueous humor drainage may be segmental rather than uniform. Additionally, morphological studies have demonstrated that the number of giant vacuoles is increased near collector channel ostia suggesting aqueous outflow across the inner wall is sensitive to downstream pressure (Parc, Johnson, Brilakis, 2000). Parc et al. (2000) noted that the variability observed in giant vacuole distribution was in part due to the distance the vacuoles are located from the collector channels. In our study, the variability observed in the microsphere distribution may have been due to the horizontal distance microspheres were bound from the collector channel ostia. Therefore, this unexpected finding of segmental outflow may have complicated our study by drastically influencing the results since only radial sections were used. Radial sections between collector channel ostia may differ significantly in their microsphere distributions from those cut at the collector channel ostia. Therefore, a future corollary of this study would be a morphometric analysis of pre and post-washout microsphere distributions as viewed in frontal sections (See Figure 4.1).

In summary, we focused on the relationship between changes in patterns of aqueous humor drainage and changes in outflow facility by inducing washout in bovine eyes. Although the scope of this study was limited, it has provided some evidence that washout may regulate outflow facility by changing patterns of aqueous humor drainage. Whether or not there is a relationship between the degree of inner wall/JCT separation that occurs with washout and the effective filtration area for aqueous humor outflow was not determinable from this study. A better understanding of the mechanisms that augment the total area for flow could be exploited to increase facility in eyes with elevated intraocular pressure.

Finally, based upon our observations:

i. ***The pattern of aqueous humor drainage before washout is more punctate while the post-washout pattern is more uniform in enucleated bovine eyes***

ii. ***Pre and Post-washout microsphere distributions do not correlate with changes in outflow facility in radial optic sections***

iii. ***Outflow appears segmental in enucleated bovine eyes perfused at 15 mmHg***

CHAPTER 4: CONCLUSIONS AND RECOMMENDATIONS FOR FUTURE WORK

It was the goal of this thesis to better understand the mechanism of washout and describe the role of washout in governing aqueous humor outflow resistance in bovine eyes. We investigated structural differences that differentiate eyes that do and do not exhibit washout and compared changes in outflow facility with changes in aqueous humor drainage patterns. We focused upon the following three specific aims:

i. *Determine whether the absence of washout in human eyes relates to morphological differences unique to the human outflow pathway as compared to bovine eyes in which washout occurs after prolonged intraocular perfusion.*

ii. *Review previous filtration studies and conclusions therein to develop a better method for tracing patterns of aqueous humor drainage in enucleated bovine eyes.*

iii. *Investigate the relationship between outflow facility and patterns of aqueous humor drainage in enucleated bovine eyes.*

In this chapter, we review relevant conclusions from the previous chapters in light of our overall goal to understand the mechanism of washout and the possible role it may play in governing patterns of aqueous humor drainage in enucleated bovine eyes. We also offer recommendations for future work in aqueous humor outflow filtration studies.

4.1 COMPARATIVE STUDIES BETWEEN SPECIES THAT DO AND DO NOT EXHIBIT A WASHOUT EFFECT

Ocular perfusion experiments were performed to investigate for morphological differences between human and bovine eyes to differentiate eyes that do and do not exhibit washout. In this study, we hypothesized that if the structural correlate for washout is separation between the inner wall and JCT in bovine eyes then similar morphological changes should not be found in human eyes subjected to prolonged perfusion since human eyes do not exhibit washout (Erickson-Lamy et al., 1990). Our hypothesis was derived from a previous study (Overby et al., 2002) where we documented that, in bovine eyes, the structural correlate to the facility increase during washout is a detachment of the JCT from the inner wall of the aqueous plexus. We therefore investigated whether the absence of washout in human eyes after long-duration perfusion is due to morphological differences unique to the human outflow pathway as compared to bovine eyes, in which morphological correlates to the increase in outflow facility have been reported after washout (Overby, 2002). From this study we concluded that:

i. *Washout in the bovine eye correlates with separation of JCT from the inner wall of the aqueous plexus, which does not occur in human eyes and may possibly account for the lack of washout.*

ii. *Human eyes uniquely possess an enhanced mechanical connectivity between the inner wall of Schlemm's canal and*

underlying JCT region that resists the separation between the JCT and inner wall that attends washout in bovine eyes.

iii. *Morphological comparison of electron micrographs shows human eyes appear to have more elastic fiber in the JCT region, especially in the region immediately underneath the inner wall of Schlemm's canal, that may aid in inner wall/JCT tethering; whereas, the bovine eye exhibits less elastic fiber in the JCT region, which may allow for easier separation of the inner wall/JCT tissue region.*

Clinical Relevance: Developing a pharmacological means by which these elastic fibers beneath the inner wall of Schlemm's canal can be digested to induce separation between the inner wall and underlying JCT tissue matrix may provide a way for inducing washout in the human eye, potentially providing a novel effective anti-glaucoma treatment.

4.2 PATTERNS OF AQUEOUS HUMOR DRAINAGE – PRELIMINARY STUDY

In this study, we investigated the relationship between changes in outflow facility and changes in patterns of aqueous humor drainage before and after washout in enucleated bovine eyes. Two colors of fluorescent microspheres were used to probe for changes in outflow drainage patterns before and after washout using laser scanning confocal microscopy. We hypothesized that that post-washout drainage patterns would demonstrate a more uniform pattern along the inner wall of the AP due to a decrease in tethering between the inner wall and JCT increasing the effective area for aqueous humor filtration along the inner wall, while pre-washout outflow patterns would show a more punctate tracer pattern due to the lack of inner wall/JCT separation.

From this study, we were able to conclude that

i. *Pre-washout aqueous humor drainage patterns are more punctate along the inner wall, whereas, post-washout aqueous humor drainage patterns show are more uniform.*

ii. *Pre and post-washout microsphere distributions do not correlate with changes in outflow facility in radial tissue sections.*

iii. *Outflow appears segmental in enucleated bovine eyes perfused at 15 mmHg.*

Clinical Relevance: Understanding the mechanism by which washout changes the effective filtration area along the inner wall may be exploited to decrease outflow resistance pharmacologically in eyes with elevated IOP.

4.3 FUTURE WORK

In our laboratory, a morphometric study is currently underway to extend the study of the relationship between changes in outflow facility and changes in patterns of aqueous humor drainage to include frontal sections. In Chapter 3B, the inability to correlate changes in microsphere distribution with changes in outflow facility may have been complicated by segmental outflow throughout the bovine eye (See Section 3B.4 Figure 3B.8). Therefore, frontal sections of the bovine aqueous plexus should provide greater visibility for assessing preferential outflow patterns before and after washout (Figure 4.1).

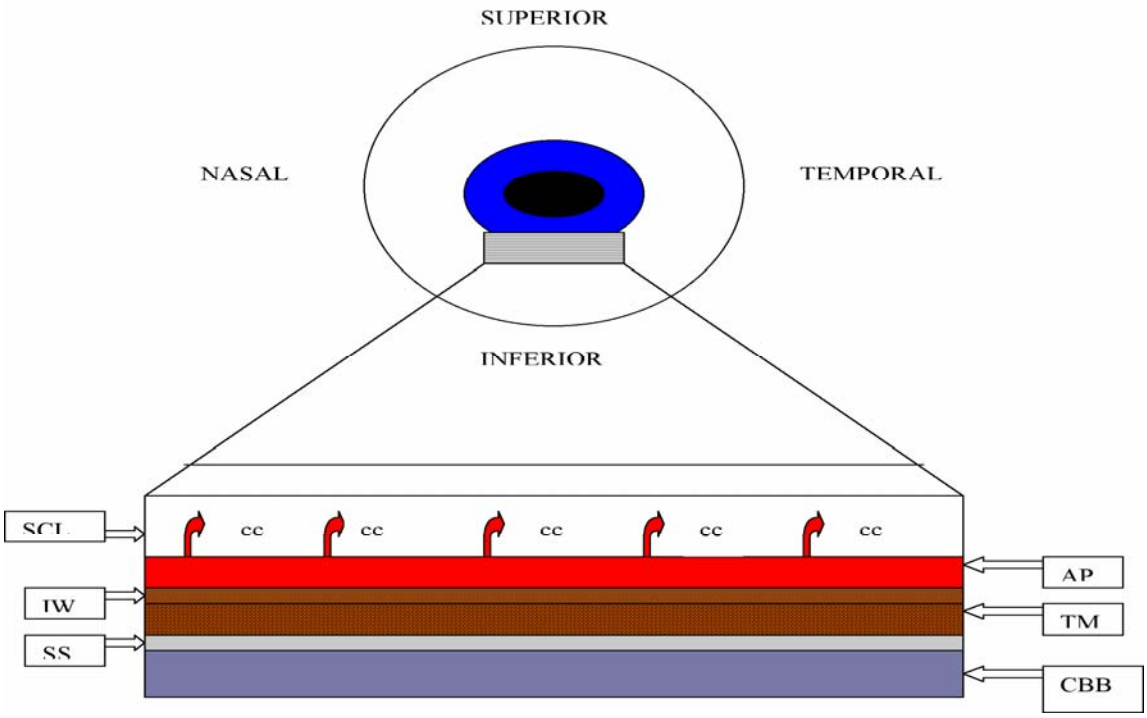


Figure 4.1 *Frontal Sectioning along the Bovine Aqueous Plexus.*

Future studies in our laboratory include: investigating the relationship between IOP and patterns of aqueous humor drainage, the relationship between outflow facility enhancing drugs such as Y-27632, a acto-myosin contractibility inhibitor, and patterns of aqueous humor drainage in human and bovine eyes, and the mechanism of increasing outflow facility by matrix-metalloproteinases and elastinase in human eyes.

APPENDIX: PRE AND POST-WASHOUT FLUOSPHERE PERCENT DISTRIBUTION ALONG THE INNER WALL OF THE BOVINE AQUEOUS PLEXUS ASSIGNED IN CHAPTER 3B

This appendix lists the percent distribution of fluorescent microsphere tracers assigned to each confocal image in Chapter 3B that investigated the relationship between changes in outflow facility and changes in patterns of aqueous humor drainage before and after washout in enucleated bovine eyes. The distribution of percentages were calculated as follows: the total length (TL) and the tracer-decorated length (L) of inner wall for both FluoSpheres were measured in at least 4 (n=3 to 21) images/eye, and the average percent effective filtration length (PEFL=L/TL) in each eye was calculated (See Figure 3.3). All scores were assigned by myself and are presented here as a permanent record of these results. Each confocal image is referenced according to the group and perfusion number (Eye ID). These images are kept on file and may be obtained by contacting Professor Haiyan Gong at

Boston University School of Medicine
Department of Ophthalmology
Lions Eye Research Laboratory, L914
715 Albany Street
Boston, MA 20118
(617) 638-4434
hgong@bu.edu

Table 1A: *Control Low-Volume Pre-Washout Microsphere Distribution Scores*

Eye ID	Quadrant	R	CC	Plex Tot length	Bead tot length	% Bead Distribution
Control 4	Superior	R1		186.82	113.95	60.99%
Control 4	Superior	R2		402.79	114.29	28.37
Control 4	Superior	R5		245.19	79.3	32.34
Control 4	Superior	R6	CC	565.15	346.05	61.23
Control 4	Superior	R8		381.15	134.42	35.27
Control 4	Superior	R9	CC	521.21	521.21	100
Control 4	Superior	R10		473.56	281.69	59.48
AVE				396.55	227.27	45.32%
Control4	Inferior	R1		387.08	338.29	87.4
Control4	Inferior	R3		354.49	80.8	22.79
Control4	Inferior	R4		574.54	178.97	31.15
AVE				438.70	199.35	47.11
Control4	Temporal	R2		573.99	202.01	35.19
Control4	Temporal	R3		644.61	87.04	13.5
Control4	Temporal	R4		378.41	378.41	100
AVE				532.34	222.49	49.56
Control4	Nasal	R1	CC	546.72	334.37	61.16
Control4	Nasal	R5	CC	946.34	351.97	37.19
Control4	Nasal	R7	CC	512.7	270.73	52.8
AVE				668.59	319.02	50.38

Control3	Superior	R2		440.85	224.14	50.84
Control3	Superior	R3		629.74	286.31	45.46
AVE				535.30	255.23	48.15
Control3	Inferior	R5		374.91	0	0
Control3	Inferior	R6		560.37	36.7	6.55
AVE				467.64	18.35	3.28
Control3	Temporal	R2		692.47	247.3	35.71
Control3	Temporal	R3		307.66	128.95	41.91
Control3	Temporal	R4		496.47	228.14	45.95
Control3	Temporal	R5		556.86	126.15	22.65
Control3	Temporal	R8		768.18	222.29	28.94

AVE				564.33	190.57	35.03
Control3	Nasal	R1	CC	593.66	167.62	28.24
Control1	Superior	R1		207.44	136.39	65.75
Control1	Superior	R2		469.11	260.08	55.44
Control1	Superior	R3		594.73	197.66	33.24
Control1	Superior	R4		428.43	162.83	38.01
AVE				424.9275	189.24	48.11
Control1	Inferior	R2		533.98	378.95	70.97
Control1	Temporal	R1		344.59	125.22	36.34
Control1	Nasal	R2		421.84	54.26	12.86
Control1	Nasal	R3	CC	313.27	216.57	69.13
AVE				367.56	135.42	40.99
Control5	Superior	R5		368.01	0	0
Control5	Inferior	NA				
Control5	Nasal	R1		189	82.18	43.48
Control5	Temporal	NA				
AVE	SUPERIOR			368.01	0	0
	NASAL			189	82.18	43.48
	OVERALL			278.51	41.10	21.74
Control6	Superior	R1		107.48	0	0
Control6	Inferior	NA				
Control6	Temporal	R2		66.32	0	0
Control6	Nasal	R1		441.22	80.15	18.17
Control6	Nasal	R2		330.03	65.7	19.91
AVE				385.63	72.93	19.04

Table 1B: *Experimental Pre and Post-Washout Microsphere Distribution (Red = Pre-Washout, Green = Post-Washout)*

EYE ID	QUAD	R		Plexus Length	Red Bead	Green Bead	% Dis Red	% Dis Green
EXP1	Superior	R		364.18	101.47	204.77	27.86	56.23
EXP1	Superior	R		227.97	234.29	261	100.00	114.5
EXP1	Superior	R		208.75	64.32	89.7	30.80	42.97
EXP1	Inferior	R1		364.4	329.25	55.37	90.35	15.19
EXP1	Nasal	R1		175.47	53.59	105.37	30.54	60.0
EXP4	Nasal	R5	CC	209.21	155.92	199.2	75.43	95.22
EXP4	Nasal	R4	CC	271.01	159.06	192.87	58.69	71.15
EXP4	Nasal	R3		452.02	144.11	144.13	31.88	31.89
EXP4	Nasal	R2		742.23	459.89	409.08	61.96	55.11
EXP4	Nasal	R1	CC	379.73	253.33	241.72	66.71	63.66
EXP4	Temporal	R2	CC	158.68	49.61	64.92	31.26	40.91
EXP4	Temporal	R1	CC	738.49	273.54	350.98	37.04	47.53
EXP4	Inferior	R5		400.18	303.74	257.41	75.90	64.32
EXP4	Inferior	R4		775.84	504.22	744.48	64.99	95.96
EXP4	Inferior	R2	CC	201.4	82.58	87.42	41.00	43.41
EXP4	Superior	R1		177.73	171.43	163.94	96.46	92.24
EXP4	Superior	R2	CC	615.1	473.12	384.75	76.92	62.55
EXP4	Superior	R2a	CC	676.32	415.97	483.8	61.50	71.53
EXP4	Superior	R3	CC	687.52	475.26	534.99	69.13	77.81
EXP4	Superior	R4		711.34	711.34	711.34	100.00	100.0
EXP5	Inferior	R2		611.53	78.47	291.25	12.83	47.63
EXP5	Superior	R3		183.69	NONE	NONE		
EXP5	Superior	R4		181.5	104.4	39.39	57.52	21.70
EXP5	Nasal	R1	CC	276.92	16.46	23.87	05.90	08.60
EXP6	Superior	R1		477.47	87.7	94.84	18.37	19.86
EXP6	Superior	R4		425.06	158.41	251.7	37.26	59.22
EXP6	Superior	R5		465.32	322.84	269.92	69.38	58.0
EXP6	Temporal	R1		246.79	150.64	91.52	61.00	37.08
EXP6	Temporal	R2		287.4	77.3	46.31	29.60	16.11

BIBLIOGRAPHY:

Allingham RR, deKater AW, Ethier CR, et al. The relationship between pore density and outflow facility in human eyes. *Invest Ophthalmol Vis Sci.* 1992:33:1661.

Allingham RR, deKater AW, Ethier CR. Schlemm's canal and primary open angle glaucoma: correlation between schlemm's canal dimensions and outflow facility. *Exp Eye Res.* 1996:62:101-109.

Ascher KW. Aqueous veins: physiologic importance of visible elimination of intraocular fluid. *Am J Ophthalmol*. 1942;25:1174.

Ashton, N. Anatomical study of Schlemm's canal and aqueous veins by means of neoprene casts. Part I. Aqueous Veins. *Br J Ophthalmol.* 1951;35:391.

Barany EH, Scotchbrook S. Influence of testicular hyaluronidase on the resistance to flow through the angle of the anterior chamber. *Acta Physiol Scand*. 1954;30:240-248.

Barany EH, Woodin AM. Hyaluronic Acid and hyaluronidase in the aqueous humor and the angle of the anterior chamber. *Acta Physiol Scand*. 1955;33:257-290.

Barany EH. The mode of action of pilocarpine on outflow resistance in the eye of a primate (*Cercopithecus aethiops*). *Invest Ophthalmol Vis Sci*. 1962;1:712-727.

Barany EH. Simultaneous measurement of changing intraocular pressure and outflow facility in the vervet monkey by constant pressure infusion. *Invest Ophthalmol Vis Sci*. 1964;3:135-143.

Bartels SP, Lawrence BA, Kolodny NH. Conformation by magnetic resonance imaging of the diffusional pathway between the ciliary processes and the anterior chamber. ARVO Abstracts. *Invest Ophthalmol Vis Sci* 33(4,suppl):1412, 1992.

Bill, A. The aqueous humor drainage mechanism in the cynomolgus monkey (*Macaca irus)* with evidence for unconventional routes. *Invest Ophthalmol Vis Sci.* 1965:4:911-919.

Bill, A. Conventional and uveo-scleral drainage of aqueous humor in the cynomolgus monkey (*Macaca irus)* at normal and high intraocular pressures. *Exp Eye Res.* 1966:5:45-54.

Bill A, Maepea O. Mechanisms and routes of aqueous humor drainage. In: Albert DM, Jacobeic FA, eds. *Principles and Practice of Ophthalmology*. Philadelphia: WB Saunders; 1994:206-225.

Bill, A, Phillips I. Uveoscleral scleral drainage of aqueous humor in human eyes. *Exp Eye Res*. 1971;2l:275-281.

Bill A, Svedbergh B. Scanning electron microscopic studies of the trabecular meshwork and the canal of Schlemm: An attempt to localize the main resistance to outflow of aqueous humor in man. *Acta Ophthalmol.* 1972:50:295-320.

Boofel CG. Intraocular pressure in vitamin A deficient Holstein male calves. *J Dairy Sci.* 1964;47:655

Brubaker RF. The effect of intraocular pressure on conventional outflow resistance in the enucleated human eye. *Invest Ophthalmol Vis Sci.* 1975;14:286-292.

de Kater AW, Melamed S, Epstein DL. Patterns of aqueous humor outflow in glaucomatous and nonglaucomatous human eyes. *Arch Ophthalmol*. 1989;107:572-76.

Dreyer EB, Zurakowski D, Schumer RA, Podos SM, Lipton SA. Elevated glutamate levels in the vitreous body of humans and monkeys with glaucoma. *Arch Ophthalmol*. 1996;114:299-

Duane TD, Jaeger EA (eds.) *Biomedical Foundations of Ophthalmology*. 1971:10:33.

Ellingsen B, Grant W. Influence of intraocular pressure and trabeculotomy on aqueous outflow in enucleated monkey eyes. *Invest Ophthalmol Vis Sci*. 1971;10:705-709.

Ellingsen B, Grant W. Trabeculotomy and sinusotomy in enucleated human eyes. *Invest Ophthalmol Vis Sci*. 1972;11:21-28.

Epstein DL, Hashimoto JM, Grant WM. Serum obstruction of aqueous outflow in enucleated eyes. *American Journal of Ophthalmology* 1978;86:101-105.

Epstein DL, Patterson MM, Rivers SC, and Anderson PJ. N-ethylmaleimide increases the facility of aqueous outflow of excised monkey and calf eyes. *Invest Ophthalmol Vis Sci*. 1982;22:752-756.

Epstein DL, Rohen JW. Morphology of the trabecular meshwork and inner wall endothelium after cationized ferritin perfusion in the monkey eye. *Invest Ophthalmol Vis Sci.* 1991;32:160-71.

Erickson KA, Kaufman PL. Comparative effects of three perfusates on outflow facility in the cynomolgus monkey. *Curr Eye Res*. 1981;1:211-216.

Erickson-Lamy K, Rohen JW, Grant WM. Outflow facility studies in the perfused bovine aqueous outflow pathways. *Eye Research*. 1988;7:799-807.

Erickson-Lamy K, Schroeder AM, Bassett-Chu S, Epstein DL. Absence of time-dependent facility increase ("washout") in the perfused enucleated human eye. *Invest Ophthalmol Vis Sci*. 1990;31:2384-2388.

Erikkson A, Svedbergh B. Transcellular aqueous humor outflow: A theoretical and experimental study. *Graefes Arch Clin Exp Ophthalmol.* 1980;212:187-197.

Ethier CR, Kamm RD, Palaszewski BA, Johnson M, Richardson TM. Calculations of flow resistance in the juxtacanalicular meshwork. *Invest. Ophthalmol. Vis. Sci*. 1986;27:1741-1750.

Ethier CR, Coloma FM, Sit AJ, Johnson M. Two pore populations in the inner wall endothelium of Schlemm's canal. *Invest Ophthalmol Vis Sci.* 1998;39:2041.

Ethier CR, Chan DWH. Cationic ferritin changes outflow facility in human eyes whereas anionic ferritin does not. *Invest Ophthalmol Vis Sci.* 2001;42:1795-1802.

Ethier CR, Read AT, Chan D. Biomechanics of Schlemm's canal endothelial cells: influence on F-actin architecture. *Biophys J.* 2004;87:2828-2837.

Flugel C, Tamm E, Lutjen-Drecoll E. Different cell populations in bovine trabecular meshwork: an ultrastructural and immunocytochemical study. *Exp Eye Res*. 1991;52:681-690.

Fourman S, Fourman MB. Correlation of tonography and constant pressure perfusion measurements of outflow facility in the rabbit. *Cur Eye Res*. 1989;9:963-969.

Francois J, Rabaey M, Neetens A. Perfusion studies on the outflow of aqueous humor in human eyes. *A.M.A Arch of Ophthalmol*. 1955; 54:193-204.

Freddo TF, Bartels SP, Barsotti MF, Kamm RD. The source of proteins in the aqueous humor of the normal rabbit. *Invest Ophthalmol Vis Sci*. 1990;31:125-137.

Gaasterland DE, Pederson JE, McLellan HM. Perfusate effects upon resistance to aqueous humor outflow in the rhesus monkey. *Invest Ophthalmol Vis Sci*. 1978;17: 391-397.

Gaasterland DE, Pederson JE, McLellan HM, Reddy VN. Rhesus monkey aqueous humor composition and a primate ocular perfusate. *Invest Ophthalmol Vis Sci*. 1979;18:1139-1150.

Gabelt BT, Gottanka J, Lutjen-Drecoll E, Kaufmann PL. Aqueous humor dynamics and trabecular meshwork and anterior ciliary muscle morphologic changes with age in rhesus monkeys. *Invest Ophthalmol Vis Sci.* 2003;44:2118-2125.

Gelatt KN. Animal models for glaucoma. *Invest Ophthalmol Vis Sci*. 1977;16:592-596.

Goldmann H. Weitere Mitteilungber den Abfluss des Kammerwassers beim Menschen. *Ophthalmologica.* 1946:112:344.

Gong H, Tripathi R, Tripathi B. Morphology of the aqueous humor outflow pathway. Microscopy Research and Technique. 1996;33:336-367.

Gong H, Ruberti J, Overby D, Johnson M, Freddo TF. A new view of the human trabecular meshwork using quick-freeze, deep-etch electron microscopy. *Exp Eye Res.* 2002;75:347-358.

Gottanka J, Johnson DH, Martus P, Lutjen-Drecoll E. Beta-adrenergic blocker therapy and the trabecular meshwork. *Graefes Arch Clin Exp Ophthalmol.* 2001;239:138-144.

Grant WM. Experimental aqueous perfusion in enucleated human eyes. *Arch Ophthalmol*. 1963:69:783-801.

Grierson I, Lee WR, Abraham S. Effects of pilocarpine on the morphology of the human outflow apparatus. *Br J Ophthalmol.* 1978;62:302-313.

Grierson I, Lee WR, Abraham S, Howes RC. Associations between the cells of the walls of Schlemm's canal. *Albrecht. Von Graefes Arch. Klin. Exp Ophthalmol.* 1978:208:33-47.

Grierson I, Lee WR, Moseley H, Abraham S. The trabecular wall of Schlemm's canal: A study of the effects of pilocarpine by scanning electron microscopy. *Br J Ophthalmol.* 1979:63:9-16.

Hann CR, Bahler CK, Johnson DH. Cationic ferritin and segmental flow through the trabecular meshwork. *Invest Ophthalmol Vis Sci.* 2005;46:1-7.

Hashimoto JM and Epstein PL. Influence of intraocular pressure on aqueous outflow facility in enucleated eyes of different mammals. *Invest Ophthalmol Vis Sci*. 1980;19:1483-1489.

Hayreh SS. Progress in the understanding of the vascular etiology of glaucoma. *Curr Opin Ophthalmol.* 1994;5:11.

Hayreh SS, Zimmerman MB, Podhajsky P, Alward WL. Nocturnal arterial hypotension and its role in optic nerve head and ocular ischemic disorders. *Am J Ophthal.* 1994; 117:603-624.

Hubbard WC, Johnson M, Gong H, Gabelt BT, Peterson JA, Sawhney R, Freddo T and Kaufman PL. Intraocular pressure and outflow facility are unchanged following acute and chronic intracameral chondratenase ABC and hyaluronidase in monkey. *Exp Eye Res* 1997;65:177-190.

Huggert A. Pore size in the filtration angle of the eye. *Acta Ophthalmol.* 1955:33:271.

Huggert A. An experiment in determining the pore size distribution curve to the filtration angle of the eye. *Acta Ophthalmol.* 1957;12-19, 104-112.

Huggert A, Holmberg A, Esklund A. Further studies concerning the filtration angle of the eye. *Acta Ophthalmol.* 1955:33:429.

http://www.glaucom.com/Meetings/4-3/iser.htm.

Inomata H, Bill A, Smelser GK. Aqueous humor pathways through the trabecular meshwork and into Schlemm's canal in the cynomolgus monkey (*Macaca Irus*). *Am J Ophthalmol.* 1972;73:760-89.

Jackson GM, James DF. The hydrodynamic resistance of hyaluronic acid and its contribution to tissue permeability. *Biorheology.* 1982;19:317-330.

Johnson M, Kamm RD. The role of Schlemm's canal in aqueous outflow from the human eye. *Invest Ophthalmol Vis Sci.* 1983:24:320.

Johnson M. Transport through the aqueous outflow system of the eye. *Ph.D. thesis*. Cambridge, MA. Massachusetts Institute of Technology. 1987.

Johnson M, Johnson DH, Kamm RD, deKater AW, Epstein DL. The filtration characteristics of the aqueous outflow system. *Exp Eye Res*. 1990:50:407-418.

Johnson M, Chen A, Epstein DL, Kamm RD. The pressure and volume dependence of the rate of wash-out in the bovine eye. *Current Eye Research* 1991;10: 373-375.

Johnson M, Shapiro A, Ethier CR, Kamm RD. Modulation of outflow resistance by the pores of the inner wall endothelium. *Invest Ophthalmol Vis Sci.* 1992:33:1670-1675.

Johnson M, Gong H, Freddo TF, Ritter N, Kamm R. Serum proteins and aqueous outflow resistance in bovine eyes. *Invest Ophthalmol Vis Sci.* 1993;34:3549-3557.

Johnson M, Chan D, Read TA, Christensen C, Sit A, and Ethier CR. The pore density in the inner wall endothelium of schlemm's canal of glaucomatous eyes. *Invest Ophthalmol Vis Sci*. 2002;43: 2950-2955.

Johnson M, Erickson K. Mechanisms and routes of aqueous humor drainage. Albert, DM Jakobiec, FA eds. *Principles and Practice of Ophthalmology.* WB Saunders Philadelphia. 2000;2577-2595.

Johnstone MA, Grant WM. Pressure dependent changes in the structures of the aqueous outflow system of human and monkey eyes. *Am J Ophthalmol.* 1973:75:365.

Johnstone MA. Pressure-dependent changes in configuration of the endothelial tubules of Schlemm's canal. *Am J Ophthalmol.* 1974:78:630-638.

Johnstone MA. Pressure-dependent changes in nuclei and the process origins of the endothelial cells lining Schlemm's canalconfiguration of the endothelial tubules of Schlemm's canal. *Invest Ophthalmol Vis Sci.* 1979:18:44-51.

Johnstone MA. The aqueous outflow system as a mechanical pump. In: *Glaucoma.* 2004;13:421-438.

Kanski JJ. Clinical Ophthalmology (4th ed.) Chapter 6: The glaucomas. 2000; 206.

Kaufman PL, True-Gabelt B, Erickson-Lamy KA. Time dependence of perfusion outflow facility in the cynomolgus monkey. *Curr Eye Res*. 1988;7:721-726.

Kee C, Gabelt BT, Croft MA, Gange SJ, Menage MJ, Kaufman PL. Serum effects on aqueous outflow during anterior chamber perfusion in monkeys. *Invest Ophthalmol Vis Sci*. 1996;37:1840-1848.

Knepper PA, Farbman AI, Tesler AG. Exogenous hyaluronidases and degradation of hyaluronic acid in the rabbit eye. *Invest Ophthalmol Vis Sci.* 1984;25:286-293.

Knies M. Die resorption von blut in der vorderen augenkammer. *Arch Pathol Anat Phsyiol Klin Med.* 1875:62:537.

Kwon YH, Caprioli J. Primary open-angle glaucoma. Duanes Clinical Ophthalmology. 2005:Chapter 52.

Laurent TC, Pietruszkiewicz A. The effect of hyaluronic acid on the sedimentation rate of other substances. *Biochem Biophys Acta*. 1961;49:258-264.

Leber T. Studien ber den Flussigkeitswechsel in Auge. *Graefes Arch Clin Exp Ophthalmol.* 1873:19:87.

Lee WR, Grierson I. Pressure effects on the endothelium of the trabecular wall of Schlemm's canal: a study by scanning electron microscopy. *Graefes Arch Clin Exp Ophthalmol.* 1975:196:255-265.

Levick JR. Flow through interstitium and other fibrous matrices (review article). *Q J Exp Physiol.* 1987;72:409-437.

Lutjen-Drecoll E, Kaufman PL. Morophological changes in primate aqueous humor formation and drainage tissues after long-term treatment with antiglaucomatous drugs. *J Glaucoma.* 1993;2:316-328.

Lutjen-Drecoll E, Tamm E, Kaufmann PL. Age changes in rhesus monkey ciliary muscle: light and electron microscopy. *Exp Eye Res.* 1988(a);47:885-899.

Lutjen-Drecoll E, Tamm E, Kaufmann PL. Age-related loss of morphologic responses to pilocarpine in rhesus monkey ciliary muscle. *Arch Ophthal*. 1988(b);106:1591-1598.

Maepea O, Bill A. The pressures in the episcleral veins, Schlemm's canal and the trabecular meshwork in monkeys: Effects of changes in intraocular pressure. *Exp Eye Res.* 1989:49:645-663.

Maepea O, Bill A. Pressures in the juxtacanalicular connective tissue and Schlemm's canal in monkeys. *Exp Eye Res.* 1992:54:879-883.

McEwen WK. Application of Poiseuille's law to aqueous outflow. *Arch Ophthalmol.* 1958:60:290.

Melamed S, Freddo TF, Epstein DL. Use of cationized ferritin to trace aqueous humor outflow in the monkey eye. *Exp Eye Res.* 1986;43:273-278.

Millar C, Kaufman PL: Aqueous humor: Secretion and dynamics. In Tasman W, Jaeger EA (eds): Duane's Foundations of Clinical Ophthalmology. Philadelphia: Lippincott-Raven, 1995

Moncada S, Palmer R, Higgs EA: Nitric oxide physiology, pathophysiology, and pharmacology. *Pharmacol Rev.* 1991;43:109.

Moseley H, Grierson I, Lee WR. Mathematical modeling of aqueous humor outflow from the eye through pores in the lining of Schlemm's canal. *Clin Phys Physiol Meas*. 1983:4:47.

Moses RA. Circumferential flow in Schlemm's canal. *Am J Ophthalmol.* 1979:88:585.

Moses RA, Grodzki WJ Jr, Etheridge EL, Wilson CD. Schlemm's canal: The effect of Intraocular Pressure. *Invest Ophthalmol Vis Sci.* 1981:20:61.

Nesterov AP. Role of blockade of Schlemm's canal in pathogenesis of primary open-angle glaucoma. *Am J Ophthalmol.* 1970:70:691-696.

Nilsson SF et al. Increased uveoscleral outflow as a possible mechanism of ocular hypertension caused by prostaglandin $F_{2\alpha}$-1-isopropylester in the cynomolgus monkey. *Exp Eye Res.* 1989;48:707.

Overby D, Gong H, Qiu G, Freddo TF, Johnson M. The mechanism of increasing outflow facility during washout in the bovine eye. *Invest Ophthalmol Vis Sci*. 2002;43:3455-3464.

Parc CE, Johnson DH, Brilakis HS. Giant vacuoles are found preferentially near collector channels. *Invest Ophthalmol Vis Sci.* 2000;41(10):2984-90.

Peterson WS, Joscon VL. Hyaluronidase effects on aqueous outflow resistance: Quantitative and localizing studies in the rhesus monkey eye. *Am J Ophthalmol.* 1974;77:573-577.

Pillunat LE, Stodtmeister R, Wilmanns I et al. Autoregulation of ocular blood flow during changes in intraocular pressure: Preliminary results. *Graefes Arch Clin Exp Ophthalmol.* 1985;223:219-

Quigley HA, Hohman RM, Addicks EM et al. Morphologic changes in the lamina cribrosa correlated with neural loss in open-angle glaucoma. *Am J Ophthalmol.* 1983; 95:673-691.

Quigley, HA. Number of people with glaucoma worldwide. *Br J Ophthalmol.* 1996;80:389-393.

Rao PV, Deng PF, Kumar J, Epstein DL. Modulation of Aqueous Humor Outflow Facility by the Rho Kinase-Specific Inhibitor Y-27632. *Invest Ophthalmol Vis Sci*. 2001;42:1029-1037.

Robert Y, Steiner D, Hendrickson P. Papillary circulation dynamics in glaucoma. *Graefes Arch Clin Exp Ophthalmol*. 1989;227:436-439.

Rohen, J. In *Glaucoma*. Ch. 14: Anatomy of the aqueous outflow channels. 1986; 277-296.

Rohen JW, Unger HH: Zur Morphologie und Pathologie der Kammerbucht des Auges, Abhandlung der Akademie der Wissenschaften und der Literatur, Mainz, Nr. 3. Wiesbaden, Steiner Verlag, 1959.

Rohen JW, Lutjen E, Barany E. The relation between the ciliary muscle and the trabecular meshwork and its importance for the effect of miotics on aqueous outflow resistance. *Albrecht Von Graefes Klin Exp Ophthalmol.* 1967;172:23-47.

Rohen JW, Futa R, Lutjen-Drecoll E. The fine structure of the cribriform meshwork in normal and glaucomatous eye as seen in tangential sections. *Invest Ophthalmol Vis Sci*. 1981;21:574-585.

Rosenquist R, Epstein D, Melamed S, Johnson M, Grant WM. Outflow resistance of enucleated human eyes at two different perfusion pressures and different extents of trabeculotomy. *Curr Eye Res.* 1989;8:1233-1240.

Ruben JB, Moses RA, Grodski WJ Jr. Perfusion outflow facility in the rabbit eye: Stabilization by EACA. *Invest Ophthalmol Vis Sci.* 1985;26:153-158.

Sabanay I, Tian B, Gabelt BT, Geiger B, Kaufman, PL. Functional and structural reversibility of H-7 effects on the conventional aqueous outflow pathway in monkeys. *Exp Eye Res 2004;*78:137-150.

Schottenstein EM. Intraocular pressure and tonometry. In Ritch R, Shields B, Krupin T, eds. The Glaucomas: Basic Sciences. 2nd ed. St. Louis, Missouri; Mosby. Chapter 20;407-428.

Schwalbe G. Untersuchen ber die Lympbahen des Auges und ihre Begrenzungen. *Arch Mikrosk Anat.* 1870:6:261.

Seidel E. Weitere experimentelle Untersuchungen ber die Quelle und den Verlauf der intraokularen Saftstrmung. XVIII. Mikroskopische Beobachtungen ber den Mechanisms des Abfluss aud der Vorderdammer des debenden Tieres bei physiologischem Augendrucke. *Graefes Arch Clin Exp Ophthalmol.* 1923:111:167.

Sit AJ, Coloma FM, Ethier CR, Johnson M. Factors affecting the pores of the inner wall endothelium of Schlemm's canal. *Invest Ophthalmol Vis Sci.* 1997:38:1517-1525.

Sit AJ, Gong H, Ritter N, Freddo TF, Kamm R, Johnson M. The role of soluble proteins in generating aqueous outflow resistance in the bovine and human eye. *Exp Eye Res 1997;*64:813-821.

Smith P. On the escape of fluid from the aqueous and vitreous chambers under different pressure. *Ophthalmol Rev.* 1888:7:193.

Sperber GO, Bill A. A method for near-continuous determination of aqueous humor flow: effects of anesthetics, tempertature and indomethacin. *Exp Eye Res.* 1984;39:435-453.

Spielman LA. Particle capture from low speed laminar flows. *Annu. Rev. Fluid Mech.* 1977:9:277-96.

Tanchel NA, et al. *IOVS* 1984;25:ARVO Abstract 7.

Theobald, GD. Schlemm's canal. Its anastamosis and anatomic relations. *Trans. Am Ophthal Soc.* 1934;32:574.

Thomassen TL. On aqueous veins. *Acta Ophthalmol Rev.* 1947:25:369.

Tian B, Kaufmann PL, Volberg T, Gabelt BT, Geiger B. H-7 disrupts the actin cytoskeleton and increases outflow facility. *Arch Ophthamol.* 1998;116:633-643.

Tian B, Gabelt BT, Peterson JA, Kiland JA, Kaufman PL. H-7 increases trabecular facility and facility after ciliary muscle disinsertion in monkeys. *Invest Ophthalmol Vis Sci*. 1998;40:239-242.

Toris CB, Yablonski ME, Wang YL, Camras CB. Aqueous humor dynamics in the aging human eye. *Am J Ophthalmol.* 1999;127:407-412.

Townsend BJ, Brubaker RF. Immediate effect of epinephrine on aqueous humor formation in the normal human eye as measured by fluorophotometry. *Invest Ophthalmol Vis Sci.* 1980;19:256-266.

Tripathi RC. Ultrastructure of the exit pathway of the aqueouos in lower mammals (a preliminary report on the “angular aqueous plexus”). *Exp Eye Res.* 1971;12:311-314.

Tripathi RC, Tripathi BJ. The mechanism of aqueous outflow in lower mammals. *Exp Eye Res.* 1972(a);14:73-79.

Tripathi RC. Comparative aspects of aqueous outflow in *The Eye*, H. Davson ed. New York: Academic Press, 1974.

Van Buskirk EM. Changes in the facility of aqueous outflow induced by lens depression and intraocular pressure in excised human eyes. *Am J Ophthalmol.* 1976:82:736-740.

Van Buskirk MS, Brett J. The canine eye: in vitro dissolution of the barriers to aqueous outflow. *Invest Ophthalmol Vis Sci.* 1978;17:258-263.

Yan DB, Trope GE, Ethier CR, Menon IA, Wakeham A. Effects of hydrogen peroxide-induced oxidative damage on outflow facility and washout in pig eyes. *Invest Ophthalmol Vis Sci*. 1991;32:2515-2520.

Yektashenas B, Read AT, Ethier CR, Johnson M. Cationized ferritin decoration as a marker of true pores in the inner wall endothelium of Schlemm’s canal. ARVO abstract #1848, 2006.

Yue, B YJT. (2000). Cellular mechanisms in the trabecular meshwork affecting the aqueous humor outflow pathway. In *Principle and Practices of Ophthalmology.* Vol. 4(Albert, DM and Jakobiec FA, Eds.) pp. 2596-2613. WB Saunders Co: Philadelphia, PA, USA.